Title
Little String Defects and Nilpotent Orbits

Author
Schmid, Christian

Publication Date
2020

Peer reviewed|Thesis/dissertation

Little String Defects and Nilpotent Orbits

by

Christian Schmid

A dissertation submitted in partial satisfaction of the

requirements for the degree of

Doctor of Philosophy

in

Physics

in the

Graduate Division

of the

University of California, Berkeley

Committee in charge:

Professor Mina Aganagic, Chair
Professor Ori Ganor
Professor Nicolai Reshetikhin

Spring 2020

Little String Defects and Nilpotent Orbits

Abstract

Little String Defects and Nilpotent Orbits

by

Christian Schmid

Doctor of Philosophy in Physics

University of California, Berkeley

Professor Mina Aganagic, Chair

In this thesis, we first derive and analyze the Gukov–Witten surface defects of four-dimensional $\mathcal{N} = 4$ Super Yang-Mills (SYM) theory from little string theory. The little string theory arises from type IIB string theory compactified on an ADE singularity. Defects are introduced as D-branes wrapping the 2-cycles of the singularity. In a suitable limit, these become defects of the six-dimensional superconformal $\mathcal{N} = (2, 0)$ field theory, which reduces to SYM after further compactification.

We then use this geometric setting to connect to the complete nilpotent orbit classification of codimension-two defects, and find relations to ADE-type Toda CFT. We highlight the differences between the defect classification in the little string theory and its $(2, 0)$ CFT limit, and find physical insights into nilpotent orbits and their classification by Bala–Carter labels and weighted Dynkin diagrams.

Contents

Acknowledgments

This thesis would not exist without the guidance of my PhD advisor, Mina Aganagic. Thank you for always being available to answer my questions, and for coming up with novel project ideas and suggestions. I also want to thank my other two committee members, Ori Ganor and Nicolai Reshetikhin, for enlightening conversations about mathematics and physics.

I also owe gratitude to Nathan Haouzi, for collaborating on the ideas in this thesis, and to Shamil Shakirov, for teaching me his style of 'experimental mathematics'. Furthermore, I want to thank Benjamin Gammage, Patrick Jefferson, Alex Takeda for their insight into some of these topics.

Finally, I'd like to thank my best friend Niklas and my family for always supporting me.

Chapter 1

Introduction

In this thesis, we will explore topics that lie at the intersection of physics and mathematics – concretely, of string theory and representation theory. Because we can take the string theory setups we build and 'zoom out', we can also use our results to gain insight into particle physics.

This general approach of using string theory, with its symmetries and dualities, to deepen our understanding of mathematics and physics has proven extremely fruitful in the past [1]. It led to results in areas like knot theory [58], condensed matter physics [34], and enumerative geometry [60].

A more recent result is the Alday-Gaiotto-Tachikawa (AGT) correspondence: It relates partition functions of a 6d $\mathcal{N} = (2, 0)$ superconformal field theory (SCFT) compactified on a Riemann surface to conformal blocks of a 2d Toda field theory on the surface. It has since been extended and proven in [3] in the context of *little string theory*. In this thesis, we want to review these results and relate them to various other physical setups. Most importantly, we want to connect to the nilpotent orbit classification of codimension two defects of the $(2, 0)$ SCFT in [17]. We also want to study relations of the little string setup to surface defects of four-dimensional $\mathcal{N} = 4$ Yang–Mills theories [26] and to $\mathcal{W}$ algebras.

Concretely, this thesis is based on the papers [33] and [32]. In this introduction, we will review the main physics actors – a limit of string theory called 'little string theory' ([53, 59, 40]; see [7] for a review) and a related particle theory called the '6d (2,0) superconformal field theory' [59]. At the end, we will recall the description of two-dimensional surface defects in 4d $\mathcal{N} = 4$ SYM given by Gukov and Witten in [26].

In chapter 2, we will first review the results of [3], and understand how to construct codimension-two defects of little string theory. Then we will study their relations to Gukov–Witten type surface defects and derive their S-duality transformation from the string theory setup. This chapter is based on [33].

In chapter 3, we will relate the little string defects to parabolic subalgebras of simple Lie algebras, and we will study the physical objects in which they appear. This chapter is based on [33].

In chapter 4, we will finally introduce nilpotent orbits, and we will see how they relate to

our defects. In chapter 5, the defects are related to $\mathcal{W}$ algebras, and we will study how the nilpotent orbits fit into that picture. In chapter 6, we analyze the difference between defects of the little string and defects of the SCFT. In chapter 7, we will study many examples. All of these chapters are also based on [33].

In chapter 8, we will give a more direct interpretation of the relation between little string defects and nilpotent orbits by using *Bala-Carter theory*. In chapter 9, we will study how our classification relates to weighted Dynkin diagrams, and give a physical interpretation of a dimension formula for nilpotent orbits. Finally, in appendix A, we give a complete list of little string defects for the exceptional algebras E_6, E_7 and E_8. These chapters are based on [32].

Finally, in chapter 10, we give an outlook to future work and directions.

1.1 Little string theory

In this section, we will review constructions of two six-dimensional 'little' string theories with 16 preserved supercharges. These were first introduced in [53] by considering type II string theory in the presence of k parallel NS5 branes: In this setup, we take the $g_s \to 0$ limit, where g_s is the string coupling constant. Because g_s is a factor in the gravitaton vertex operator (which is fixed by unitarity), this turns off gravitational interactions (from a low-energy point of view, this can also be seen by considering the coupling constant of the supergravity action).

Interestingly, this limit does not lead to a trivial theory: The theory on the NS5 branes decouples, and the strings on the world-volume give rise to a non-local, but non-gravitational theory:

In type IIA theory, the NS5 branes preserve six-dimensional $(2,0)$ supersymmetry, and support the $(2,0)$ *little string theory*. In type IIB, the worldvolume theory has $(1,1)$ supersymmetry and is T-dual to the $(2,0)$ theory – we call this the $(1,1)$ *little string theory*.

By using the results of [50], the k parallel NS5 branes (on a transverse circle, which doesn't play a role here) are T-dual to an A_{k-1} singularity. This allows us to generalize these A_{k-1} *little string theories* to an ADE classification, and to introduce additional branes:

$(2,0)$ ADE Little String Theory

The ADE little string theory with $(2,0)$ supersymmetry is a six dimensional string theory, and therefore has 16 supercharges. It is obtained by sending the string coupling g_s to zero in type IIB string theory on an ADE surface X; this has the effect of decoupling the bulk modes of the full type IIB string theory. X is a hyperkähler manifold, obtained by resolving a $\mathbb{C}^2/\Gamma$ singularity where Γ is a discrete subgroup of $SU(2)$, related to $\mathbf{g}$ by the McKay correspondence [51]. As mentioned, the little string is not a local QFT – it has a T-dual, and the strings have a tension m_s^2. The moduli space of the little string is $(\mathbb{R}^4 \times S^1)^{\mathrm{rk}(\mathfrak{g})}/W$, with W the Weyl group of $\mathfrak{g}$. The scalars parametrizing this moduli space come from the periods of the NS B-field $m_s^2/g_s \int_{S_a} B_{NS}$, the RR B-field $m_s^2 \int_{S_a} B_{RR}$, and a triplet of self-dual

two-forms obtained from deformations of the metric on X, $m_s^4/g_s \int_{S_a} \omega_{I,J,K}$. Here, S_a are two-cycles generating the homology group $H_2(X,\mathbb{Z})$. The $(S^1)^{\mathrm{rk}(\mathfrak{g})}$ have radius m_s^2 and are parametrized by the periods of B_{RR}. When g_s is sent to zero, we keep the above periods fixed in that limit. We set for all a's

$$\int_{S_a} \omega_{J,K} = 0, \ \int_{S_a} B_{NS} = 0, \tag{1.1}$$

and let

$$\tau_a = \int_{S_a} (m_s^2 \, \omega_I/g_s + i \, B_{RR}) \tag{1.2}$$

be arbitrary complex numbers with $\mathrm{R}e(\tau_a) > 0$.

1.2 Six-Dimensional $(2,0)$ Superconformal Field Theory

As mentioned above, the low-energy description of little string theory, for energies well below m_s, becomes a superconformal field theory (note that six is the highest dimension supporting a superconformal algebra). The $(1,1)$ little string simply becomes 6d $\mathcal{N} = (1,1)$ Super Yang–Mills theory.

Unfortunately, the limit of the $(2,0)$ little string is harder to understand. Its superconformal symmetry is $OSp(6,2|2) \supset O(2,8) \times Sp(2)_R$,[1] where the R symmetry $Sp(2)_R \cong SO(5)_R$ comes from the rotations transverse to the NS5 branes. In M-theory, it can be understood as the worldvolume theory of parallel M5 branes. M2 branes stretching between them give rise to strings in the 6d theory, which have to be tensionless (we can't have a dimensionful parameter).

Notably, this theory has $O(k^3)$ degrees of freedom (as can be shown by calculating the free energy [42]), and a two-form potential with self-dual field strength. This couples to the tensionless strings, but unfortunately, due to the presence of this field, there is no known Lagrangian description of these theories. Fortunately, its compactifications are much simpler: On an S^1, the theory already reduces to $5d$ maximally supersymmetric Yang-Mills theory.

For more information about this theory, and some interesting relations to the geometric Langlands correspondence, see [57].

1.3 Gukov–Witten Surface Defects of $\mathcal{N} = 4$ SYM

Surface defects of $\mathcal{N} = 4$ SYM are $\frac{1}{2}$-BPS operators; to describe them, one starts with a four-dimensional manifold M, which is locally $M = D \times D'$, where D is two-dimensional, and

[1] We're using the convention where the real dimension of $Sp(n)$ is $n(2n+1)$.

D' is a fiber to the normal bundle to D. Surface defects are then codimension-two objects living on D, and located at a point on D'; they are introduced by specifying the singular behavior of the gauge field near this defect. A surface operator naturally breaks the gauge group G to a subgroup $\mathbb{L} \subset G$, called a Levi subgroup.

The story so far is in fact valid for $\mathcal{N} = 2$ SUSY, but $\mathcal{N} = 4$ SUSY has additional parameters $\vec{\beta}$ and $\vec{\gamma}$, which describe the singular behavior of the Higgs field ϕ near the surface operator; choosing $D' = \mathbb{C}$ with coordinate $z = re^{i\theta} = x_2 + ix_3$, we have:

$$A = \vec{\alpha} d\theta + \dots, \tag{1.3}$$

$$\phi = \frac{1}{2}\left(\vec{\beta} + i\vec{\gamma}\right)\frac{dz}{z} + \dots, \tag{1.4}$$

which solve the Hitchin equations [35]:

$$F = [\phi, \overline{\phi}], \tag{1.5}$$

$$\overline{D}_z \phi = 0 = D_z \overline{\phi}. \tag{1.6}$$

As written above, we have chosen a complex structure which depends holomorphically on $\beta + i\gamma$, while the Kähler structure depends on α. Quantum mechanics also requires the consideration of the Theta angle, denoted by η; by supersymmetry, it will complexify the Kähler parameter α.

S-duality is the statement that this theory is equivalent to $\mathcal{N} = 4$ gauge theory with a dual gauge group and coupling constant

$$g'_{4d} = 1/g_{4d}.$$

The action of S-duality on the surface defect parameters is a rescaling of the Higgs field residue

$$(\beta, \gamma) \to \left(\frac{4\pi}{g^2_{4d}}\right)(\beta, \gamma), \tag{1.7}$$

and an exchange of the gauge field and Theta angle parameters [26]

$$(\alpha, \eta) \to (\eta, -\alpha). \tag{1.8}$$

The analysis of [26] gives a second description of the surface operators of $\mathcal{N} = 4$ SYM, which will be of great relevance to us; one couples the 4d theory to a 2d non-linear sigma model on D. In the $\mathcal{N} = 4$ case, the 2d theory is a sigma model to $T^*(G/\mathcal{P})$, where $\mathcal{P} \subset G$ is a parabolic subgroup of the Lie group. The quotient describes a partial flag manifold when the Lie algebra $\mathfrak{g}$ is A_n. In the case of a general Lie algebra, the quotient is a generalized flag variety. This target space is in fact the moduli space of solutions to the Hitchin equations (1.5).

Then, to describe a surface operator, one can either specify the parameters (β, γ, α) for the singular Higgs and gauge fields, or spell out the sigma model $T^*(G/\mathcal{P})$. It turns out that both of these descriptions have an origin in string theory, and we will now show this explicitly; our starting point will be the $(2, 0)$ little string theory.

Chapter 2

SYM Surface Defects From Little String Theory

Let's review the analysis of little string theory on a Riemann surface [3], and use it to describe these surface defects and derive their S-duality transformation.

2.1 Little String on a Riemann surface and D5 Branes

We start by compactifying the $(2,0)$ little string theory on a fixed Riemann surface $\mathcal{C}$, which is chosen to have a flat metric. This guarantees $X \times \mathcal{C}$ to be a solution of type IIB string theory. We want to introduce codimension-two defects in the little string, at points on $\mathcal{C}$ and filling the four remaining directions $\mathbb{C}^2$. These correspond to D5 branes in IIB string theory, wrapping non-compact 2-cycles in X and $\mathbb{C}^2$ [3]. Their tension remains finite in the little string limit, so they are the correct objects to study (D3 branes also keep finite tension, but they do not describe the codimension-two defects we are after; other objects of type IIB either decouple or get infinite tension when $g_s \to 0$).

In [3], it is argued that the dynamics of the $(2,0)$ little string theory on $\mathcal{C} \times \mathbb{C}^2$, with an arbitrary collection of D5 brane defects at points on $\mathcal{C}$, is captured by the theory on the branes themselves. Because the Riemann surface $\mathcal{C}$, which is transverse to the D5 branes, has a flat metric, the theory on the D5 branes is four dimensional at low energies. In fact, it has 4d $\mathcal{N} = 2$ super Poincare invariance, since the D5 branes break half the supersymmetry. We will focus specifically on the class of D5 branes that retain some conformal invariance in the resulting low energy 4d theory. This corresponds to a very specific choice of non-compact 2 cycles of X wrapped by the D5 branes, which we review here. For definiteness, we will choose the Riemann surface $\mathcal{C}$ to be the complex plane in what follows (one could equally choose to work on the cylinder as in [3], or on the torus.) The four-dimensional theory on the D5 branes is a quiver gauge theory, of shape the Dynkin diagram of $\mathfrak{g}$ [22]. The 4d gauge couplings are the τ_a defined in equation (1.2), which are the moduli of the $(2,0)$ theory in

6d. The masses of fundamental hypermultiplets are the positions of the D5 branes on $\mathcal{C}$ wrapping non-compact two-cycles of X. Finally, the Coulomb moduli are the positions of the D5 branes on $\mathcal{C}$ wrapping compact two-cycles of X.

In order to specify a defect D5 brane charge, we pick a class $[S^*]$ corresponding to non-compact two-cycles in the relative homology $H_2(X, \partial X; \mathbb{Z}) = \Lambda_*$, which we identify with the (co-)weight lattice of $\mathbf{g}$:

$$[S^*] = -\sum_{a=1}^{n} m_a \, w_a \quad \in \Lambda_* \tag{2.1}$$

with non-negative integers m_a and fundamental weights w_a. A necessary condition for conformal invariance in 4d is that the net D5 brane flux vanishes at infinity. This constrains the form of the coefficients m_a. To satisfy the condition, we add D5 branes that wrap a compact homology class $[S]$ in $H_2(X, \mathbb{Z}) = \Lambda$, which we identify with the root lattice of $\mathbf{g}$:

$$[S] = \sum_{a=1}^{n} d_a \, e_a \quad \in \Lambda \tag{2.2}$$

with non-negative integers d_a and the simple roots e_a, such that

$$[S + S_*] = 0. \tag{2.3}$$

The vanishing of $S + S^*$ in homology is equivalent to vanishing of $\#(S_a \cap (S + S_*))$ for all a. We can therefore rewrite (2.3) as

$$\sum_{b=1}^{n} C_{ab} \, d_b = m_a \tag{2.4}$$

where C_{ab} is the Cartan matrix of $\mathfrak{g}$. On the Higgs branch of the low energy gauge theory, the gauge group $\prod_{a=1}^{n} U(d_a)$ is broken to its $U(1)$ centers, one for each node. There, the D5 branes wrapping the compact cycles S and the non-compact cycles S^* recombine to form D5 branes wrapping a collection of non-compact cycles S_i^*, whose homology classes are elements ω_i of the weight lattice $\Lambda^* = H_2(X, \partial X; \mathbb{Z})$:

$$\omega_i = [S_i^*] \qquad \in \Lambda^*. \tag{2.5}$$

It is these weights ω_i that will classify the defects of the little string. Each of the ω_i's comes from one of the non-compact D5 branes on S^*. The branes can bind when the positions on $\mathcal{C}$ of the compact branes coincides with the positions of one of the non-compact D5 branes. Recall that the positions of non-compact D5 branes are mass parameters of the quiver gauge theory, while the positions of compact D5 branes on $\mathcal{C}$ are Coulomb moduli; when a Coulomb modulus coincides with one of the masses, the corresponding fundamental hypermultiplet becomes massless and can get expectation values, describing the root of the Higgs branch. One can reasonably worry that the binding of the D5 branes will break supersymmetry, but

it is in fact preserved when one turns on the FI terms, which are the periods $\int_{S_a} \omega_{J,K}$, $\int_{S_a} B_{NS}$.

Then, the ω_i's can always be written as a negative fundamental weight $-w_a$ plus the sum of positive simple roots e_a, from bound compact branes. Not any such combination will correspond to truly bound branes: a sufficient condition is that ω_i is in the Weyl orbit of $-w_a = [S_a^*]$ (we will relax this condition in section 6.3 and end up with a new class of defects of the little string). Furthermore, the collection of weights

$$\mathcal{W}_{\mathcal{S}} = \{\omega_i\} \tag{2.6}$$

we get must be such that it accounts for all the D5 brane charges in $[S^*]$ and in $[S]$. One simple consequence is that the number of ω_i's is the total rank of the 4d flavor group, $\sum_{a=1}^{n} m_a$. The fact that the net D5 charge is zero, $[S + S^*] = 0$, implies that

$$\sum_{\omega_i \in \mathcal{W}_{\mathcal{S}}} \omega_i = 0,$$

which is equivalent to (2.4).

The most canonical type of defect is the one analyzed in [3], which makes use of the fact that the weight lattice of a Lie algebra of rank n is n-dimensional. Then we can construct a set $\mathcal{W}_{\mathcal{S}}$ by picking any $n+1$ weight vectors which lie in the Weyl group orbits of the fundamental weights $-w_a$ such that they sum up to zero and n of them span Λ_*. This leads to a full puncture defect of the $(2,0)$ little string on $\mathcal{C}$. The example below features $\mathfrak{g} = A_3$.

Example 2.1.1. Let us look at the set of all the weights in the antifundamental representation of A_3; these weights all add up to 0, and all weights are in the orbit of (minus) the fundamental weight $[-1,0,0]$, written in Dynkin labels, so this set defines a valid set $\mathcal{W}_{\mathcal{S}}$. Writing w_i for the i-th fundamental weight, we note that:

$$\begin{aligned}
\omega_1 &= [-1, \quad 0, \quad 0] = -w_1, \\
\omega_2 &= [\ \ 1, -1, \quad 0] = -w_1 + e_1, \\
\omega_3 &= [\ \ 0, \quad 1, -1] = -w_1 + e_1 + e_2, \\
\omega_4 &= [\ \ 0, \quad 0, \quad 1] = -w_1 + e_1 + e_2 + e_3.
\end{aligned}$$

Written in this fashion, the set $\mathcal{W}_{\mathcal{S}}$ defines a 4d quiver gauge theory, shown in Figure 2.1. This is called the full puncture.

The full classification of defects for simply-laced $\mathfrak{g}$ is obtained by constructing the set $\mathcal{W}_{\mathcal{S}}$ to have size $n+1$ *or less*. As we will explain in later sections, this is where the rich structure of the parabolic subalgebras of $\mathfrak{g}$ will emerge, and it will be our main object of study.

When the string scale m_s is taken to infinity, the $(2,0)$ little string reduces to the $(2,0)$ CFT of type $\mathfrak{g}$ compactified on $\mathcal{C}$; we lose the Lagrangian description in general, and the

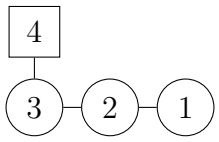

Figure 2.1: The quiver theory describing a full puncture for $\mathfrak{g} = A_3$

Coulomb branch dimension, previously equal to $\sum_{a=1}^{n} d_a$, generically decreases. This loss of Coulomb moduli is expected, as the theory loses degrees of freedom in the limit. This distinction in counting Coulomb moduli between the little string and CFT cases will be important to keep in mind throughout the rest of our discussion.

2.2 Little String Theory origin of SYM surface defects and S-duality

–Hitchin System and Higgs Field Data–

In the little string theory, the brane defects we are studying are solutions to Bogomolny equations on $\mathcal{C}$ times an extra circle $S^1(R_1)$ [3]:

$$D\phi = *F. \tag{2.7}$$

Little string theory enjoys T-duality, so in particular, the $(2,0)$ ADE Little String of type IIB compatified on $S^1(R_1)$ is dual to the (1,1) ADE Little String of type IIA compatified on $S^1(\hat{R}_1)$ of radius $\hat{R}_1 = 1/m_s^2 R_1$. The defects are then D4 branes after T-dualizing, and are points on $\mathcal{C} \times S^1(\hat{R}_1)$. These are monopoles, magnetically charged under the gauge field coming from the (1,1) little string. The n scalars are $\phi_a = \int_{S_a^2} m_s^3 \omega^I / g_s'$, where g_s' is the IIA string coupling, related to the IIB one by $1/g_s' = R_1 m_s / g_s$. F is the curvature of the gauge field coming from the (1,1) little string.

If we want to recover the original description of the defects as D5 branes, we can take the dual circle size $\hat{R}_1$ to be very small; the upshot is that the Bogomolny equations simplify and we recover the Hitchin equations (1.5) we considered previously:

$$F = [\phi, \overline{\phi}], \tag{2.8}$$

$$\overline{D}_z \phi = 0 = D_z \overline{\phi}. \tag{2.9}$$

A subtlety here is that the field ϕ got complexified in passing from D4 branes back to D5 branes. The imaginary part of ϕ is the holonomy of the (1,1) gauge field around $S^1(\hat{R}_1)$; this comes from the fact that the D4 branes are magnetically charged under the RR 3-form:

$R_1 \int_{S^2_a \times S^1(R_1)} m_s^2 \; C^{(3)}_{RR}$. In type IIB language, after T-duality, the D5 branes are charged under the RR 2-form instead: $1/\hat{R}_1 \int_{S^2_a} B_{RR}$. All in all, the Higgs field is then written in IIB variables as

$$\phi_a = (e_a, \phi) = 1/\hat{R}_1 \int_{S^2_a} (m_s^2 \omega_I / g_s + i B_{RR}) = \tau_a / \hat{R}_1. \tag{2.10}$$

The Seiberg-Witten curve of the quiver gauge theory on the D5 branes arises as the spectral curve of the Higgs field ϕ, taken in some representation $\mathfrak{R}$ of $\mathfrak{g}$:

$$\det{}_{\mathfrak{R}}(e^{\hat{R}_1 \phi} - e^{\hat{R}_1 p}) = 0. \tag{2.11}$$

In the absence of monopoles, ϕ is constant: the vacuum expectation value of the Higgs field is $\hat{R}_1 \phi = \tau$.

By construction, then, the Coulomb branch of the ADE quiver theory on the D5 branes is the moduli space of monopoles on $\mathcal{C} \times S^1(\hat{R}_1)$. As we described in the previous section, we ultimately want to go on the Higgs branch of the theory, where we get a description of quiver theories as a fixed set of weights $\mathcal{W}_{\mathcal{S}}$ in $\mathfrak{g}$; there, all the non-abelian monopoles reduce to Dirac monopoles. The effect on ϕ of adding a Dirac monopole of charge $\omega_i^\vee$, at a point $x_i = \hat{R}_1 \hat{\beta}_i$ on $\mathcal{C}$, is to shift:

$$e^{\hat{R}_1 \phi} \to e^{\hat{R}_1 \phi} \cdot (1 - z \, e^{-\hat{R}_1 \hat{\beta}_i})^{-w_i^\vee}. \tag{2.12}$$

Here, z is the complex coordinate on $\mathcal{C} = \mathbb{C}$. Thus, the Higgs field solving the Hitchin equations at the point where the Higgs and the Coulomb branches meet is

$$e^{\hat{R}_1 \phi(x)} = e^{\tau} \prod_{\omega_i^V \in \mathcal{W}_{\mathcal{S}}} (1 - z \, e^{-\hat{R}_1 \hat{\beta}_i})^{-\omega_i^\vee}. \tag{2.13}$$

To take the string mass m_s to infinity, we relabel $e^{\hat{R}_1 \hat{\beta}_i} = z_{\mathcal{P}} \, e^{\hat{R}_1 \alpha_{i,\mathcal{P}}}$. We can then safely take the limit $\hat{R}_1 \to 0$; the imaginary part of ϕ decompactifies, and equation (2.11) becomes the spectral curve of the Hitchin integrable system [24]:

$$\det{}_{\mathfrak{R}}(\phi - p) = 0. \tag{2.14}$$

In this limit, the Higgs field near a puncture of $\mathcal{C}$ has a pole of order one, and takes the form

$$\phi(z) = \frac{\alpha_0}{z} + \sum_{\mathcal{P}} \sum_{\omega_i \in \mathcal{W}_{\mathcal{P}}} \frac{\alpha_{i,\mathcal{P}} \, \omega_i^\vee}{z_{\mathcal{P}} - z}, \tag{2.15}$$

with $\alpha_0 = \tau / \hat{R}_1$ and $\mathcal{P}$ the set of punctures. Therefore, in the $(2,0)$ CFT, we have poles on $\mathcal{C}$ at $z = z_{\mathcal{P}}$, with residues

$$\alpha_{\mathcal{P}} = \sum_{\omega_i \in \mathcal{W}_{\mathcal{P}}} \alpha_{i,\mathcal{P}} \, \omega_i^\vee.$$

These residues are what we called $\beta + i\gamma$ in the $\mathcal{N} = 4$ SYM setup of eq. (1.4).

– 4d S-duality is T-duality of the Little String–

To provide evidence that the surface defects of $\mathcal{N} = 4$ SYM really are branes at points on $\mathcal{C}$ in the $(2, 0)$ little string, we now derive four-dimensional S-duality from T-duality of the string theory, compactified on an additional torus T^2. Here, T^2 is the product of two S^1's, one from each of the two complex planes $\mathbb{C}^2$. We label those circles as $S^1(R_1)$ and $S^1(R_2)$, of radius R_1 and R_2 respectively.

$$\boxed{(1,1) \text{ string on } S^1(\hat{R}_1) \times S^1(R_2) \times \mathbb{R}^2 \times \mathcal{C} \text{ with } (\text{D4}, \text{D4}) \text{ branes}}$$
$$\updownarrow\ T_1\text{-duality}$$
$$\boxed{(2,0) \text{ string on } S^1(R_1) \times S^1(R_2) \times \mathbb{R}^2 \times \mathcal{C} \text{ with } (\text{D3}, \text{D5}) \text{ branes}}$$
$$\updownarrow\ T_2\text{-duality}$$
$$\boxed{(1,1) \text{ string on } S^1(R_1) \times S^1(\hat{R}_2) \times \mathbb{R}^2 \times \mathcal{C} \text{ with } (\text{D4}, \text{D4}) \text{ branes}}$$

Figure 2.2: One starts with the $(1, 1)$ little string theory on $T^2 \times \mathbb{R}^2 \times \mathcal{C}$. After doing two T-dualities in the torus directions, we get the $(1, 1)$ little string theory on the T-dual torus; in the low energy limit, the pair of $(1, 1)$ theories gives an S-dual pair of $\mathcal{N} = 4$ SYM theories. D3 branes at a point on T^2 map to D4 branes in either $(1, 1)$ theory, while D5 branes wrapping T^2 map to another set of D4 branes.

First, without any D5 branes, S-duality was derived in [56], and the line of reasoning went as follows: suppose we first compactify on, say, $S^1(R_1)$; this is what we just did in the previous section to make contact with D4 branes as magnetic monopoles. Then we are equivalently studying the (1,1) little string on $S^1(\hat{R}_1)$. Compactifying further on $S^1(R_2)$, this theory is the same as the (1,1) little string on $S^1(R_1) \times S^1(\hat{R}_2)$, by T^2-duality. 4d SYM S-duality then naturally follows from the T^2-duality of this pair of (1,1) theories. Indeed, at low energies, both $(1, 1)$ little string theories become the maximally supersymmetric 6d SYM, with gauge group dictated by $\mathfrak{g}$ and gauge coupling $1/g_{6d}^2 = m_s^2$. We wish to take the string scale m_s to infinity; in the case of the $(1, 1)$ string on $S^1(\hat{R}_1)$, since $m_s^2 \hat{R}_1 = 1/R_1$, the radius $\hat{R}_1$ goes to 0 in that limit. The theory then becomes 5d $\mathcal{N} = 2$ SYM, with inverse gauge coupling $1/g_{5d}^2 = 1/R_1$. After the further compactification on $S^1(R_2)$, we obtain at low energies 4d $\mathcal{N} = 4$ SYM, with inverse gauge coupling $1/g_{4d}^2 = R_2/g_{5d}^2 = R_2/R_1$.

Now, the same reasoning applied to the T^2-dual theory $S^1(R_1) \times S^1(\hat{R}_2)$ gives 4d $\mathcal{N} = 4$ SYM in the m_s to infinity limit, with inverse gauge coupling $1/g_{4d}'^2 = R_1/R_2$.

Note that $1/g'_{4d} = g_{4d}$. This is just the action of S-duality on the gauge coupling of $\mathcal{N} = 4$ SYM. Writing $R_2/R_1 \equiv \text{Im}(\tau')$, with τ' the modular parameter of the T^2, we see

that S-duality is a consequence of T^2-duality for the pair of $(1,1)$ little string theories. An illustration of the dualities is shown in Figure 2.2.

Now, we extend this argument and introduce the D5 brane defects; since the D5 branes were initially wrapping $T^2 \times \mathbb{C}$, note that we can equivalently consider the defects to be D3 branes at a point on T^2. We now argue that the S-duality action on the half BPS surface defects of SYM has its origin in the same T^2-duality of $(1,1)$ theories we presented in the previous paragraph.

First, recall that after $S^1(R_1)$ compactification, the D5 branes are charged magnetically, with period:

$$\phi_a = 1/\hat{R}_1 \int_{S_a} (m_s^2 \omega_I / g_s + i B_{RR}).$$

In type IIB variables, we call this period $\beta + i\gamma$. By T-dualizing along $S^1(R_1)$ we obtain D4 branes wrapping $S^1(R_2)$ in the $(1,1)$ little string. Now suppose we T-dualize the D5 branes along $S^1(R_2)$ instead; then we have D4 branes wrapping $S^1(R_1)$, in the T^2-dual $(1,1)$ little string. The D4 brane tensions in both $(1,1)$ theories are proportional to each other, with factor R_2/R_1. But then $(\beta,\gamma) \to R_2/R_1\,(\beta,\gamma)$ after T^2-duality. The D4 branes are then heavy, magnetic objects in one $(1,1)$ theory, while they are light, electric objects in the other. In the $m_s \to \infty$ limit, (β,γ) are the parameters of the Higgs field in 4d SYM. This is precisely the action of S-duality for the Higgs field data: $(\beta,\gamma) \to \mathrm{Im}(\tau')(\beta,\gamma)$ (1.7).

Second, after T^2 compactification, the D3 branes, which are points on T^2, are charged under the RR 4-form: $\int_{S_a \times \widetilde{S^1} \times S^1(R_1)} C^{(4)}_{RR}$, where $\widetilde{S^1}$ is a circle around the point defect on $\mathcal{C}$. As before, $S^1(R_1)$ is one of the 1-cycles of T^2, and S_a is a compact 2-cycle in the ALE space X. We call this period α. The D3 branes are also charged under $\int_{S_a \times \widetilde{S^1} \times S^1(R_2)} C^{(4)}_{RR}$, where $S^1(R_2)$ is the other 1-cycle of T^2; we call this period η.

Suppose we T-dualize in the $S^1(R_1)$ direction. Then α becomes the period of the RR 3-form on $S_a \times \widetilde{S^1}$; this period is in fact an electric coupling for the holonomy of the $(1,1)$ gauge field around $\widetilde{S^1}$. Also, η becomes the period of the RR 5-form on $S_a \times \widetilde{S^1} \times S^1(R_2) \times S^1(\hat{R}_1)$; this period is in fact a magnetic coupling for the holonomy of the $(1,1)$ gauge field around $\widetilde{S^1}$. T-dualizing on $S^1(R_2)$ instead, we reach the T^2-dual $(1,1)$ theory. We see that α gets mapped to η, while η gets mapped to $-\alpha$ (the minus sign arises because the 5-form is antisymmetric). So in the end, under T^2-duality, the periods change as $(\alpha,\eta) \to (\eta,-\alpha)$.

Note that because the 1-cycles generating the T^2 appear explicitly in the definition of these periods, T^2-duality does not amount to a simple rescaling of (α,η), as was the case for (β,γ). In the low energy limit, we recover the S-duality of the gauge field and Theta angle parameters of 4d SYM α and η in the presence of a defect (1.8).

– $T^*(G/\mathcal{P})$ sigma model and Coulomb branch of the Defect Theory–

We made contact with the surface defects of Gukov and Witten after compactifying the $(2,0)$ little string on T^2 and T-dualizing the D5 branes to D3 branes. In this process, as long as m_s is kept finite, the 4d ADE quiver gauge theory that describes the D5 branes at low energies simply becomes a two-dimensional quiver theory for the D3 branes, with the same gauge gauge groups and fundamental matter. In the rest of this paper, we will label this low energy ADE quiver theory on the D3 branes, together with the set of weights $\mathcal{W}_{\mathcal{S}}$ that specified it, as T^{2d}. In the CFT limit, we will label the theory as $T^{2d}_{m_s\to\infty}$. As we mentioned already, unlike T^{2d}, the theory $T^{2d}_{m_s\to\infty}$ generically has no Lagrangian description.

Now, Gukov and Witten showed that surface operators of $\mathcal{N}=4$ SYM can also be described by a 2d sigma model $T^*(G/\mathcal{P})$, which then coincides with the moduli space of solutions to the Hitchin equations (1.5). After taking the CFT limit of the little string theory, we saw that this moduli space is also the Coulomb branch of the $(2,0)$ CFT theory on the Riemann surface $\mathcal{C}$ times a circle $S^1(R_1)$ (the radius R_1 here being very big). As an algebraic variety, this Coulomb branch is singular, while $T^*(G/\mathcal{P})$ is smooth. The statement is then that the (resolution of the) Coulomb branch of the 2d ADE quiver gauge theories on the D3 branes we presented, in the appropriate m_s to infinity limit, is expected to be the sigma model to $T^*(G/\mathcal{P})$. In other terms, the Coulomb branch of $T^{2d}_{m_s\to\infty}$ can be identified with $T^*(G/\mathcal{P})$.

A natural question arises: how do parabolic subgroups $\mathcal{P}$ in $T^*(G/\mathcal{P})$ arise from the point of view of the defects of the $(2,0)$ little string?

We will now see that to every ADE theory T^{2d} on the D3 branes, we will be able to associate a unique parabolic subalgebra from the geometry (specifically, the non-compact 2-cycles of X), or equivalently, from the representation theory of $\mathfrak{g}$ (the Higgs field we introduced is valued in the Lie algebra $\mathfrak{g}$, so we will speak of parabolic subalgebras rather than parabolic subgroups); in particular, after taking the CFT limit, we will be able to read it from the data of the weight system $\mathcal{W}_{\mathcal{S}}$ that defines the theory $T^{2d}_{m_s\to\infty}$.

As a side note, it is known ([17, 25, 28, 20]) that $T^*(G/\mathcal{P})$ is the resolution of the Higgs branch of different theories from the ones we have been considering. In the little string setup, as we reviewed, the moduli space of monopoles naturally arises as a Coulomb branch instead of a Higgs branch. A natural guess is that those two descriptions could be related by mirror symmetry, and this is indeed the case in all the cases we could explicitly check (all defects in the A_n case, and some low rank defects in the D_n case; see also [27]). We will not investigate this point further here, but it would be important to get a clear understanding of the mirror map.

Chapter 3

From Brane Defects to Parabolic Subalgebras

We now explain how the ADE quiver theories T^{2d} determine the parabolic subalgebras of $\mathfrak{g}$.

3.1 Mathematics Preliminaries

Because they will be so crucial to our story, we review here the mathematics of parabolic and Levi subalgebras of a Lie algebra $\mathfrak{g}$.

A *Borel subalgebra* of $\mathfrak{g}$ is a maximal solvable subalgebra of $\mathfrak{g}$, and always has the form $\mathfrak{b} = \mathfrak{h} \oplus \mathfrak{m}$, where $\mathfrak{h}$ is a Cartan subalgebra of $\mathfrak{g}$ and $\mathfrak{m} = \sum_{\alpha \in \Phi^+} \mathfrak{g}_\alpha$ for some choice of positive roots Φ^+. A *parabolic subalgebra* $\mathfrak{p}$ is defined to be a subalgebra of $\mathfrak{g}$ that contains a Borel subalgebra $\mathfrak{b}$, so $\mathfrak{b} \subseteq \mathfrak{p} \subseteq \mathfrak{g}$.

There are many different choices of Borel subalgebras of $\mathfrak{g}$, but we will choose one for each $\mathfrak{g}$ and keep it fixed. Since the Borel subalgebra is the sum of all the positive root spaces, we can get any $\mathfrak{p}$ by adding the root spaces associated to any closed system of negative roots.

Let us extend our notations to differentiate between distinct parabolic subalgebras: We denote the set of positive simple roots by Δ. Take an arbitrary subset $\Theta \subset \Delta$. We define $\mathfrak{p}_\Theta$ to be the subalgebra of $\mathfrak{g}$ generated by $\mathfrak{h}$ and all of the root spaces $\mathfrak{g}_\alpha$, with $\alpha \in \Delta$ or $-\alpha \in \Theta$. Then $\mathfrak{p}_\Theta$ is a parabolic subalgebra of $\mathfrak{g}$ containing $\mathfrak{b}$, and every parabolic subalgebra of $\mathfrak{g}$ containing $\mathfrak{b}$ is of the form $\mathfrak{p}_\Theta$ for some $\Theta \subset \Delta$. In fact, every parabolic subalgebra of $\mathfrak{g}$ is conjugate to one of the form $\mathfrak{p}_\Theta$ for some $\Theta \subset \Delta$. We state the important result:

Let $\langle \Theta \rangle$ denote the subroot system generated by Θ and write $\langle \Theta \rangle^+ = \langle \Theta \rangle \cap \Phi^+$. There is a *direct sum decomposition* $\mathfrak{p}_\Theta = \mathfrak{l}_\Theta \oplus \mathfrak{n}_\Theta$, where $\mathfrak{l}_\Theta = \mathfrak{h} \oplus \sum_{\alpha \in \langle \Theta \rangle} \mathfrak{g}_\alpha$ is a reductive subalgebra (a reductive Lie algebra is a direct sum of a semi-simple and an abelian Lie algebra), called a Levi

subalgebra, and $\mathfrak{n}_\Theta = \sum_{\alpha\in\Phi^+\setminus\langle\Theta\rangle^+}\mathfrak{g}_\alpha$, is called the nilradical of $\mathfrak{p}_\Theta$. Here, $\alpha\in\Phi^+\setminus\langle\Theta\rangle^+$ means that α is a positive root not in $\langle\Theta\rangle^+$. Note that $\mathfrak{n}_\Theta \cong \sum_{\alpha\in\Phi^-\setminus\langle\Theta\rangle^-}\mathfrak{g}_\alpha \cong \mathfrak{g}/\mathfrak{p}_\Theta$. Furthermore, all Levi subalgebras of a given parabolic subalgebra are conjugate to each other [41]. We illustrate the above statements in the examples below:

Example 3.1.1. Consider $\mathfrak{g} = A_2$ in the fundamental, three-dimensional representation. Then the elements in the Cartan subalgebra have the form

$$\mathfrak{h} = \begin{pmatrix} * & 0 & 0 \\ 0 & * & 0 \\ 0 & 0 & * \end{pmatrix}. \tag{3.1}$$

We associate to a root $\alpha_{ij} = h_i - h_j$ the space $\mathbb{C}E_{ij}$, where E_{ij} is the matrix that has a $+1$ in the i-th row and j-th column, and zeroes everywhere else. Thus, we see that

$$\mathfrak{b} = \begin{pmatrix} * & * & * \\ 0 & * & * \\ 0 & 0 & * \end{pmatrix}, \tag{3.2}$$

and the parabolic subalgebras are

$$\mathfrak{p}_\varnothing = \mathfrak{b} = \begin{pmatrix} * & * & * \\ 0 & * & * \\ 0 & 0 & * \end{pmatrix}, \tag{3.3}$$

$$\mathfrak{p}_{\{\alpha_1\}} = \begin{pmatrix} * & * & * \\ * & * & * \\ 0 & 0 & * \end{pmatrix}, \tag{3.4}$$

$$\mathfrak{p}_{\{\alpha_2\}} = \begin{pmatrix} * & * & * \\ 0 & * & * \\ 0 & * & * \end{pmatrix}, \tag{3.5}$$

$$\mathfrak{p}_{\{\alpha_1,\alpha_2\}} = \mathfrak{g} = \begin{pmatrix} * & * & * \\ * & * & * \\ * & * & * \end{pmatrix}. \tag{3.6}$$

Let us look at the Levi decompositions of the above:

Example 3.1.2. For $\mathfrak{g} = A_2$, we get the following decompositions:

$$\mathfrak{p}_{\varnothing} = \begin{pmatrix} * & * & * \\ 0 & * & * \\ 0 & 0 & * \end{pmatrix} = \begin{pmatrix} * & 0 & 0 \\ 0 & * & 0 \\ 0 & 0 & * \end{pmatrix} \oplus \begin{pmatrix} 0 & * & * \\ 0 & 0 & * \\ 0 & 0 & 0 \end{pmatrix} = \mathfrak{l}_{\varnothing} \oplus \mathfrak{n}_{\varnothing}, \tag{3.7}$$

$$\mathfrak{p}_{\{\alpha_1\}} = \begin{pmatrix} * & * & * \\ * & * & * \\ 0 & 0 & * \end{pmatrix} = \begin{pmatrix} * & * & 0 \\ * & * & 0 \\ 0 & 0 & * \end{pmatrix} \oplus \begin{pmatrix} 0 & 0 & * \\ 0 & 0 & * \\ 0 & 0 & 0 \end{pmatrix} = \mathfrak{l}_{\{\alpha_1\}} \oplus \mathfrak{n}_{\{\alpha_1\}}, \tag{3.8}$$

$$\mathfrak{p}_{\{\alpha_2\}} = \begin{pmatrix} * & * & * \\ 0 & * & * \\ 0 & * & * \end{pmatrix} = \begin{pmatrix} * & 0 & 0 \\ 0 & * & * \\ 0 & * & * \end{pmatrix} \oplus \begin{pmatrix} 0 & * & * \\ 0 & 0 & 0 \\ 0 & 0 & 0 \end{pmatrix} = \mathfrak{l}_{\{\alpha_2\}} \oplus \mathfrak{n}_{\{\alpha_2\}}, \tag{3.9}$$

$$\mathfrak{p}_{\{\alpha_1,\alpha_2\}} = \begin{pmatrix} * & * & * \\ * & * & * \\ * & * & * \end{pmatrix} = \begin{pmatrix} * & * & * \\ * & * & * \\ * & * & * \end{pmatrix} \oplus \begin{pmatrix} 0 & 0 & 0 \\ 0 & 0 & 0 \\ 0 & 0 & 0 \end{pmatrix} = \mathfrak{l}_{\{\alpha_1,\alpha_2\}} \oplus \mathfrak{n}_{\{\alpha_1,\alpha_2\}}. \tag{3.10}$$

Example 3.1.3. In the table below, we show the root spaces that the Borel subalgebra of A_3 is made of:

Θ	$\mathfrak{p}_\Theta$	$\mathfrak{l}_\Theta$	$\mathfrak{n}_\Theta$
$\varnothing$	$\begin{pmatrix} * & * & * & * \\ 0 & * & * & * \\ 0 & 0 & * & * \\ 0 & 0 & 0 & * \end{pmatrix}$	$\begin{pmatrix} * & 0 & 0 & 0 \\ 0 & * & 0 & 0 \\ 0 & 0 & * & 0 \\ 0 & 0 & 0 & * \end{pmatrix}$	$\begin{pmatrix} 0 & * & * & * \\ 0 & 0 & * & * \\ 0 & 0 & 0 & * \\ 0 & 0 & 0 & 0 \end{pmatrix}$

: α_1 : $(\alpha_1 + \alpha_2)$:$(\alpha_1 + \alpha_2 + \alpha_3)$
: α_2 : $(\alpha_2 + \alpha_3)$
: α_3

Table 3.1: This table illustrates the Levi decomposition of fp_Θ, when Θ is the empty set and $\mathfrak{g} = A_3$. $\mathfrak{p}_\Theta$ consists of all the matrices in A_3 with zeroes in the indicated places and the other entries are arbitrary. The color code shows which positive root is denoted by which nonzero entry.

3.2 Parabolic Subalgebras from Weight Data

We reviewed in chapter 2 how we could specify a defect of the little string from a set of weights

$$\mathcal{W}_{\mathcal{S}} = \{\omega_i\}, \tag{3.11}$$

all in the orbit of some (possibly different) fundamental weights, and adding up to 0. We make the claim that to each parabolic subalgebra of $\mathfrak{g}$ we can associate such a set; the map is many-to-one, as many different sets $\mathcal{W}_\mathcal{S}$ will typically determine one and the same parabolic subalgebra.

Our strategy will be to extract a nilradical of the algebra from a given $\mathcal{W}_\mathcal{S}$. We do so by first computing the inner product $\langle e_\gamma, \omega_i \rangle$, for all weights ω_i in $\mathcal{W}_\mathcal{S}$, and for all positive roots e_γ of $\mathfrak{g}$. Here, $\langle \cdot, \cdot \rangle$ denotes the Killing form of $\mathfrak{g}$. The postive roots e_γ that satisfy

$$\langle e_\gamma, \omega_i \rangle < 0, \tag{3.12}$$ [1]

for at least one $\omega_i \in \mathcal{W}_\mathcal{S}$, form a set, which we call $\tilde{\Phi}$. The root spaces associated to these $e_\gamma \in \tilde{\Phi}$ make up a nilradical $\mathfrak{n}$.

We claim that for each parabolic subalgebra $\mathfrak{p}$, there exists at least one set $\mathcal{W}_\mathcal{S}$ from which we can read off a set of positive roots $\tilde{\Phi}$ that defines the nilradical $\mathfrak{n} = \mathfrak{g}/\mathfrak{p}$ of the algebra as above. In fact, $\mathfrak{n}$ specifies the Coulomb branch of $T^{2d}_{m_s \to \infty}$.

This nilradical can always be obtained from the Levi decomposition $\mathfrak{p}_\Theta = \mathfrak{l}_\Theta \oplus \mathfrak{n}_\Theta$ of some parabolic algebra $\mathfrak{p}_\Theta$, which we now index by positive *simple* roots (recall from our definitions that Θ is taken in the set of positive simple roots Δ). In the notation of section 3.1, we write $\tilde{\Phi} = \langle \Theta \rangle^+$.

As mentioned already, we emphasize here that the Coulomb branch of T^{2d} is generically bigger than the Coulomb branch of $T^{2d}_{m_s \to \infty}$. In the little string case, the Coulomb branch of T^{2d} has dimension $\sum_{a=1}^n d_a$, where d_a are the ranks of the gauge groups (here, we include the $U(1)$ centers of the $U(d_a)$ gauge groups). In the CFT limit, the space $X \times \mathcal{C}$ can be reinterpreted as a Calabi–Yau manifold. Thus, one can use the techniques of complex geometry to count the Coulomb moduli of $T^{2d}_{m_s \to \infty}$ as the complex structure deformations of this Calabi–Yau [14]. For instance, for $\mathcal{C}$ a sphere with 3 full punctures, meaning the residues of the Higgs fields $\phi(z)$ are generic, the dimension of the Coulomb branch of $T^{2d}_{m_s \to \infty}$ is the number $|\Phi^+|$ of positive roots of $\mathfrak{g}$. Note that for A_n, the full puncture of T^{2d} has Coulomb branch dimension $\sum_{a=1}^n d_a = |\Phi^+|$, so in that specific case the CFT counting is the same as the little string counting. This is generally not so for $\mathfrak{g} = D_n$ and E_n.

The dimension of $T^{2d}_{m_s \to \infty}$ can be conveniently recovered from the representation theory of $\mathfrak{g}$. Indeed, by just keeping track of which positive roots satisfy $\langle e_\gamma, \omega_i \rangle < 0$ for an $\omega_i \in \mathcal{W}_\mathcal{S}$, and not recording the actual value of the inner product, the positive roots are counting Coulomb moduli of the defect theory in the CFT limit. This point is irrelevant in the A_n case, but crucial in the D_n and E_n cases, where higher positive root multiplicity has to be ignored to identify a nilradical of $\mathfrak{g}$.

[1] Or equivalently, $\langle e_\gamma, \omega_i \rangle > 0$.

Example 3.2.1. From Table 3.1 above, we will read off a unique parabolic subalgebra from a set of weights $\mathcal{W}_{\mathcal{S}}$ for an A_3 theory. We choose $\mathcal{W}_{\mathcal{S}}$ to be the set of all four weights in the antifundamental representation (note that they add up to 0, as they should); they make up the full puncture of A_3. Next, we note the following:

$[-1, \ 0, \ 0]$ has a negative inner product with $h_1 - h_2, h_1 - h_3, h_1 - h_4$.
$[\ 1, -1, \ 0]$ has a negative inner product with $h_2 - h_3, h_2 - h_4$.
$[\ 0, \ 1, -1]$ has a negative inner product with $h_3 - h_4$.
$[\ 0, \ 0, \ 1]$ has no negative inner product with any of the positive roots.

We see that all positive roots of $\mathfrak{g}$ are accounted for, so the nilradical $\mathfrak{n}_\Theta$ is constructed using all the positive roots, and thus, $\Theta = \varnothing$. From the Levi decomposition, we therefore identify the parabolic subalgebra as $\mathfrak{p}_\varnothing$. This is summarized in Figure 3.1.

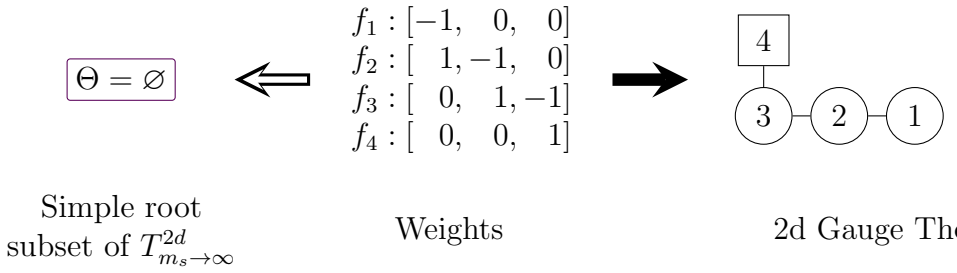

Figure 3.1: From the set of weights $\mathcal{W}_{\mathcal{S}}$, we read off the parabolic subalgebra $\mathfrak{p}_\varnothing$ of A_3 (in this case, the choice of weights is unique up to global $\mathbb{Z}_2$ action on the set). Reinterpreting each weight as a sum of "minus a fundamental weight and simple roots," we obtain the 2d quiver gauge theory shown on the right. The white arrow implies we take the CFT limit.

Example 3.2.2. As a nontrivial example, let us first study the set at the top of Figure 3.2 for $\mathfrak{g} = D_4$: $\mathcal{W}_{\mathcal{S}} = \{[-1, 0, 0, 0], [1, -1, 0, 0], [0, 1, 0, 0]\}$. Except for the two simple roots α_3 and α_4, all the other positive roots e_γ satisfy $\langle e_\gamma, \omega_i \rangle < 0$ for at least one $\omega_i \in \mathcal{W}_{\mathcal{S}}$. Indeed, it is easy to check that $\langle \alpha_3, \omega_i \rangle = 0 = \langle \alpha_4, \omega_i \rangle$ for all the $\omega_i \in \mathcal{W}_{\mathcal{S}}$; the set of positive roots we obtain defines the nilradical $\mathfrak{n}_{\{\alpha_3, \alpha_4\}}$. We then conclude from the Levi decomposition that $\mathcal{W}_{\mathcal{S}}$ characterizes the parabolic subalgebra $\mathfrak{p}_{\{\alpha_3, \alpha_4\}}$.

Now, in this example, we could have very well studied a different set:

$$\mathcal{W}_{\mathcal{S}} = \{[1, 0, 0, 0], [1, 0, 0, 0], [-2, 1, 0, 0], [0, -1, 0, 0]\},$$

shown at the bottom of Figure 3.2. It is an easy exercise to show that one identifies the same nilradical $\mathfrak{n}_{\{\alpha_3, \alpha_4\}}$ as previously, so the same parabolic subalgebra $\mathfrak{p}_{\{\alpha_3, \alpha_4\}}$. This illustrates

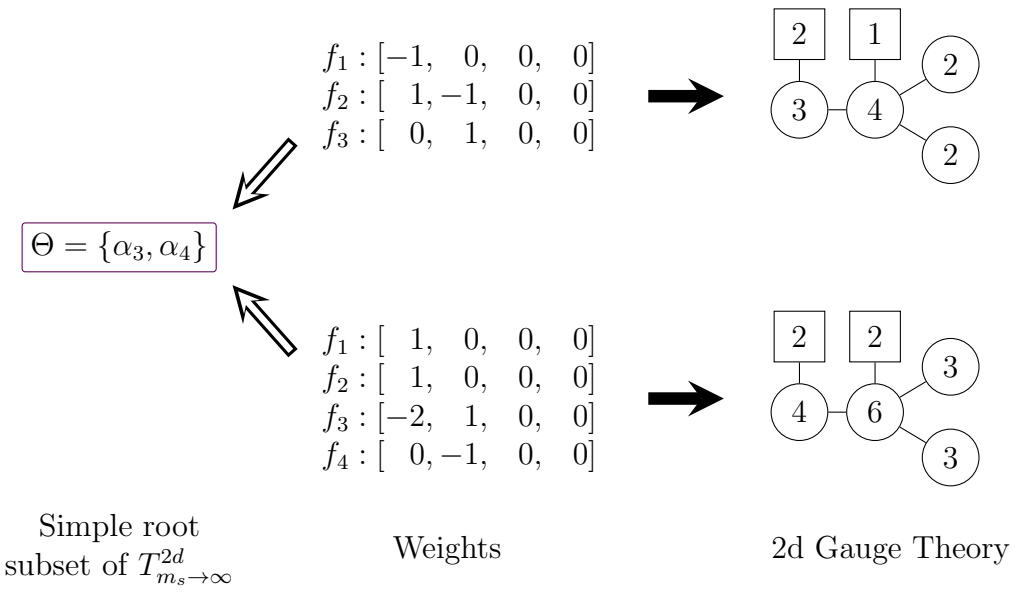

Figure 3.2: From the two sets of weights $\mathcal{W}_\mathcal{S}$, we read off the parabolic subalgebra $\mathfrak{p}_{\{\alpha_3,\alpha_4\}}$ of D_4. Reinterpreting each weight as a sum of "minus a fundamental weight and simple roots," we obtain two different 2d quiver gauge theories shown on the right. The white arrows imply we take the CFT limit.

that theories T^{2d} that have different quiver descriptions can end up determining the same parabolic subalgebra after taking m_s to infinity.

In particular, the two 2d theories of Figure 3.2 have different Coulomb branch dimensions. In the CFT limit, we lose the quiver description of the theories, and the complex Coulomb branch dimension of both theories reduces to 10, which is the dimension of $\mathfrak{n}_{\{\alpha_3,\alpha_4\}}$.

What about all the other possible sets $\mathcal{W}_\mathcal{S}$ one can write down, but for which a nilradical is not directly readable? After all, there are many more sets $\mathcal{W}_\mathcal{S}$ one can construct than the number of parabolic subalgebras of $\mathfrak{g}$. A parabolic subalgebra is in some sense associated to a specific *representative* set of weights $\mathcal{W}_\mathcal{S}$ (not necessarily unique), such that the above procedure can be carried through. It turns out that any admissible set $\mathcal{W}_\mathcal{S}$ is always in the Weyl orbit of such a representative set, which determines a parabolic subalgebra.

Note that all the sets $\mathcal{W}_\mathcal{S}$ featured in the examples so far were such representative sets. We also emphasize that throughout this discussion, it really is the set of weights $\mathcal{W}_\mathcal{S}$, not the resulting quiver, that characterizes a defect, since two different defects in the CFT limit can have the same quiver origin in the little string; see Figure 3.3 for an illustration.

Note that the case of $\mathfrak{g} = A_n$ is special, in that a parabolic subalgebra of A_n *defines* a 2d quiver theory, without any explicit reference to a set of weights; see Figure 3.4 for an illustration. A direct consequence is that for A_n, we do not need to assume that the 2d quiver

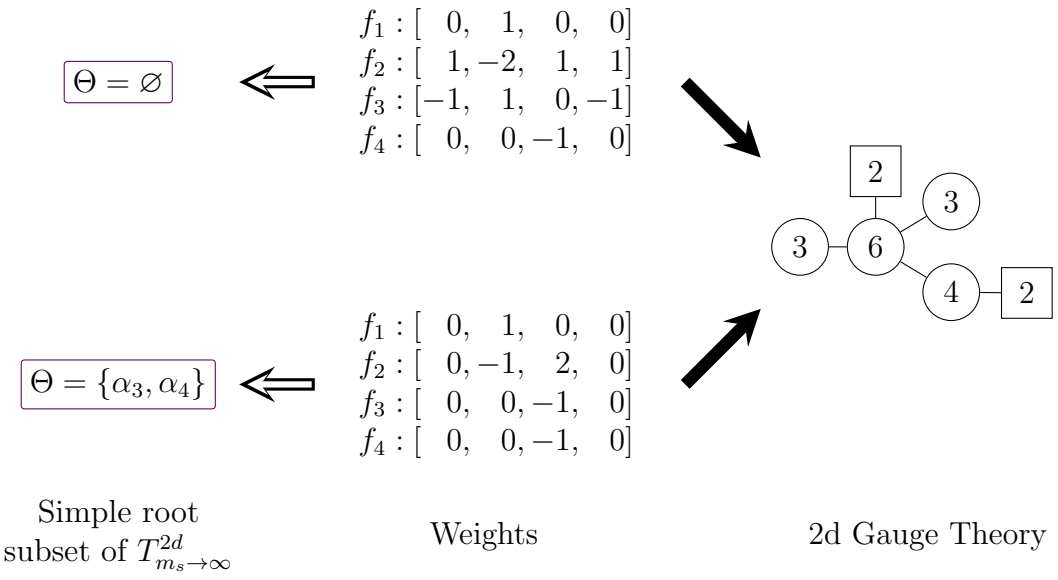

Figure 3.3: Two sets of weights $\mathcal{W}_{\mathcal{S}}$ which spell out the same quiver, but denote two different defects; we see it is really the weights, and not quivers, that define a defect. This is clear in the CFT limit, where two distinct parabolic subalgebras are distinguished.

is superconformal (in other words, we don't need to assume that the weights add up to zero, which was a necessary condition for conformality). This condition is *derived* from the Levi decomposition. Indeed, the nilradical gives the exact Coulomb moduli of the quiver, read in a diagonal fashion from a matrix representative. And the masses are read off from the Levi subalgebra, since the latter specifies a partition (this partition is just the Cartan subalgebra mass matrix). The resulting quiver *ends up* superconformal, since it obeys equation 2.4.

Lastly, there are extra "special" punctures which cannot be obtained from the sets of weights $\mathcal{W}_{\mathcal{S}}$ as defined so far. They are special in the sense that they do not determine a parabolic subalgebra of $\mathfrak{g}$. We defer the analysis of these extra theories to section 6.3.

3.3 Parabolic subalgebras from Higgs field data

The characterization of defects so far has relied on identifying a nilradical of the algebra. There is yet another way the above classification can be recovered, which relies on identifying a Levi subalgebra of $\mathfrak{g}$ instead. The Levi decomposition $\mathfrak{p}_\Theta = \mathfrak{l}_\Theta \oplus \mathfrak{n}_\Theta$ guarantees that specifying the Levi subalgebra $\mathfrak{l}_\Theta$ is equivalent to determining the nilradical $\mathfrak{n}_\Theta$ as done in the previous section. Either way, we obtain the same parabolic subalgebra $\mathfrak{p}_\Theta$. Let us derive this explicitly.

Recall that the Seiberg–Witten curve of the quiver gauge theory on the D5 branes is the

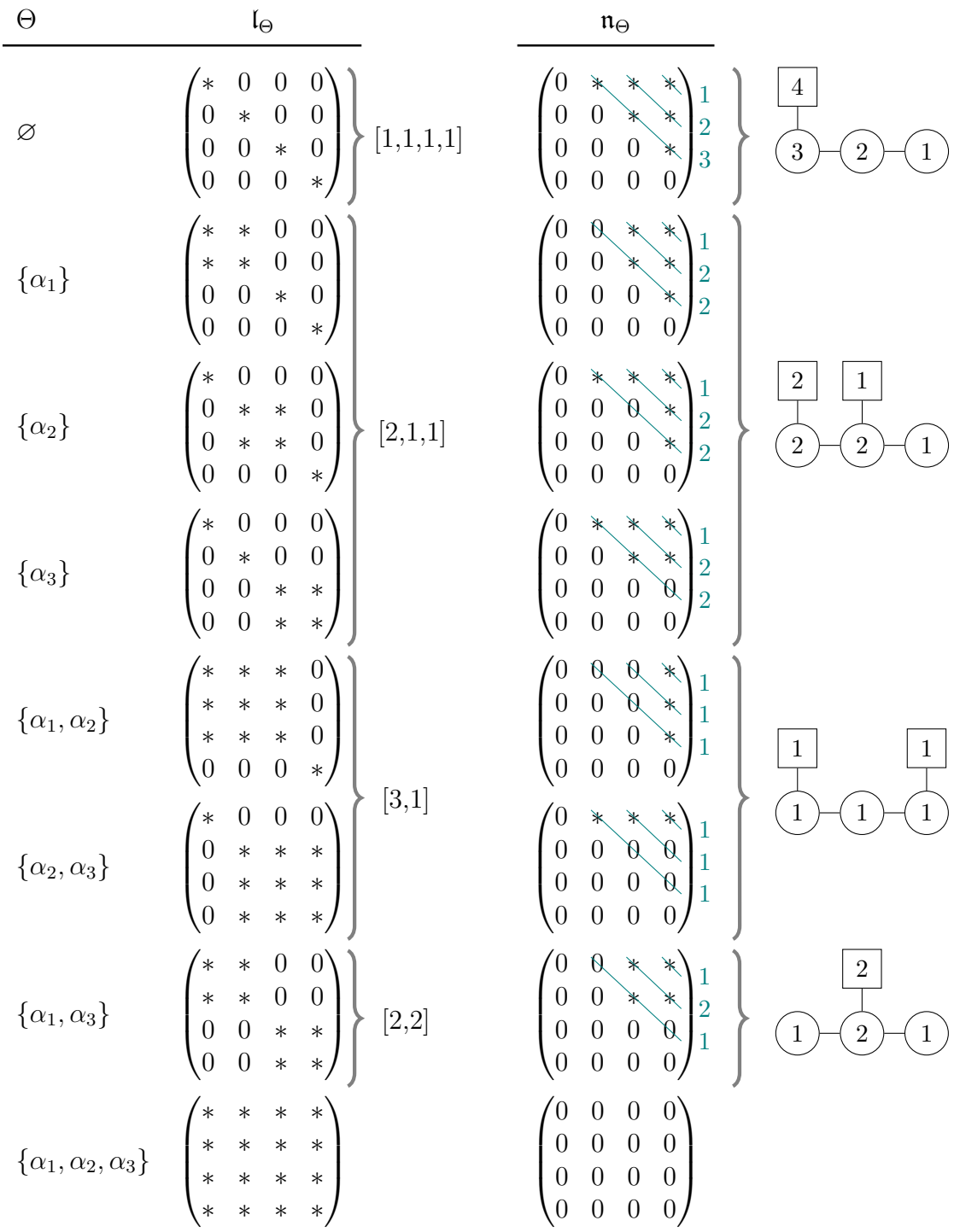

Figure 3.4: How to read off A_n quiver theories directly from the Levi decomposition of a parabolic subalgebra; here we show $n = 3$. The matter content is written as a partition, specified by the Levi subalgebra. The nilradical, read off in diagonal fashion in the upper triangular matrix, gives the Coulomb content. Note the resulting quivers are automatically superconformal. This way of reading off quiver gauge theories directly is unique to the A_n case.

spectral curve of the Higgs field ϕ, taken in some representation $\mathfrak{R}$ of $\mathfrak{g}$ ([48, 49, 46]). We described the m_s to infinity limit after which the Seiberg–Witten curve of the theory becomes the spectral curve of the Hitchin integrable system

$$\det{}_{\mathfrak{R}}(\phi - p) = 0.$$

After T^2 compactification, the same equation is solved by D3 branes instead, so we can say that the above spectral curve is the Seiberg–Witten curve of the two-dimensional theory $T^{2d}_{m_s\to\infty}$. At the root of the Higgs branch, where the Coulomb and Higgs branches meet, this expression simplifies: the Higgs field near a puncture of $\mathcal{C}$ has a pole of order one. After shifting this pole to $z = 0$, we get

$$0 = \det\left(p \cdot \mathbb{1} - \frac{\sum_{\omega_i \in \mathcal{W}_S} \hat{\beta}_i \omega_i}{z} + \text{reg.}\right), \tag{3.13}$$

where $\mathcal{W}_S$ is the set of weights introduced in chapter 2. The $\hat{\beta}_i$ are mass parameters of the gauge theory, which correspond to insertion points of the D3 branes on $\mathcal{C}$.

Thus, the residue at the pole diagonalizes, and the diagonal entries can be interpreted as hypermultiplet masses. So at the root of the Higgs branch, the Higgs field is described by an honest semi-simple element of $\mathfrak{g}$. From this semi-simple element, we can once again recover a parabolic subalgebra $\mathfrak{p}$. Indeed, given a semi-simple (diagonalizable) element S (in our cases, we'll always have $S \in \mathfrak{h}$), its centralizer

$$\mathfrak{g}^S := \{X \in \mathfrak{g} \,\big|\, [X, S] = 0\} \tag{3.14}$$

is reductive and is in fact a Levi subalgebra $\mathfrak{l}_S$ of some parabolic subalgebra $\mathfrak{p}_S$.

Since the Higgs field at a puncture of $\mathcal{C}$ has a pole with semi-simple residue, we can use this construction to associate a Levi subalgebra $\mathfrak{l}$ to a defect. The smallest parabolic subalgebra containing $\mathfrak{l}$ is then the parabolic subalgebra defining the theory. Thus, we achieved our goal of building a parabolic subalgebra, starting from a given Higgs field of a quiver theory T^{2d}.

Example 3.3.1. For $\mathfrak{g} = A_2$, assume that the Higgs field has a pole with semi-simple residue $\phi = \frac{S}{z}$ near $z = 0$. In the fundamental representation of $\mathfrak{sl}_3$, a possible choice for S is

$$S = \begin{pmatrix} \beta & 0 & 0 \\ 0 & \beta & 0 \\ 0 & 0 & -2\beta \end{pmatrix}. \tag{3.15}$$

The Levi subalgebra of $\mathfrak{sl}_3$ associated to this semi-simple element is the centralizer of S, which has the form

$$\mathfrak{g}^S = \begin{pmatrix} * & * & 0 \\ * & * & 0 \\ 0 & 0 & * \end{pmatrix} = \mathfrak{l}_{\{\alpha_1\}} \tag{3.16}$$

The parabolic subalgebra associated to this S is then $\mathfrak{p}_{\{\alpha_1\}}$ from example 3.1.2.

Chapter 4

Surface defects and Nilpotent Orbits

We now explain how the classification of surface defects presented here is connected to the classification of codimension-two defects via nilpotent orbits.

4.1 A short review

The characterization of a puncture as studied in the 6d $(2,0)$ CFT literature [17] is given in terms of a *nilpotent orbit* of the algebra: An element $X \in \mathfrak{g}$ is nilpotent if the matrix representative (in some faithful representation) is a nilpotent matrix. If X is nilpotent, then the whole orbit $\mathcal{O}_X$ of X under the adjoint action of G is nilpotent – we call this a nilpotent orbit. For readers interested in details and applications, the textbook [19] serves as an excellent introduction.

For a simple Lie algebra, the number of such nilpotent orbits is finite, and studying their properties leads to many connections to different branches of representation theory. For $\mathfrak{g} = A_n$, these orbits are labeled by Young diagrams with $n+1$ boxes; for $\mathfrak{g} = D_n$, they are classified by Young diagrams with $2n$ boxes which satisfy some conditions (see [19] for details.)

An important fact is that for any nilpotent orbit $\mathcal{O}$, the closure $\overline{\mathcal{O}}$ is always a union of nilpotent orbits. Furthermore, there is a maximal orbit $\mathcal{O}_{\max}$ whose union contains all other nilpotent orbits of $\mathfrak{g}$. This allows us to define an ordering on these orbits:

Given two nilpotent orbits $\mathcal{O}_1, \mathcal{O}_2 \subset \mathfrak{g}$, we define the relation

$$\mathcal{O}_1 \preceq \mathcal{O}_2 :\Leftrightarrow \mathcal{O}_1 \subseteq \overline{\mathcal{O}_2}\,, \tag{4.1}$$

where $\overline{\mathcal{O}}$ is the closure in the Zariski topology. This turns the set of all nilpotent orbits into a partially ordered set.

For A_n and D_n, this order corresponds to the dominance order of the Young diagrams used to label the orbits.

Example 4.1.1. For an A_n nilpotent orbit labeled by a partition $[d_1, \ldots, d_k]$, a matrix representative is given by k Jordan blocks of size $d_i \times d_i$. Taking the example of $n = 3$, there are

five different nilpotent orbits. Their Hasse diagram can be found below in Figure 4.1. For instance, the sub-dominant diagram $[3,1]$ labels the orbit of

$$X_{[3,1]} = \begin{pmatrix} 0 & 1 & 0 & 0 \\ 0 & 0 & 1 & 0 \\ 0 & 0 & 0 & 1 \\ 0 & 0 & 0 & 0 \end{pmatrix}. \tag{4.2}$$

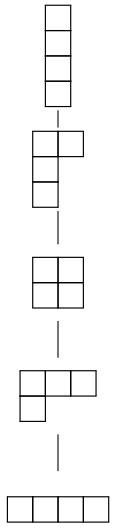

Figure 4.1: This diagram represents the inclusion relations between the nilpotent orbits of A_3.

In [17], boundary conditions of the 6d $(2,0)$ CFT are determined by solutions to Nahm's equations. These equations admit singular solutions near a puncture which are labeled by embeddings $\rho : \mathfrak{sl}_2 \to \mathfrak{g}$. Since $\sigma_+ \in \mathfrak{sl}_2$ is nilpotent, its image $\rho(\sigma_+)$ is as well, and defines a nilpotent orbit. By the Jacobson–Morozov theorem, this gives a one-to-one correspondence between such embeddings and nilpotent orbits. Thus, by dimensional reduction, $\frac{1}{2}$-BPS surface defects of 4d $\mathcal{N} = 4$ super Yang–Mills are typically labeled by nilpotent orbits.

4.2 Nilpotent orbits from Levi subalgebras

Since we now have two different constructions of surface defects, we should explain how we can relate them (a related discussion can be found in [17]):

Given a parabolic subalgebra $\mathfrak{p} = \mathfrak{l} \oplus \mathfrak{n}$, the nilpotent orbit $\mathcal{O}_\mathfrak{p}$ associated to it is the maximal orbit that has a representative $X \in \mathcal{O}_\mathfrak{p}$ for which $X \in \mathfrak{n}$. This induced orbit agrees with what is referred to as the Richardson orbit of $\mathfrak{p}$.

If $\mathfrak{g}$ is A_n or D_n, this map can be most easily described using the semi-simple pole of the Higgs field. We represent the pole in the first fundamental representation, and assign a Young diagram (with $n+1$ or $2n$ boxes, respectively) to it by counting the multiplicities of the eigenvalues. For A_n, these Young diagrams are given by the sizes of the blocks making up the Levi subalgebra $\mathfrak{l}$ (see Figure 3.4).

To this Young diagram, we can apply the so-called Spaltenstein map [54], which gives another Young diagram of the same size [19]. For A_n, this map is just the transposition.

This Young diagram labels the nilpotent orbit describing a defect according to [17]; adding this nilpotent element to the Higgs field describes a Coulomb deformation of the theory $T^{2d}_{m_s\to\infty}$, meaning we are moving away from the root of the Higgs branch.

Young diagrams are not available for exceptional Lie algebras, but this correspondence can be described at any rate by using the so-called Bala-Carter labels [8, 9].

Thus, we get a map which associates one of the theories in [17] to the 2d theory $T^{2d}_{m_s\to\infty}$. This was checked explicitly by comparing to the data in [16, 15, 18]. Furthermore, we will revisit this correspondence when considering the Seiberg–Witten curves of our theories in section 5.3.

Example 4.2.1. Let us show how to get the nilpotent orbits of A_3 in Figure 4.1 from parabolic subalgebras. To assign the right nilpotent orbit to them, we take the transpose of the partition describing the Levi subalgebra. The resulting Young diagram labels a nilpotent orbit, which describes a Coulomb deformation of the theory. Since this partition is the same one that is assigned to the pole of the Higgs field (in the first fundamental representation), we can also directly get the nilpotent orbit from the Higgs field data.

The correspondence we get can be read off from Table 4.1 below.

Θ	$\mathcal{O}$
$\varnothing$	[4]
$\{\alpha_i\}_{\,i=1,2,3}$	[3,1]
$\{\alpha_1,\alpha_2\}$	[2,2]
$\{\alpha_1,\alpha_3\}$	[2,1,1]
$\{\alpha_1,\alpha_2,\alpha_3\}$	[1,1,1,1]

Table 4.1: In this table, we read off which parabolic subalgebras of A_3 (labelled by a subset Θ of positive simple roots) induce which nilpotent orbits $\mathcal{O}$ (labelled by Young diagrams).

Chapter 5

Surface Defect classification and $\mathcal{W}(\mathfrak{g})$-algebras

In [3], the partition function of the $(2,0)$ $\mathfrak{g} = ADE$ little string on $\mathcal{C}$ with certain D5 brane defects is shown to be equal to a q-deformation of the $\mathfrak{g}$-Toda CFT conformal block on $\mathcal{C}$, with vertex operators determined by positions and types of defects. In this section, we analyze the previous classification of defects of the little string and its relation to parabolic subalgebras from the point of view of the dual $\mathfrak{g}$-type Toda CFT. Strictly speaking, the theory dual to the little string is a q-deformation of $\mathfrak{g}$-type Toda, which has a deformed $\mathcal{W}(\mathfrak{g})$-algebra symmetry, and is therefore not a CFT [23]; for an analysis in this deformed setting, see [39]. For our purposes, it will be enough to turn off that deformation and work with the usual Toda CFT and its $\mathcal{W}(\mathfrak{g})$-algebra symmetry; this is the counterpart to the m_s to infinity limit in the $(2,0)$ little string description, which gives the $(2,0)$ 6d CFT.

5.1 Levi subalgebras from level-1 null states of Toda CFT

In free field formalism, the ADE Toda field theory can be written in terms of $n = \mathrm{r}k(\mathbf{g})$ free bosons in two dimensions with a background charge contribution and the Toda potential that couples them:

$$S_{Toda} = \int dz d\bar{z}\ \sqrt{g}\ g^{z\bar{z}}[(\partial_z\vec{\varphi}\cdot\partial_{\bar{z}}\vec{\varphi}) + (\vec{\rho}\cdot\vec{\varphi})\ QR + \sum_{a=1}^{n} e^{\vec{e}_a\cdot\vec{\varphi}/b}]. \tag{5.1}$$

The field φ is a vector in the n-dimensional (co-)weight space, the inner product is the Killing form on the Cartan subalgebra of $\mathbf{g}$, $\vec{\rho}$ is the Weyl vector, and $Q = b + 1/b$. The $\vec{e}_a$ label the simple positive roots.

The Toda CFT has an extended conformal symmetry, a $\mathcal{W}(\mathfrak{g})$-algebra symmetry. The elements of the Cartan subalgeba $\mathfrak{h} \subset \mathfrak{g}$ define the highest weight states $|\vec{\beta}\rangle$ of the $\mathcal{W}(\mathfrak{g})$-algebra. It turns out that null states of this algebra play a crucial role in classifying the defects we have identified from the gauge theory perspective. Indeed, as shown in [37] for $\mathfrak{g} = A_n$, punctures can be classified via level 1 null states of the Toda CFT. This is also true for D_n and E_n; in this section, we will review how to construct these null states, and we will see that they distinguish the same parabolic subalgebras $\mathfrak{p}_\Theta$ of $\mathfrak{g}$ we encountered before. As we will explain, the set of simple roots Θ plays a very clear role in the $\mathcal{W}(\mathfrak{g})$-algebra null state condition.

We can use the vertex operators to construct highest weight states $|\vec{\beta}\rangle$ of the $\mathcal{W}(\mathfrak{g})$-algebra by acting on the vacuum, $|\vec{\beta}\rangle = \lim_{z\to 0} e^{\vec{\beta}\cdot\vec{\phi}(z)}|0\rangle$. These give rise to a Verma module over $|\vec{\beta}\rangle$ by acting with $\mathcal{W}(\mathfrak{g})$-algebra generators. For some of the $|\vec{\beta}\rangle$, these representations are degenerate, because they contain a null state; we say that $|\chi\rangle$, in the Verma module over $|\vec{\beta}\rangle$, is a *level k null state* of the $\mathcal{W}(\mathfrak{g})$-algebra if for all spins s:

$$W_n^{(s)}|\chi\rangle = 0, \quad \forall n > 0, \tag{5.2}$$

$$W_0^{(2)}|\chi\rangle = (E_\beta + k)|\chi\rangle, \tag{5.3}$$

where $W_0^{(2)}|\vec{\beta}\rangle = E_\beta|\vec{\beta}\rangle$.

The Verma module over $|\vec{\beta}\rangle$ contains such a null state at level k if the Kač determinant at level k vanishes. For any semi-simple $\mathfrak{g}$, this determinant at level k is a non-zero factor times

$$\prod_{\substack{\vec{\alpha}\in\Phi \\ m,n\leq k}} \Big((\vec{\beta} + \alpha_+\vec{\rho} + \alpha_-\vec{\rho}^\vee)\cdot\vec{\alpha} - (\tfrac{1}{2}\vec{\alpha}^2\, m\alpha_+ + n\alpha_-)\Big)^{p_N(k-mn)}, \tag{5.4}$$

where $p_N(l)$ counts the partitions of l with N colours and Φ is the set of all roots of $\mathfrak{g}$ [11]. For us, $(\alpha_+, \alpha_-) = (b, 1/b)$.

Note that this determinant is invariant only under the shifted action of the Weyl group,

$$\vec{\beta} \mapsto w(\vec{\beta} + \alpha_+\vec{\rho} + \alpha_-\vec{\rho}^\vee) - (\alpha_+\vec{\rho} + \alpha_-\vec{\rho}^\vee), \tag{5.5}$$

where w is the ordinary Weyl action.

If $\mathfrak{g}$ is simply laced, and $\vec{\alpha} = \vec{\alpha}_i$ is a simple root, the condition that this determinant vanishes can be phrased as

$$\vec{\beta}\cdot\vec{\alpha}_i = (1-m)\alpha_+ + (1-n)\alpha_-. \tag{5.6}$$

We see that any $\vec{\beta}$ with $\vec{\beta}\cdot\vec{\alpha}_i = 0$ for a *simple root* $\vec{\alpha}_i$ gives rise to a level 1 null state, and if $Q := (\alpha_+ + \alpha_-) \to 0$, a null state at level 1 occurs if $\vec{\beta}\cdot\vec{\alpha} = 0$ for any $\vec{\alpha} \in \Phi$. Furthermore, in this limit, the shift in the Weyl group action disappears. It is enough to work in this

"semi-classical" limit for our purposes, so we will set Q to 0 in what follows.

We can explicitly construct these null states: Consider the *screening charge operators*

$$Q_i^{\pm} = \oint \frac{dz}{2\pi i} \exp(i\alpha_{\pm}\vec{\alpha}_i \cdot \vec{\phi}) \tag{5.7}$$

and observe that

$$[W_n^{(k)}, Q_i^{\pm}] = 0. \tag{5.8}$$

The level 1 null state is then

$$S_i^+ |\vec{\beta} - \alpha_+ \vec{\alpha}_i\rangle. \tag{5.9}$$

Explicit forms of these null states for $\mathfrak{g} = A_n$ or D_n are shown in the examples of section 7. The relation to the parabolic subalgebras introduced in chapter 3 is immediate: we simply associate a generic null state $|\vec{\beta}\rangle$ satisfying

$$\vec{\beta} \cdot \vec{\alpha}_i = 0 \quad \forall \vec{\alpha}_i \in \Theta$$

with the parabolic subalgebra $\mathfrak{p}_\Theta$.

We also note that this $\vec{\beta}$ defines a semi-simple element in $\mathfrak{g}$; this is just the residue of the Higgs field at the puncture, as explained in section 3.3.

We show next that these these null states induce relations in the Seiberg–Witten curve of the theory $T^{2d}_{m_s \to \infty}$. Indeed, the Seiberg–Witten curve of $T^{2d}_{m_s \to \infty}$ (3.13) can be obtained from a free field realization of the $\mathcal{W}(\mathfrak{g})$-algebra. We will simply read off the null states as relations between the curve coefficients. Generically, these relations only involve semi-simple elements of the algebra $\mathfrak{g}$. In 5.3, we will see these relations are still preserved when one additionally introduces certain nilpotent deformations.

When working in the q-deformed setting, the formula for the Kač determinant is an exponentiated version of (5.4) [10]. This implies that the null states can be defined analogously for the q-deformed $\mathcal{W}(\mathfrak{g})$-algebra.

5.2 Seiberg–Witten curves from $\mathcal{W}(\mathfrak{g})$-algebras

As we reviewed previously, the Seiberg–Witten curve of $T^{2d}_{m_s \to \infty}$ is the spectral curve equation

$$\det_{\mathfrak{R}}(\phi - p) = 0. \tag{5.10}$$

In our case, ϕ has a simple pole such that the residue is a semi-simple element of $\mathfrak{g}$, which we can write as

$$\vec{\beta} = \sum_{\omega_i \in W_S} \hat{\beta}^i \omega_i. \tag{5.11}$$

To find the curve near the pole, which we assume to be at $z = 0$, we can just choose some convenient representation $\mathfrak{R}$, where the residue of ϕ is diagonal, and given by $\mathrm{diag}(\beta_1, \beta_2, \ldots) =: M$. Then $\phi = \frac{M}{z} + A$, with A a generic element in $\mathfrak{g}$.

We now expand eq. (5.10) and write the curve as

$$0 = \det\left(-p \cdot \mathbb{1} + \frac{M}{z} + A\right) = (-p)^{\dim(\mathfrak{R})} + \sum_s p^{\dim(\mathfrak{R})-s}\varphi^{(s)}, \tag{5.12}$$

where $\varphi^{(s)}$ is a meromorphic differential, i.e. $\varphi^{(s)} = \sum_{k=0}^{s} \frac{\varphi_k^{(s)}}{z^k}$, where the $\varphi_k^{(s)}$ are regular functions of β^i and a_{ij} (the entries of A).

Since M is diagonal, this determinant just picks up the diagonal terms a_{ii} of A, which we identify with the gauge couplings of the quiver theory.

Now, we can also construct the Seiberg–Witten curve of $T^{2d}_{m_s\to\infty}$ from the $\mathcal{W}(\mathfrak{g})$-algebra [37, 38]: For this, we need to perform a Drinfeld–Sokolov reduction to obtain explicit $\mathcal{W}(\mathfrak{g})$-algebra generators in the free field realization[1]. Setting $Q = 0$ gives us a direct connection to the two dimensional quiver defined by the semi-simple element $\vec{\beta} \in \mathfrak{g}$ (cf. section 3.3): We can identify the poles of the Seiberg-Witten differentials with expectation values of these $\mathcal{W}(\mathfrak{g})$ algebra generators in the state $|\vec{\beta}\rangle$:

$$\varphi^{(s)} = \langle\vec{\beta}|W^{(s)}|\vec{\beta}\rangle. \tag{5.13}$$

We checked this relation explicitly for A_n and D_n theories.

Example 5.2.1. Let us look at the curve describing the full puncture for $\mathfrak{g} = A_2$:

Take the fundamental three-dimensional representation of $\mathfrak{sl}_3$ and write

$$M = \begin{pmatrix} \beta_1 & 0 & 0 \\ 0 & \beta_2 & 0 \\ 0 & 0 & -\beta_1 - \beta_2 \end{pmatrix}, \quad A = \begin{pmatrix} a_{11} & a_{12} & a_{13} \\ a_{21} & a_{22} & a_{23} \\ a_{31} & a_{32} & -a_{11} - a_{22} \end{pmatrix}. \tag{5.14}$$

Then the curve can be expanded, and we read off the differentials. For example, $\varphi^{(2)}$, the coefficient multiplying p, has the form

$$\varphi^{(2)} = \frac{\varphi_2^{(2)}}{z^2} + \frac{\varphi_1^{(2)}}{z} + \varphi_0^{(2)}, \tag{5.15}$$

where

$$\varphi_2^{(2)} = \frac{1}{2}\left(\beta_1^2 + \beta_2^2 + (-\beta_1 - \beta_2)^2\right) := \frac{1}{2}(\vec{\beta})^2, \tag{5.16}$$

$$\varphi_1^{(2)} = a_{11}(2\beta_1 + \beta_2) + a_{22}(\beta_1 + 2\beta_2). \tag{5.17}$$

[1] We thank Kris Thielemans for sending us his `OPEDefs.m` package [55], which allowed us to do these calculations

Furthermore,

$$\begin{aligned}\varphi_3^{(3)} &= -\beta_1^2\beta_2 - \beta_2^2\beta_1, \\ \varphi_2^{(3)} &= a_{11}(-2\beta_1\beta_2 - \beta_2^2) + a_{22}(-2\beta_1\beta_2 - \beta_1^2).\end{aligned} \tag{5.18}$$

Now from the CFT side, for $\mathfrak{g} = A_2$, define $X^j = i\partial\phi^j$. In the fundamental representation, $X^1 + X^2 + X^3 = 0$. Then the generators are just the energy momentum tensor

$$T(z) = W^{(2)}(z) = \frac{1}{3}(:X^1X^1: + :X^2X^2: + :X^3X^3: - :X^1X^2: - :X^1X^3: - :X^2X^3:)$$

and the spin 3 operator

$$\begin{aligned}W^{(3)}(z) = :&\left(\frac{2}{3}X^1 - \frac{1}{3}X^2 - \frac{1}{3}X^3\right)\cdot\left(-\frac{1}{3}X^1 + \frac{2}{3}X^2 - \frac{1}{3}X^3\right)\cdot \\ &\cdot\left(-\frac{1}{3}X^1 - \frac{1}{3}X^2 + \frac{2}{3}X^3\right):.\end{aligned}$$

For the full puncture, we find at once that $\langle\vec{\beta}|L_0|\vec{\beta}\rangle$ is equal to $\varphi_2^{(2)}$ from above, while $\langle\vec{\beta}|W_0^{(3)}|\vec{\beta}\rangle$ is equal to $\varphi_3^{(3)}$, as expected. For the level 1 modes, one finds

$$\langle\vec{\beta}|W_{-1}^{(2)}|\vec{\beta}\rangle = (2\beta_1 + \beta_2)\langle\vec{\beta}|j_{-1}^1|\vec{\beta}\rangle + (\beta_1 + 2\beta_2)\langle\vec{\beta}|j_{-1}^2|\vec{\beta}\rangle, \tag{5.19}$$

$$\langle\vec{\beta}|W_{-1}^{(3)}|\vec{\beta}\rangle = (-2\beta_1\beta_2 - \beta_2^2)\langle\vec{\beta}|j_{-1}^1|\vec{\beta}\rangle + (-\beta_1^2 - 2\beta_1\beta_2)\langle\vec{\beta}|j_{-1}^2|\vec{\beta}\rangle, \tag{5.20}$$

where j_k^i denotes the k-th mode of X^i.

Observe that this has the form (5.18) if we identify $\langle\vec{\beta}|j_{-1}^i|\vec{\beta}\rangle$ with the i-th gauge coupling constant.

For more complicated defects, the $\mathcal{W}(\mathfrak{g})$-algebra generators will have terms that are derivatives of X — these are set to zero in the semiclassical $Q \to 0$ limit we are considering; after doing so, the reasoning is as above.

5.3 Null state relations

Punctures that are not fully generic are determined by semi-simple elements $\vec{\beta} \in \mathfrak{g}$ whose Verma modules contain null states at level one. Since the eigenvalues of the level one $\mathcal{W}(\mathfrak{g})$-algebra generators appear as coefficients in the curve, the existence of these null states induces some relations between these coefficients.

For $\mathfrak{g} = A_n$ and D_n in the fundamental representation, the pattern is easy to see. The condition $\vec{\beta}\cdot\vec{\alpha} = 0$ for some positive root $\vec{\alpha}$ will cause some of the entries of $M = \mathrm{diag}(\beta_1, \beta_2, \ldots)$ to be equal to each other; if the entry β_i occurs k times, we get null states by letting the operator

$$\sum_s \beta_i^s W_{-1}^{(\dim(\mathfrak{R})-s)}, \tag{5.21}$$

and its $k-1$ derivatives with respect to β_i, act on $|\vec{\beta}\rangle$. Thus, each theory induces some characteristic null state relations which are realized in the Seiberg–Witten curve.

We now use this observation to connect these curves to nilpotent orbits: note that all the curves considered so far were written as

$$\det\left(-p\cdot\mathbb{1}+\frac{M}{z}+A\right)=0 \tag{5.22}$$

for some diagonal M and a generic A in $\mathfrak{g}$. In the nilpotent orbit literature, the curves considered in [15, 16, 18] have the form

$$\det\left(-p\cdot\mathbb{1}+\frac{X}{z}+A\right)=0, \tag{5.23}$$

where, again, A is a generic element in $\mathfrak{g}$, and X is a representative of a nilpotent orbit $\mathcal{O}_X$.

We can now simply combine these two poles and form a curve of the form

$$\det\left(-p\cdot\mathbb{1}+e\frac{X}{z}+\frac{M}{z}+A\right)=0, \tag{5.24}$$

where M is semi-simple, $X\in\mathcal{O}_X$ is nilpotent and e is a parameter. We will test the correspondence between theories defined by nilpotent orbits and theories defined by semi-simple elements from this vantage point. Recall from section 4 that the semi-simple element $M\in\mathfrak{g}$ induces a nilpotent orbit $\mathcal{O}$. We observe the following facts:

- Whenever an orbit $\mathcal{O}'\preceq\mathcal{O}$, it is *always* possible to find an $X\in\mathcal{O}'$ such that all the null state relations of the curve (5.22) are still satisfied by the curve (5.24).
- Whenever an orbit $\mathcal{O}'\not\preceq\mathcal{O}$, it is *never* possible find an $X\in\mathcal{O}'$ such that all the null state relations of the curve (5.22) are still satisfied by the curve (5.24).

This gives a prescription for allowed deformations; from the perspective of the theory $T^{2d}_{m_s\to\infty}$, this corresponds to leaving the root of the Higgs branch by turning on certain Coulomb moduli.

Example 5.3.1. For $\mathfrak{g}=A_2$, the only interesting state is $\vec{\beta}=(\beta_1,\beta_1,-2\beta_1)$; we can get the level one coefficients of the curve by setting $\beta_1=\beta_2$ in example 5.2.1:

$$\begin{aligned}\phi_1^{(2)}&=\langle W_{-1}^{(2)}\rangle=3\beta_1(a_{11}+a_{22}),\\ \phi_2^{(3)}&=\langle W_{-1}^{(3)}\rangle=-3\beta_1^2(a_{11}+a_{22}),\end{aligned} \tag{5.25}$$

so we see that

$$\langle W_{-1}^{(3)}\rangle+\beta_1\langle W_{-1}^{(2)}\rangle=0. \tag{5.26}$$

If we now add the nilpotent element $X = \begin{pmatrix} 0 & 0 & 1 \\ 0 & 0 & 0 \\ 0 & 0 & 0 \end{pmatrix}$, then

$$\begin{aligned} \phi_1^{(2)} &= 3\beta_1(a_{11} + a_{22}) + ea_{31}, \\ \phi_2^{(3)} &= -3\beta_1^2(a_{11} + a_{22}) - e\beta_1 a_{31}, \end{aligned} \tag{5.27}$$

and the null state relation (5.26) is still satisfied.

Chapter 6

Defects of the Little String and their CFT limit

Up until now, we have been been using the little string theory as a tool to derive codimension-two defects of the $(2,0)$ CFT, and in particular exhibit the parabolic subalgebras that arise in that limit. In this section, we keep m_s finite, and comment on the classification of defects of the $(2,0)$ little string proper. In particular, as we have emphasized in chapter 3, when we work with the little string and not its conformal field theory limit, parabolic subalgebras are in general not visible (exceptions are when $\mathfrak{g} = A_n$, as we had illustrated in Figure 3.4, and in a few low rank cases when $\mathfrak{g} = D_n$ and $\mathfrak{g} = E_n$.)

We also address a question that was not answered so far: certain nilpotent orbits of $\mathfrak{g}$ are not induced from any parabolic subalgebra. The simplest example would be the minimal nilpotent orbit of D_4. These denote nontrivial defects of the $(2,0)$ CFT, so one should ask if they arise at all from the little string, since so far all the quiver theories we constructed distinguished a parabolic subalgebra. We will see that these exotic defects do indeed originate from the little string. To properly analyze them, we must first understand how flowing on the Higgs branch of a defect is realized from representation theory.

6.1 T^{2d} and Higgs flow as Weight Addition

In this section, we describe an effective and purely group-theoretical way to flow on the Higgs branch of different 2d quiver theories T^{2d}, for any simple $\mathfrak{g}$. We show that in the A_n case, this agrees with standard brane engineering and Hanany-Witten transitions [29]. As an application, this procedure will be used to analyze the punctures that fall outside of the parabolic subalgebra classification we have spelled out so far.

Our setup will be the usual one in this paper: we consider the quiver gauge theory T^{2d} that describes the low energy limit of D3 branes wrapping 2-cycles of the ALE space X times $\mathbb{C}$. The D3 branes are points on the Riemann surface $\mathcal{C}$ and on the torus T^2.

We claim that moving on the Higgs branch of T^{2d} translates to a weight addition procedure in the algebra: this makes use of the fact that a weight belonging to a fundamental representation can always be written as the sum of new weights. Each of them should be in the orbit of some fundamental weight (the two orbits do not have to be the same, here), while obeying the rule that no subset adds up to the zero weight.

After moving on the Higgs branch of T^{2d}, we obtain a new 2d theory $T^{2d'}$ with a new set of weights, but the same curve. When the gauge theory can be engineered using branes, going from T^{2d} to $T^{2d'}$ is called a Hanany–Witten transition [29]. There, as we will see, a D5 brane passing an NS5 brane creates or removes D3 branes stretching between the two. When a brane construction is not available, the weight description we give is still valid, for an arbitrary simply laced Lie algebra..

Note that this weight addition formalism also gives a generalization of the S-configuration [29]: No weight in a fundamental representation can ever be written as the sum of two identical weights.

In the A_n case, where we have a brane picture, this statement translates immediately to the S-rule, which is then automatically satisfied. This argument is however applicable to D_n and E_n theories as well, so this gives an ADE-type S-rule.

6.2 Brane Engineering and Weights

For A_n theories and D_n theories obtainable by an orbifolding procedure, the above discussion can be realized by brane engineering of the theory. We can conveniently represent the weights of the algebra, and in particular, their Dynkin labels, using a configuration of D3 branes stretching between NS5's and D5 branes. To see how this works, let us focus on the i-th Dynkin label of a weight:

- A D3 brane coming from the left ending on the $i-th$ NS5 contributes -1 to the weight's i-th label.
- A D3 brane coming from the right ending on the i-th NS5 contributes $+1$ to the weight's i-th label.
- A D3 brane coming from the left ending on the $i+1$-th NS5 contributes $+1$ to the weight's i-th label.
- A D3 brane coming from the right ending on the $i+1$-th NS5 contributes -1 to the weight's i-th label.
- Finally, a D5 brane present between the i-th and $i+1$-th NS5's contributes -1 to the weight's i-th label.

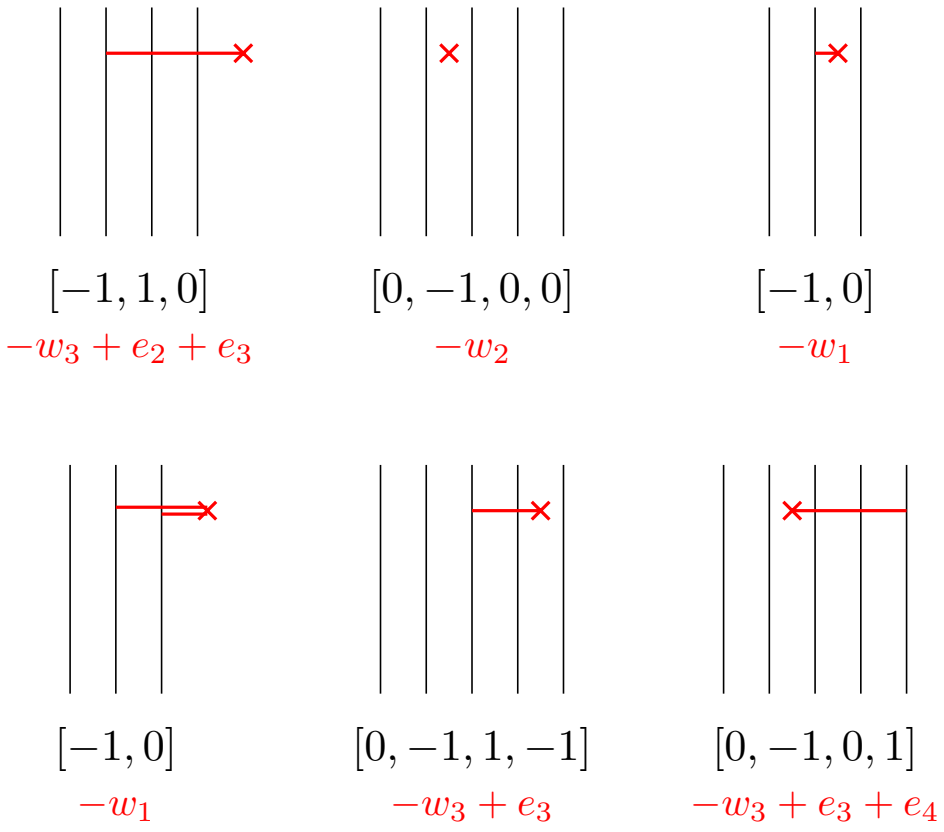

Figure 6.1: How to read off weights from a system of D3, D5, and NS5 branes.

All in all, a D3 brane stretching between a D5 brane and an NS5 brane (while possibly going through some other NS5 branes) produces a weight, whose Dynkin labels are a combination of 1's, -1's, and 0's. The map is not injective: for a given weight, there can be many brane configurations.

So the Dynkin labels record the total charge of the D3 brane configuration. The statement that the sum of weights is 0 is then a statement about vanishing of D3 brane flux. Note that the configuration of branes spells out a quiver gauge theory at low energies, which is the expected theory T^{2d} we would write based on the weight data $\mathcal{W}_S$. See Figure 6.2 for some examples.

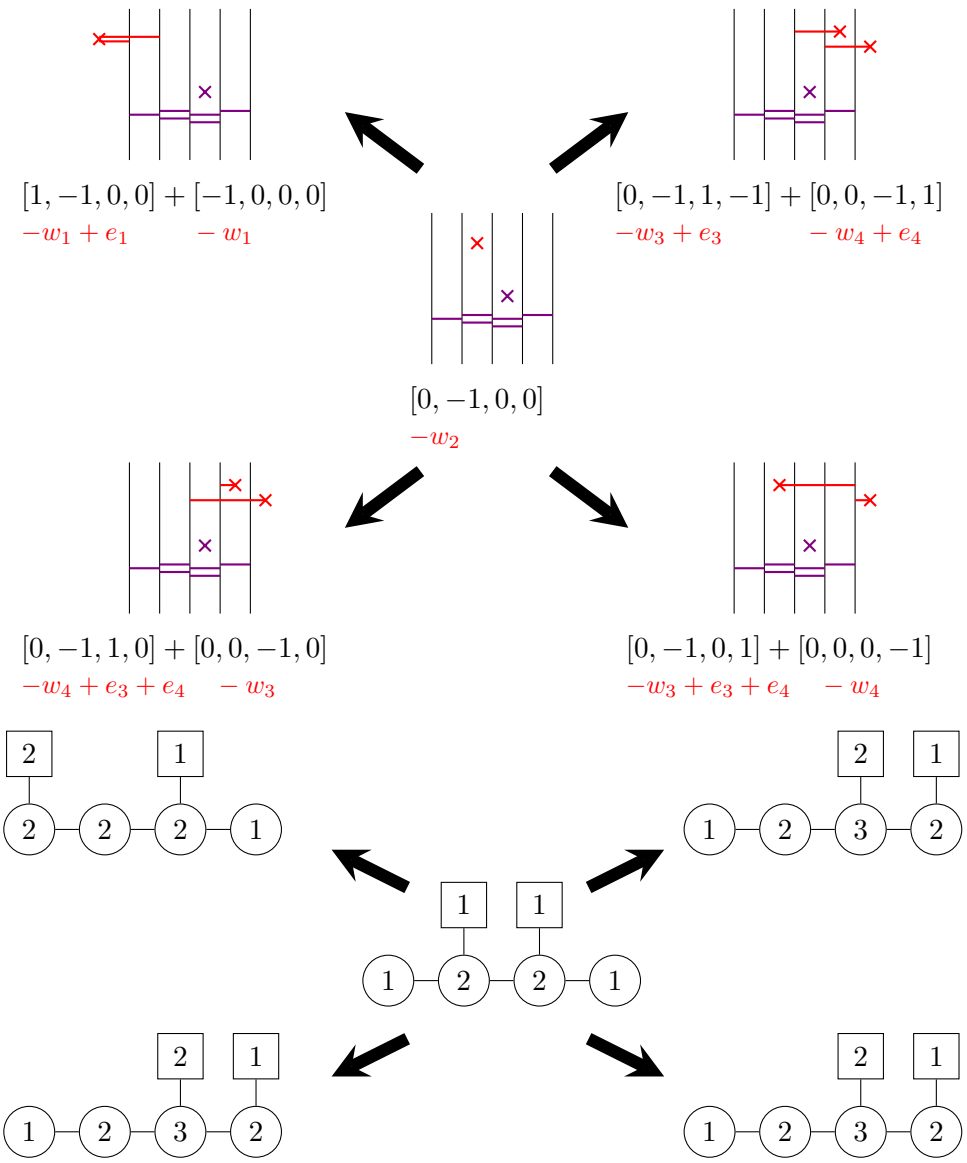

Figure 6.2: Flowing on the Higgs branch of T^{2d}: starting from the theory in the middle, these are all the theories one can obtain by replacing the weight on node 2 by a sum of two weights. The top picture shows the detailed brane picture for each of the quivers. These all have a low-energy 2d quiver gauge theory description (the ones shown below). At the root of the Higgs branch, the partition functions of all 5 theories are equal.

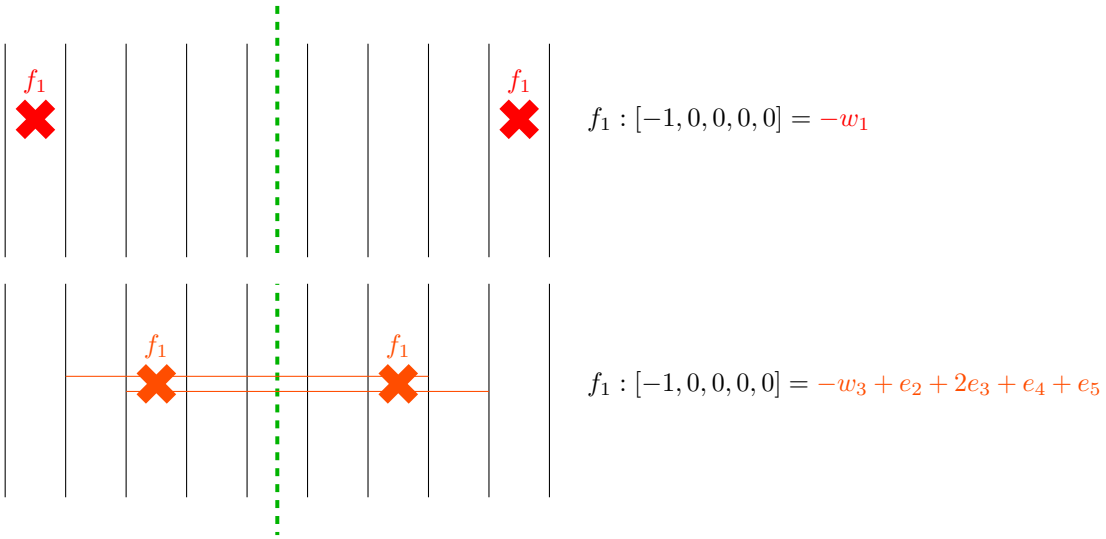

(a) The brane realization of the weight $[-1,0,0,0,0]$ of D_5. We started with A_9 theory and performed a $\mathbb{Z}_2$ orbifold to obtain the picture. This weight can be written in two ways: by placing the D5 brane between the first two NS5 branes (top), the weight is written in an "appropriate way" . By placing the D5 brane between the "wrong" set of NS5 branes (bottom), the resulting quiver will be unpolarized and will not distinguish a parabolic subalgebra.

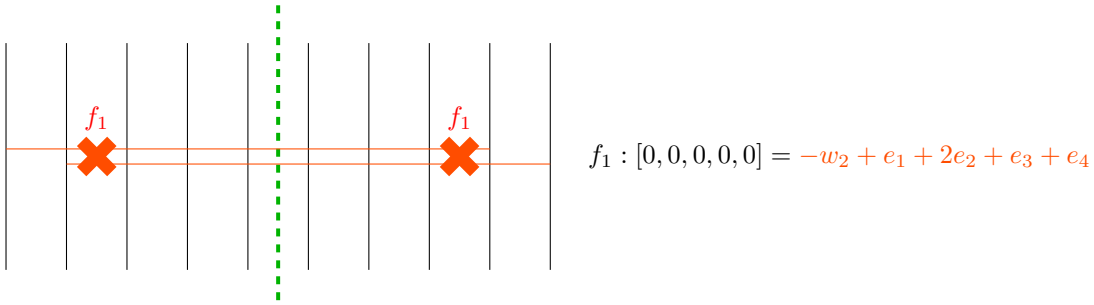

(b) Simplest unpolarized defect: the null weight $[0,0,0,0]$ of D_4, realized here with branes. We started with A_7 theory and performed a $\mathbb{Z}_2$ orbifold to obtain the picture. This theory does not distinguish a parabolic subalgebra.

6.3 Polarized and Unpolarized Punctures of the Little String

We finally come to the description of defects in the little string that happen to fall outside the parabolic subalgebra classification we have spelled out so far.

Suppose we pick a weight in the i-th fundamental representation. Unless it is the null weight, it is in the orbit of one and only one fundamental weight, say the j-th one. In our entire discussion so far, and in all the examples of [3], we had $i = j$. In terms of the gauge theory, if all weights are chosen so that $i = j$, then $T^{2d}_{m_s \to \infty}$ distinguishes a parabolic

subalgebra, as explained in section 3.2. We call such a 2d theory *polarized*. [1]

However, in the D_n and E_n cases, it can also happen that $i \neq j$, or that the weight we pick is the null weight. See Figures 6.3a and 6.3b. In terms of the gauge theory, if *at least one* of the weights in $\mathcal{W}_{\mathcal{S}}$ falls under this category, the theory $T^{2d}_{m_s \to \infty}$ does *not* distinguish a parabolic subalgebra. We call such a 2d theory *unpolarized*.

We saw in section 6.1 that if we start with a polarized theory T^{2d}, then after flowing on the Higgs branch, we still end up with a polarized theory $T^{2d'}$. What happens to unpolarized theories? If we start with a such a theory T^{2d}, then after moving on the Higgs branch, it is in fact always possible to end up with a theory $T^{2d'}$ that is polarized. This resulting polarized theory $T^{2d'}$ is of course highly specialized, since some masses have to be set equal to each other as a result of the Higgs flow.

This is the viewpoint we take to analyze all unpolarized theories: we will flow on the Higgs branch until they transition to polarized theories. In practice, it means that every "problematic" weight in an unpolarized theory can be written as a sum of weights to give a polarized theory. Note that for A_n, every quiver theory T^{2d} is polarized, while this is not the case for D_n and E_n. An illustration of how one can start with an unpolarized theory and arrive at a polarized theory is shown in Figure 6.4 below.

One should ask what happens to unpolarized defects in the context of Toda CFT. As we have seen in chapter 5, polarized defects are described by momenta that obey null state relations of the corresponding $\mathcal{W}(\mathfrak{g})$-algebra. This is consistent with what can be found in the class S literature [17]; for instance, for the minimal puncture of D_4 from Figure 6.4, the defect in the CFT limit is predicted to have no flavor symmetry. In particular, it is unclear what vertex operator one would write in D_4-Toda; indeed, in the little string formalism, the defect is the null weight, which suggests a trivial conformal block with no vertex operator insertion! To investigate this issue more carefully, it is useful to keep m_s finite and work in the little string proper; there, a computation in the spirit of [6, 4, 3], shows that the partition function of T^{2d} is in fact *not* a q-conformal block of D_4 Toda, due to subtleties of certain non-cancelling fugacities. In other words, the claim that the partition function of T^{2d} is a q-conformal block of $\mathfrak{g}$-type Toda fails precisely when T^{2d} is an unpolarized defect, and only for those cases.

[1] The terminology here comes from the fact that the parabolic subgroup $\mathcal{P}$ in $T^*(G/\mathcal{P})$ is often called a polarization of some nilpotent orbit $\mathcal{O}$, through the resolution map $T^*(G/\mathcal{P}) \to \overline{\mathcal{O}}$, with $\overline{\mathcal{O}}$ the closure of $\mathcal{O}$.

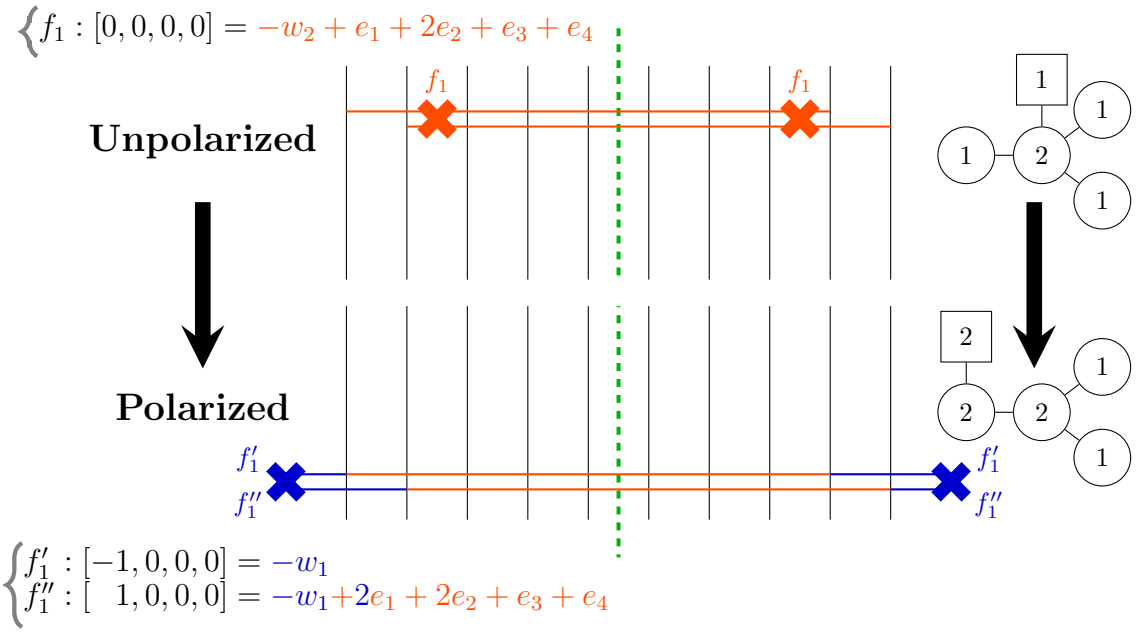

Figure 6.4: The brane picture for the zero weight of D_4 (top of the figure), which makes up an unpolarized theory at low energies. It is obtained after $\mathbb{Z}_2$ orbifolding of A_7. The D5 branes sit on top of the D3 branes, and all the D3 branes are stacked together. After flowing on the Higgs branch, we end up with a polarized theory, with the two masses equal to each other.

6.4 All Codimension-Two Defects of the (2,0) Little String

From the considerations above, we get a complete list of the D3 brane defects of the $(2,0)$ little string that are points on $\mathcal{C} \times T^2$, and which preserve conformality. These are the polarized and unpolarized punctures we presented. Each of them is characterized by a set of weights in $\mathfrak{g}$, which produce a superconformal quiver gauge theory at low energies. Enumerating the $(2,0)$ little string defects, for a given $\mathfrak{g}$, is then a *finite* counting problem. For D_n and E_n, we find that the number of resulting theories T^{2d} one obtains from specifying a set of weights, although finite, far exceeds the number of the CFT defects as enumarated in [17]. What is happening is that in the CFT limit, many distinct defect theories T^{2d} typically coalesce to one and the same defect theory $T^{2d}_{m_s \to \infty}$. The discussion in Figure 3.3 illustrates this phenomenon. See also Figure 6.5 for the example of all theories T^{2d} describing a generic full puncture of the D_4 little string.

An important point is that even though we focused on the case of a sphere with two full punctures and an additional arbitrary puncture, the formalism we developed is automatically

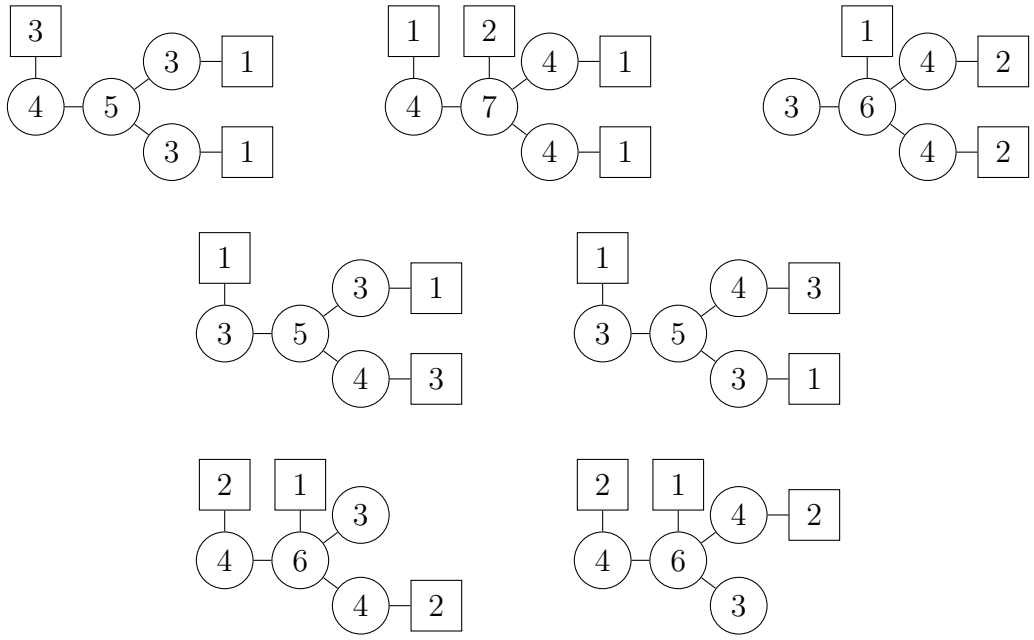

Figure 6.5: All D_4 2d quiver theories one obtains from a set $\mathcal{W}_{\mathcal{S}}$ of 5 weights, and which all denote full punctures. In the CFT limit, all these theories produce the same full puncture, denoted by the parabolic subalgebra $\mathfrak{p}_{\varnothing}$. In particular, the Coulomb branch of $T^{2d}_{m_s\to\infty}$ for all these theories has dimension twelve.

suited to study a sphere with an arbitrary number of defects. Simply choose a set of weights $\mathcal{W}_{\mathcal{S}}$, as done before. The statement is that if there are k subsets of weights which add up to zero in $\mathcal{W}_{\mathcal{S}}$, then the little string is in fact compactified on a sphere with $k+2$ punctures. This just follows from linearity of equation (2.4). In particular, for the case of the sphere with 3 punctures we have been analyzing, there are then no proper subset of weights in $\mathcal{W}_{\mathcal{S}}$ that add up to zero. An immediate consequence is that not all quiver theories characterize a sphere with two full punctures and a third arbitrary one: some quivers represent composite arbitrary defects (and two full punctures). See Figure 6.6.

As a final remark, let us mention that the techniques we used in this note to study codimension-two defects of the little string can also be applied to analyze codimension-four defects; these defects do not originate as D5 branes in the $(2,0)$ little string, but as D3 branes instead, before considering any T^2 compactification.

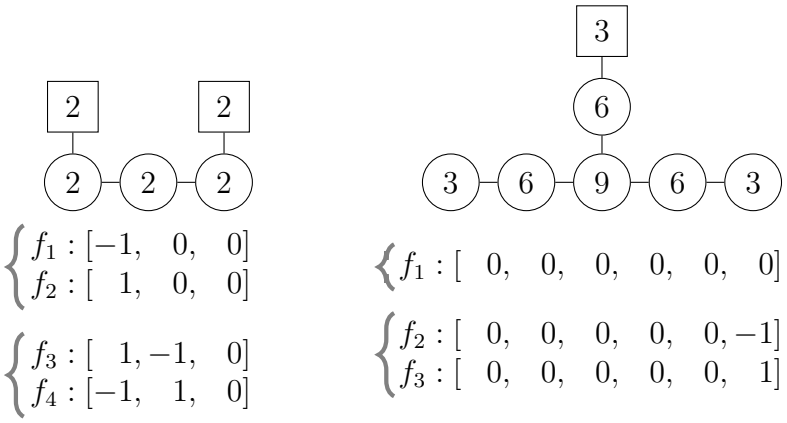

Figure 6.6: Left: a four-punctured sphere of A_3, with two maximal (full) punctures and two minimal (simple) punctures, both denoted by the parabolic subalgebra $\mathfrak{p}_{\{\alpha_2,\alpha_3\}}$. The two simple punctures indicate that there are two subsets of weights in $\mathcal{W}_{\mathcal{S}}$ that add up to zero. In this specific example, the fact that the weights $[1,-1,0]$ and $[-1,1,0]$ denote a simple puncture can easily be seen by applying a Weyl reflection about the first simple root of A_3. Right: a four-punctured sphere of E_6, with two maximal punctures and two other punctures; the first of these is the minimal puncture, denoted by the zero weight in the 6-th fundamental representation, and is unpolarized. The second puncture is polarized, and distinguishes the parabolic subalgebra $\mathfrak{p}_{\{\alpha_1,\alpha_2,\alpha_3,\alpha_4,\alpha_5\}}$.

Chapter 7

Examples

7.1 A_n Examples

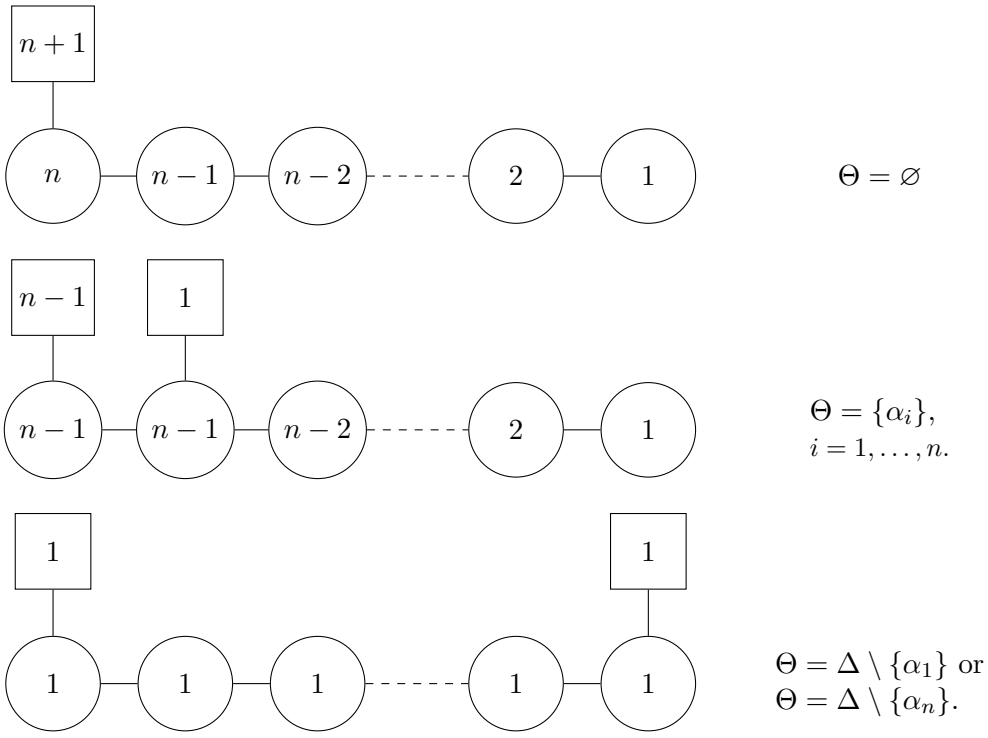

Figure 7.1: The top quiver is the full puncture, denoted by the partition $[1^{n+1}]$. The middle quiver is the next to maximal puncture, with partition $[2, 1^{n-1}]$. The bottom quiver is the simple puncture. It is denoted by the partition $[n, 1]$, and has two associated parabolic subalgebras: $\mathfrak{p}_{\Delta\setminus\{\alpha_1\}}$ and $\mathfrak{p}_{\Delta\setminus\{\alpha_n\}}$.

We can explicitly write the parabolic subalgebras in some representation; for A_n, it is customary to do so in the fundamental representation. Therefore, in what follows, the

matrices are valued in $\mathfrak{sl}(n+1)$; a star $*_i$ denotes a nonzero complex number, and the label "i" stands for the positive root e_i. A star $*_{-i}$ denotes a nonzero complex number, and the label "$-i$" stands for the negative root $-e_i$. Unless specified otherwise, a partition refers to a semi-simple element denoting the Higgs field structure of the theory. These partitions are related to the nilpotent element partitions from section 4 by transposition in the A_n case, and more generally by the Spaltenstein map (cf. [19]).

Maximal ("full") Puncture

We start with the set $\mathcal{W}_{\mathcal{S}}$ of all weights in the n-th fundamental representation (antifundamental). Writing w_i for the highest weight of the i-th fundamental representation, the weights can be written as:

$$\begin{aligned}
\omega_1 &= -w_1 \\
\omega_2 &= -w_1 + \alpha_1 \\
\omega_3 &= -w_1 + \alpha_1 + \alpha_2 \\
\vdots \quad &= \quad \vdots \\
\omega_{n+1} &= -w_1 + \alpha_1 + \alpha_2 + \ldots + \alpha_n,
\end{aligned}$$

from which we read the top 2d quiver in Figure 7.1. This is called the full puncture. We compute the inner product of the weights with the positive roots:

$\omega_1 \equiv [-1, 0, 0, \ldots, 0]$ has a negative inner product with:
$\alpha_1\ ,\ \alpha_1 + \alpha_2\ ,\ \ldots,\ \alpha_1 + \alpha_2 + \ldots + \alpha_n$

$\omega_2 \equiv [1, -1, 0, \ldots, 0]$ has a negative inner product with:
$\alpha_2\ ,\ \alpha_2 + \alpha_3\ ,\ \ldots,\ \alpha_2 + \alpha_3 + \ldots + \alpha_n$

$\omega_3 \equiv [0, 1, -1, 0, \ldots, 0]$ has a negative inner product with:
$\alpha_3\ ,\ \alpha_3 + \alpha_4\ ,\ \ldots,\ \alpha_3 + \alpha_4 + \ldots + \alpha_n$
$\vdots \qquad\qquad\qquad\qquad\qquad\qquad \vdots$
$\omega_{n+1} \equiv [0, \ldots, 0, 0, 1]$ has no negative inner product with any of the positive roots.

Since all of the positive roots of $\mathfrak{g}$ have a negative inner product with some weight, they define the nilradical $\mathfrak{n}_{\varnothing}$. The parabolic subalgebra is $\mathfrak{p}_{\varnothing}$. It is denoted by the partition $[1^{n+1}]$, which is immediately readable from the Levi subalgebra with symmetry $S(U(1)^{n+1})$.

The Levi decomposition gives:

$$\mathfrak{p}_\varnothing = \begin{pmatrix} * & *_1 & *_{1+2} & \cdots & *_{1+\ldots+(n-1)} & *_{1+\ldots+n} \\ 0 & * & *_2 & \cdots & \cdots & *_{2+\ldots+n} \\ \vdots & \ddots & \ddots & \ddots & \vdots & \vdots \\ \vdots & & \ddots & \ddots & *_{(n-1)} & *_{(n-1)+n} \\ \vdots & & & \ddots & * & *_n \\ 0 & \cdots & \cdots & \cdots & 0 & * \end{pmatrix},$$

with $\mathfrak{p}_\varnothing = \mathfrak{l}_\varnothing \oplus \mathfrak{n}_\varnothing$, where

$$\mathfrak{l}_\varnothing = \begin{pmatrix} * & 0 & \cdots & \cdots & \cdots & 0 \\ 0 & * & \ddots & & & \vdots \\ \vdots & \ddots & \ddots & \ddots & & \vdots \\ \vdots & & \ddots & \ddots & \ddots & \vdots \\ \vdots & & & \ddots & * & 0 \\ 0 & \cdots & \cdots & \cdots & 0 & * \end{pmatrix}$$

and

$$\mathfrak{n}_\varnothing = \begin{pmatrix} 0 & *_1 & *_{1+2} & \cdots & *_{1+\ldots+(n-1)} & *_{1+\ldots+n} \\ 0 & 0 & *_2 & \cdots & \cdots & *_{2+\ldots+n} \\ \vdots & \ddots & \ddots & \ddots & \vdots & \vdots \\ \vdots & & \ddots & \ddots & *_{(n-1)} & *_{(n-1)+n} \\ \vdots & & & \ddots & 0 & *_n \\ 0 & \cdots & \cdots & \cdots & 0 & 0 \end{pmatrix}.$$

We see explicitly that the nonzero inner products $\langle e_\gamma, \omega_i \rangle$ make up the i-th line of the nilradical $\mathfrak{n}_\varnothing$.

In this example, there is in fact one other set $\mathcal{W}_\mathcal{S}$ that singles out the nilradical $\mathfrak{n}_\varnothing$; it is the set of all weights in the first fundamental representation of A_n. The resulting 2d quiver is again the top one in Figure 7.1, but with reversed orientation.

Now we analyze this defect from the Toda CFT perspective: starting from our set $\mathcal{W}_\mathcal{S}$ and recalling that $\beta = \sum_{i=1}^{|\mathcal{W}_\mathcal{S}|} \hat{\beta}_i w_i$, $\mathcal{W}_\mathcal{S}$ defines the Toda momentum vector β. We can write

this momentum β explicitly as the semi-simple element $\mathrm{diag}(\beta_1, \beta_2, \ldots, \beta_{n+1})$, where all the entries add up to 0. One checks at once that the commutant of this element is the Levi subalgebra $\mathfrak{l}_\varnothing$ written above.

The flag manifold $T^*(G/\mathcal{P})$ associated to this defect also appears as the resolution of the Higgs branch of the same quiver,

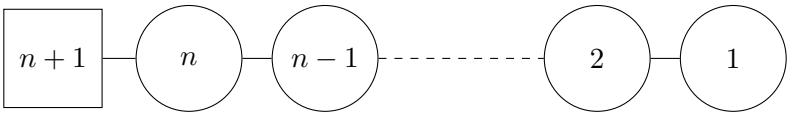

which is an instance of mirror symmetry, since the complete flag is self-mirror. Furthermore, it is easy to see from the method of section 4.2 that the nilpotent orbit associated to this theory is the maximal nilpotent orbit of A_n, denoted by the partition $[n+1]$.

Next to Maximal Puncture

We start by constructing the set $\mathcal{W}_\mathcal{S}$: Consider all the $n+1$ weights of the n-th fundamental representation. For each $1 \leq i \leq n$, the set contains two unique weights ω_i and ω_{i+1} such that $\alpha_i = \omega_i - \omega_{i+1}$, with α_i the i-th simple root. Remove ω_i and ω_{i+1} from the set, and replace them with the single weight $\omega' \equiv \omega_i + \omega_{i+1}$. ω' is always a weight in the $n-1$-th fundamental representation of A_n. Therefore, the set we consider is made of $n-1$ weights in the n-th fundamental representation, and the weight ω' in the $n-1$-th fundamental representation. It is easy to check that the sum of these weights is 0, so these n weights define a valid set $\mathcal{W}_\mathcal{S}$. The weights once again define a 2d quiver gauge theory T^{2d}; it is shown in the middle of Figure 7.1. All of the positive roots except the i-th simple root α_i have a negative inner product with at least one weight $\omega_i \in \mathcal{W}_\mathcal{S}$, so these positive roots define the nilradical $\mathfrak{n}_{\{\alpha_i\}}$.

For a given simple root α_i, the parabolic subalgebra is then $\mathfrak{p}_{\{\alpha_i\}}$. It is denoted by the partition $[2, 1^{n-1}]$, which is immediately readable from the Levi subalgebra with symmetry $S(U(2) \times U(1)^{n-1})$.

The Levi decomposition gives:

$$\mathfrak{p}_{\{\alpha_i\}} = \begin{pmatrix} * & *_1 & *_{1+2} & \cdots & \cdots & \cdots & \cdots & \cdots & *_{1+\ldots+(n-1)} & *_{1+\ldots+n} \\ 0 & * & *_2 & \cdots & \cdots & \cdots & \cdots & \cdots & \cdots & *_{2+\ldots+n} \\ \vdots & \ddots & \ddots & \ddots & & & & & \vdots & \vdots \\ \vdots & & \ddots & \ddots & \ddots & & & & \vdots & \vdots \\ \vdots & & & 0 & * & *_i & & & \vdots & \vdots \\ \vdots & & & & *_{-i} & * & \ddots & & \vdots & \vdots \\ \vdots & & & & & 0 & \ddots & \ddots & \vdots & \vdots \\ \vdots & & & & & & \ddots & \ddots & *_{(n-1)} & *_{(n-1)+n} \\ \vdots & & & & & & & \ddots & * & *_n \\ 0 & \cdots & \cdots & \cdots & \cdots & \cdots & \cdots & \cdots & 0 & * \end{pmatrix},$$

with $\mathfrak{p}_{\{\alpha_i\}} = \mathfrak{l}_{\{\alpha_i\}} \oplus \mathfrak{n}_{\{\alpha_i\}}$, where

$$\mathfrak{l}_{\{\alpha_i\}} = \begin{pmatrix} * & 0 & \cdots & \cdots & \cdots & \cdots & \cdots & 0 \\ 0 & * & \ddots & & & & & \vdots \\ \vdots & \ddots & \ddots & 0 & & & & \vdots \\ \vdots & & 0 & * & *_i & & & \vdots \\ \vdots & & & *_{-i} & * & 0 & & \vdots \\ \vdots & & & & 0 & \ddots & \ddots & \vdots \\ \vdots & & & & & \ddots & * & 0 \\ 0 & \cdots & \cdots & \cdots & \cdots & \cdots & 0 & * \end{pmatrix}$$

and

$$\mathfrak{n}_{\{\alpha_i\}} = \begin{pmatrix} 0 & *_1 & *_{1+2} & \cdots & \cdots & \cdots & \cdots & \cdots & *_{1+\ldots+(n-1)} & *_{1+\ldots+n} \\ 0 & 0 & *_2 & \cdots & \cdots & \cdots & \cdots & \cdots & \cdots & *_{2+\ldots+n} \\ \vdots & \ddots & \ddots & \ddots & & & & & \vdots & \vdots \\ \vdots & & \ddots & \ddots & *_{i-1} & & & & \vdots & \vdots \\ \vdots & & & \ddots & 0 & 0 & & & \vdots & \vdots \\ \vdots & & & & 0 & 0 & *_{i+1} & & \vdots & \vdots \\ \vdots & & & & & \ddots & \ddots & \ddots & \vdots & \vdots \\ \vdots & & & & & & \ddots & \ddots & *_{(n-1)} & *_{(n-1)+n} \\ \vdots & & & & & & & \ddots & 0 & *_n \\ 0 & \cdots & \cdots & \cdots & \cdots & \cdots & \cdots & \cdots & 0 & 0 \end{pmatrix}.$$

There is in fact another set $\mathcal{W}_\mathcal{S}$ that spells out the nilradical $\mathfrak{n}_{\{\alpha_i\}}$ for fixed α_i; just as for the full puncture, the corresponding 2d quiver would be the middle one in Figure 7.1, but again with reversed orientation.

Now we rederive this result from the Toda CFT perspective: consider once again the set $\mathcal{W}_\mathcal{S}$. We define the momentum vector β from $\beta = \sum_{i=1}^{|\mathcal{W}_\mathcal{S}|} \hat{\beta}_i \omega_i$. It is easy to check that

$$\langle \beta, \alpha_i \rangle = 0$$

for the simple root α_i, since β has a unique 0 as its i-th Dynkin label. This defines a null state at level 1 in the CFT. One can easily check that there is only one other set $\mathcal{W}_\mathcal{S}$ such that $\langle \beta, \alpha_i \rangle = 0$; this alternate choice gives the reflection of our 2d quiver. Also note that the commutant of the semi-simple element β is the Levi subalgebra $\mathfrak{l}_{\alpha_i}$ written above in the fundamental representation.

We make the following important observations:

- This puncture is in fact described by many sets $\mathcal{W}_\mathcal{S}$. To obtain them, one simply considers all possible Weyl group actions that preserve the root sign: $w(\alpha_i)$ must be a positive root. Then all possible momenta are given by $\beta' = w(\beta)$. Note that the condition $\langle \beta, \alpha_i \rangle = 0$ is Weyl invariant: $\langle \beta, \alpha_i \rangle = \langle \beta', w(\alpha_i) \rangle$. Therefore, from the CFT perspective, the momentum of this different theory satisfies instead:

  $$\langle \beta', w(\alpha_i) \rangle = 0.$$

  Because $w(\alpha_i)$ is a positive *non*-simple root, this is strictly speaking a higher than level-1 null state condition of A_n-Toda. As explained in section 5.1, this higher level distinction is not relevant in the semi-classical limit $\hbar \to 0$ (or $Q \to 0$ in Toda), which

is enough for our purposes. The explicit null state for all the theories obtained from the sets $\mathcal{W}_{\mathcal{S}}$ can then be written at level 1, it is

$$\left(W_{-1}^{(n+1)} + \beta_i W_{-1}^{(n)} + \beta_i^2 W_{-1}^{(n-2)} + \cdots + \beta_i^{n-1} W_{-1}^{(2)}\right) |\vec{\beta}\rangle. \tag{7.1}$$

Here, $W_{-1}^{(j)}$ is the mode -1 of the spin j generator, and β_i is the i-th entry of β, written in the fundamental representation, where i labels the singled-out simple root α_i. The eigenvalues of the $W_0^{(j)}$ modes are then functions of all the entries of β.

- All of the many different sets $\mathcal{W}_{\mathcal{S}}$ mentioned above give rise to the same 2d quiver gauge theory, in the middle of Figure 7.1.
- The definition of the weight $\omega' \equiv \omega_i + \omega_{i+1}$ above is an illustration of the weight addition rule from section 6.1. This corresponds to moving on the Higgs branch, and transitioning from the top quiver to the middle quiver in Figure 7.1. In gauge theory terms, when the hypermultiplet masses for ω_i and ω_{i+1} of the full puncture are set equal, one can transition from the top 2d theory to the middle 2d theory, which has a single hypermultiplet mass for ω' instead.
- The nilpotent orbit associated to this puncture is the unique subregular nilpotent orbit of A_n, with partition $[n, 1]$.

The flag manifold $T^*(G/\mathcal{P})$ also appears as the resolution of the Higgs branch of the quiver

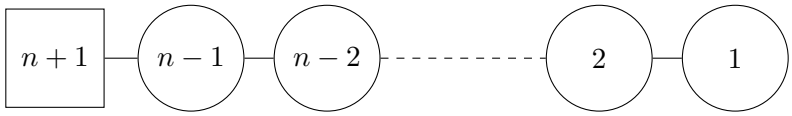

which is again mirror to ours.

Minimal ("simple") Puncture

We start by constructing the set $\mathcal{W}_{\mathcal{S}}$. Writing w_i for the highest weight of the i-th fundamental representation, we define $\mathcal{W}_{\mathcal{S}}$ as:

$$\begin{aligned} \omega_1 &= -w_n, \\ \omega_2 &= -w_1 + \alpha_1 + \alpha_2 + \ldots + \alpha_n. \end{aligned}$$

Written as above, the weights spell out the 2d quiver at the bottom of Figure 7.1. This is called the simple puncture. We compute the inner product of the weights with the positive roots:

$\omega_1 \equiv [0, 0, \ldots, 0, -1]$ has a negative inner product with:
$\alpha_n,\ \alpha_n + \alpha_{n-1},\ \ldots,\ \alpha_n + \alpha_{n-1} + \ldots + \alpha_1$

$\omega_2 \equiv [0, 0, \ldots, 0, \quad 1]$ has no negative inner product with any of the positive roots.

So the only positive roots of $\mathfrak{g}$ that have a negative inner product with some weight $\omega_i \in \mathcal{W}_{\mathcal{S}}$ are $\alpha_n,\ \alpha_n + \alpha_{n-1},\ \ldots,\ \alpha_n + \alpha_{n-1} + \ldots + \alpha_1$, and they define the nilradical $\mathfrak{n}_{\Delta\setminus\{\alpha_n\}}$. The parabolic subalgebra is then $\mathfrak{p}_{\Delta\setminus\{\alpha_n\}}$. It is denoted by the partition $[n, 1]$, which is immediately readable from the Levi subalgebra with symmetry $S(U(n) \times U(1))$. The Levi decomposition gives:

$$\mathfrak{p}_{\Delta\setminus\{\alpha_n\}} = \begin{pmatrix} * & *_1 & *_{1+2} & \cdots & \cdots & *_{1+\ldots+(n-1)} & *_{1+\ldots+n} \\ *_{-1} & * & *_2 & \cdots & \cdots & *_{2+\ldots+(n-1)} & *_{2+\ldots+n} \\ *_{-(1+2)} & *_{-2} & * & \cdots & \cdots & *_{3+\ldots+(n-1)} & *_{3+\ldots+n} \\ \vdots & \vdots & \vdots & \ddots & \cdots & \vdots & \vdots \\ \vdots & \vdots & \vdots & \cdots & \ddots & *_{(n-1)} & *_{(n-1)+n} \\ *_{-(1+\ldots+(n-1))} & *_{-(2+\ldots+(n-1))} & *_{-(3+\ldots+(n-1))} & \cdots & *_{-(n-1)} & * & *_n \\ 0 & 0 & 0 & \cdots & 0 & 0 & * \end{pmatrix},$$

with $\mathfrak{p}_{\Delta\setminus\{\alpha_n\}} = \mathfrak{l}_{\Delta\setminus\{\alpha_n\}} \oplus \mathfrak{n}_{\Delta\setminus\{\alpha_n\}}$, where

$$\mathfrak{l}_{\Delta\setminus\{\alpha_n\}} = \begin{pmatrix} * & *_1 & *_{1+2} & \cdots & \cdots & *_{1+\ldots+(n-1)} & 0 \\ *_{-1} & * & *_2 & \cdots & \cdots & *_{2+\ldots+(n-1)} & 0 \\ *_{-(1+2)} & *_{-2} & * & \cdots & \cdots & *_{3+\ldots+(n-1)} & 0 \\ \vdots & \vdots & \vdots & \ddots & \cdots & \vdots & \vdots \\ \vdots & \vdots & \vdots & \cdots & \ddots & *_{(n-1)} & 0 \\ *_{-(1+\ldots+(n-1))} & *_{-(2+\ldots+(n-1))} & *_{-(3+\ldots+(n-1))} & \cdots & *_{-(n-1)} & * & 0 \\ 0 & 0 & 0 & \cdots & 0 & 0 & * \end{pmatrix}$$

and

$$\mathfrak{n}_{\Delta\setminus\{\alpha_n\}} = \begin{pmatrix} 0 & \cdots & \cdots & \cdots & \cdots & 0 & *_{1+\ldots+n} \\ \vdots & \ddots & & & & \vdots & *_{2+\ldots+n} \\ \vdots & & \ddots & & & \vdots & *_{3+\ldots+n} \\ \vdots & & & \ddots & & \vdots & \vdots \\ \vdots & & & & \ddots & \vdots & *_{(n-1)+n} \\ 0 & \cdots & \cdots & \cdots & \cdots & 0 & *_n \\ 0 & \cdots & \cdots & \cdots & \cdots & 0 & 0 \end{pmatrix}.$$

We see explicitly that the non-zero inner products $\langle e_\gamma, \omega_i \rangle$ give the last column of the nilradical $\mathfrak{n}_{\Delta\setminus\{\alpha_n\}}$.

Now we rederive this result from the CFT perspective: consider once again the set $\mathcal{W}_\mathcal{S}$. We define the momentum vector β from $\beta = \sum_{i=1}^{|\mathcal{W}_\mathcal{S}|} \hat{\beta}_i \omega_i$. It is easy to check that

$$\langle \beta, \alpha_i \rangle = 0, \qquad\qquad i = 1, 2, \ldots, n-1$$

since β has a 0 as its i-th Dynkin label for $i = 1, 2, \ldots, n-1$. This defines many level 1 null states in the CFT. One can easily check that no other set $\mathcal{W}_\mathcal{S}$ satisfies the above vanishing inner product conditions. Also note that the commutant of the semi-simple element β is the Levi subalgebra $\mathfrak{l}_{\Delta\setminus\{\alpha_n\}}$ written above in the fundamental representation.

We make the following important observations:

- This puncture is in fact described by many sets $\mathcal{W}_\mathcal{S}$. To obtain them, one simply considers all possible Weyl group actions that preserve the root sign: $w(\alpha_i)$ must be a positive root; the details are in the previous example. The upshot is once again that the explicit null states for all these 2d theories can be written at level 1; they are:

$$\left(W_{-1}^{(n+1)} + \beta W_{-1}^{(n)} + \beta^2 W_{-1}^{(n-2)} + \ldots + \beta^{n-1} W_{-1}^{(2)}\right) |\vec{\beta}\rangle, \tag{7.2}$$

  and the $n-1$ derivatives of this equation with respect to β:

$$\begin{aligned}
&\left(W_{-1}^{(n)} + 2\beta W_{-1}^{(n-2)} + \ldots + (n-1)\beta^{n-2} W_{-1}^{(2)}\right) |\vec{\beta}\rangle \\
&\left(2W_{-1}^{(n-2)} + \ldots + (n-1)(n-2)\beta^{n-3} W_{-1}^{(2)}\right) |\vec{\beta}\rangle \\
&\quad\vdots \\
&W_{-1}^{(2)} |\vec{\beta}\rangle
\end{aligned}$$

  Here, $W_{-1}^{(j)}$ is the mode -1 of the spin j generator, and $\vec{\beta}$=diag$(\beta, \beta, \ldots, \beta, -n\beta)$, written in the fundamental representation. The eigenvalues of the $W_0^{(j)}$ modes are again functions of β.

- All the many different sets $\mathcal{W}_\mathcal{S}$ mentioned above give rise to the same 2d quiver gauge theory, in the bottom of Figure 7.1, and they all characterize the parabolic subalgebra $\mathfrak{p}_{\Delta\setminus\{\alpha_n\}}$, even if not directly readable from the positive root inner products with the Weyl reflected weights.

- Once again, we can use the weight addition procedure to move on the Higgs branch, and transition from the top quiver to the bottom quiver in Figure 7.1. In gauge theory terms, when the hypermultiplet masses for ω_1, ω_2, …, ω_n of the full puncture are set

equal, one can transition from the top 2d theory to the bottom 2d theory, which has a single hypermultiplet mass for the single weight $\omega_1 + \omega_2 + \ldots + \omega_n$ instead. Explicitly,

$$[-1, 0, 0, \ldots, 0] + [1, -1, 0, \ldots, 0] + \ldots + [0, \ldots, 0, 1, -1] = [0, 0, \ldots, 0, -1].$$

- The nilpotent orbit for this theory is the minimal non-trivial orbit of A_n, with partition $[1^{n+1}]$.

The flag manifold $T^*(G/\mathcal{P})$ associated to this defect also appears as the resolution of the Higgs branch of the quiver

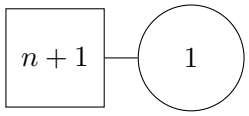

which is the Grassmanian $G(1, n+1)$. Note this is again precisely mirror to our quiver theory T^{2d}.

7.2 D_n Examples: Polarized Theories

Examples for Arbitrary n

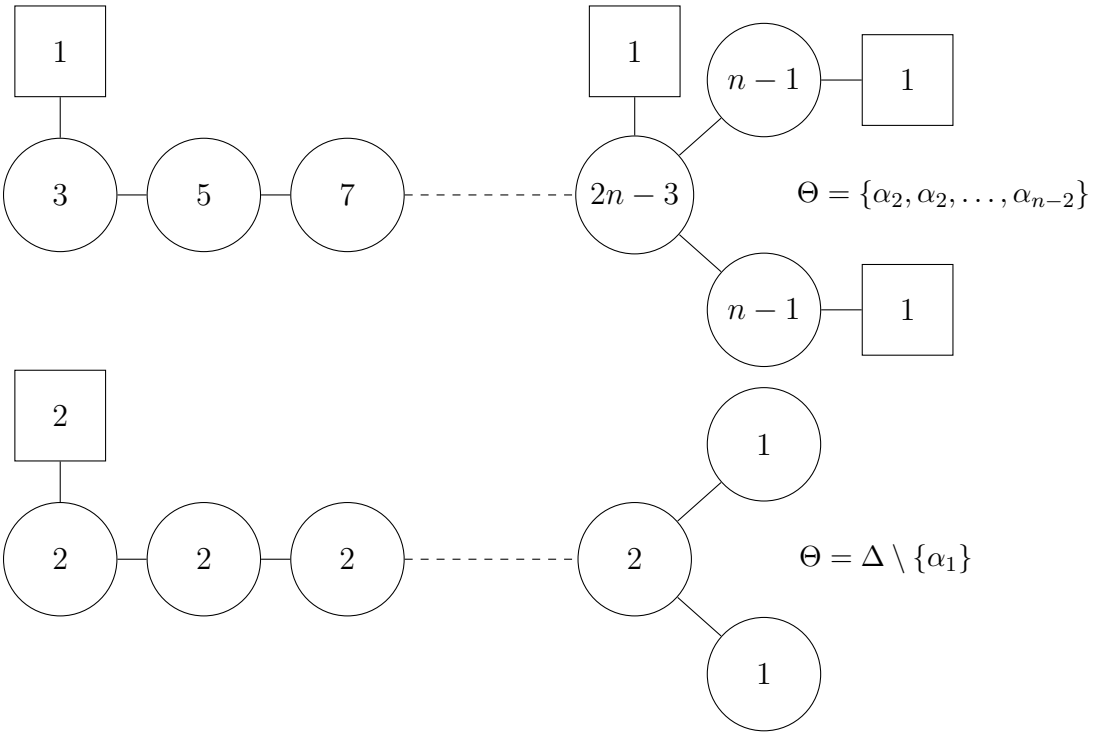

Figure 7.2: The top quiver is a nontrivial puncture characterized by the parabolic subalgebra $\mathfrak{p}_{\{\alpha_2,\alpha_3,\ldots,\alpha_{n-2}\}}$. It is denoted by the partition $[(n-2)^2, 1^4]$ in the fundamental representation. The bottom quiver is the simple puncture of D_n, characterized by the parabolic subalgebra $\mathfrak{p}_{\Delta\setminus\{\alpha_1\}}$. It is denoted by the partition $[2n-2, 1^2]$.

Here, we give two nontrivial D_n examples. We proceed as in the A_n case and start by constructing a valid set of weights $\mathcal{W}_\mathcal{S}$:

$$\begin{aligned}
\omega_1 &\equiv [\ \ 1, 0, \ldots, 0, \ \ 0, \ \ 0], \\
\omega_2 &\equiv [\ \ 0, 0, \ldots, 0, -1, \ \ 0], \\
\omega_3 &\equiv [\ \ 0, 0, \ldots, 0, \ \ 0, -1], \\
\omega_4 &\equiv [-1, 0, \ldots, 0, \ \ 1, \ \ 1].
\end{aligned}$$

These weights obviously add up to 0, so they define a valid set $\mathcal{W}_{\mathcal{S}}$. Now note that:

$$\begin{aligned}
\omega_1 &= -w_1 + 2e_1 + 2e_2 + \ldots + 2e_{n-2} + e_{n-1} + e_n \\
\omega_2 &= -w_{n-2} + e_1 + 3e_2 + 5e_3 \ldots + (2n-5)e_{n-2} + (n-2)e_{n-1} + (n-2)e_n \\
\omega_3 &= -w_{n-1} \\
\omega_4 &= -w_n
\end{aligned}$$

This defines the 2d quiver gauge theory T^{2d} shown on top of Figure 7.2. Computing $\langle e_\gamma, \omega_i \rangle$ for all positive roots e_γ, we identify the nilradical $\mathfrak{n}_{\{\alpha_2,\alpha_3,\ldots,\alpha_{n-2}\}}$. Therefore, we associate to $\mathcal{W}_{\mathcal{S}}$ the parabolic subalgebra $\mathfrak{p}_{\{\alpha_2,\alpha_3,\ldots,\alpha_{n-2}\}}$ from the Levi decomposition.

Now we rederive this result from the CFT perspective: consider once again the set $\mathcal{W}_{\mathcal{S}}$. We define the momentum vector β from $\beta = \sum_{i=1}^{|\mathcal{W}_{\mathcal{S}}|} \hat{\beta}_i \omega_i$. It is easy to check that

$$\langle \beta, \alpha_i \rangle = 0, \qquad i = 2, 3, \ldots, n-2$$

since β has a 0 as its i-th Dynkin label for $i = 2, 3, \ldots, n-2$. This defines many level 1 null states in the CFT. One can easily check that no other set $\mathcal{W}_{\mathcal{S}}$ satisfies $\langle \beta, \alpha_i \rangle = 0$. Also note that the commutant of the semi-simple element β is the Levi subalgebra $\mathfrak{l}_{\{\alpha_2,\alpha_3,\ldots,\alpha_{n-2}\}}$.

We make the following important observations:

- This puncture features the instance of a new phenomenon: there are in fact many 2d quivers associated to the parabolic subalgebra $\mathfrak{p}_{\{\alpha_2,\alpha_3,\ldots,\alpha_{n-2}\}}$. We just exhibited one possible 2d quiver among many valid others.

- Just as in the A_n case, there are many different sets $\mathcal{W}_{\mathcal{S}}$ for each 2d quiver, which do not directly allow us to read off the parabolic subalgebra. The upshot is once again that the explicit null states for all these sets $\mathcal{W}_{\mathcal{S}}$ can be written at level 1; they are given by:

$$\left((\tilde{W}^{(n)})^2_{-1} + \beta^2 W^{(2n-2)}_{-1} + \beta^4 W^{(2n-4)}_{-1} + \cdots + \beta^{2n-2} W^{(2)}_{-1} \right) |\vec{\beta}\rangle \tag{7.3}$$

  and derivatives of this equation with respect to β. Here, $W^{(j)}_{-1}$ is the mode -1 of the spin j generator. In the split representation of $\mathfrak{so}(2n)$, a generic semi-simple element is $\vec{\beta} = \mathrm{diag}(\beta_1, \beta_2, \ldots, \beta_n, -\beta_1, -\beta_2, \ldots, -\beta_n)$. The puncture we study sets $n-2$ entries β_i equal to each other; call them β (and so $n-2$ entries $-\beta_i$ become $-\beta$). It is this parameter β that appears in the null state (7.3).

- We can also identify the nilpotent orbit corresponding to this theory: for even n, it is given by the partition $[5, 3, 2^{n-4}]$, and for odd n, the orbit has the partition $[5, 3, 2^{n-5}, 1, 1]$ (this agrees with the results of [16].)

We now turn to the second example. We start with the set of weights:

$$\omega_1 \equiv [\ \ 1, 0, 0, \ldots, 0] = -w_1 + 2e_1 + 2e_2 + \ldots + 2e_{n-2} + e_{n-1} + e_n$$
$$\omega_2 \equiv [-1, 0, 0, \ldots, 0] = -w_1$$

These weights obviously add up to 0, so they define a valid set $\mathcal{W}_\mathcal{S}$. Written as above, they spell out a 2d quiver theory T^{2d} shown at the bottom of Figure 7.2. Computing $\langle e_\gamma, \omega_i \rangle$ for all positive roots e_γ, we identify the nilradical $\mathfrak{n}_{\Delta\setminus\{\alpha_1\}}$. So we associate to $\mathcal{W}_\mathcal{S}$ the parabolic subalgebra $\mathfrak{p}_{\Delta\setminus\{\alpha_1\}}$ from the Levi decomposition. Unlike the previous example, the 2d quiver theory associated to this puncture is unique. All other possible sets $\mathcal{W}_\mathcal{S}$ are then obtained by Weyl reflection.

The nilpotent orbit corresponding to this theory is the minimal non-trivial orbit in D_n, with partition $[3, 1^{2n-2}]$.

The corresponding space $T^*(G/\mathcal{P})$ also appears as the resolution of the Higgs branch of the quiver

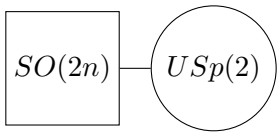

Note that this quiver theory is again mirror to ours.

Complete D_4 Classification

In Figure 7.3 we give the full classification of surface defects for D_4: the left column shows a representative quiver T^{2d} from [3] that describes each puncture. The middle column shows the subset of simple roots Θ which defines the parabolic subalgebra associated to $T^{2d}_{m_s\to\infty}$. The right column features all the nilpotent orbits, in the notation of [16], as Hitchin Young diagrams. Note that lines 2 to 5 on the left denote one and the same nilpotent orbit, but different parabolic subalgebras. More subtle is the fact that lines 2 and 3 on the right feature the same Young diagram, but that is just an unfortunate misfortune in the notation: they really denote distinct nilpotent orbits and parabolic subalgebras; the Levi decompositions indeed yield two distinct nilradicals. An asterisk is written down to differentiate those two punctures. In order to specify which of the three parabolic subalgebras the left 2d quiver of line 6 is associated to, one would need to specify explicitly the set $\mathcal{W}_\mathcal{S}$ that defines it. We omitted writing $\mathcal{W}_\mathcal{S}$ for brevity.

The nilpotent orbit classification of punctures has a disadvantage: two distinct punctures can be associated to one and the same Hitchin Young diagram (see for instance lines 2 and 3 on the right in Figure 7.3), so extra data is needed to differentiate them. Classifying the CFT defects from the little string perspective, on the other hand, every polarized puncture in the

classification is associated to a distinct parabolic subalgebra. Unpolarized punctures, however, have to be added separately. For D_4, there is exactly one such unpolarized puncture: the one featuring the null weight $[0, 0, 0, 0]$; we show the explicit quiver theory T^{2d} in the section 7.4. It is interesting to note that special and non-special punctures in the classification of [17] are treated on an equal footing in the little string formalism.

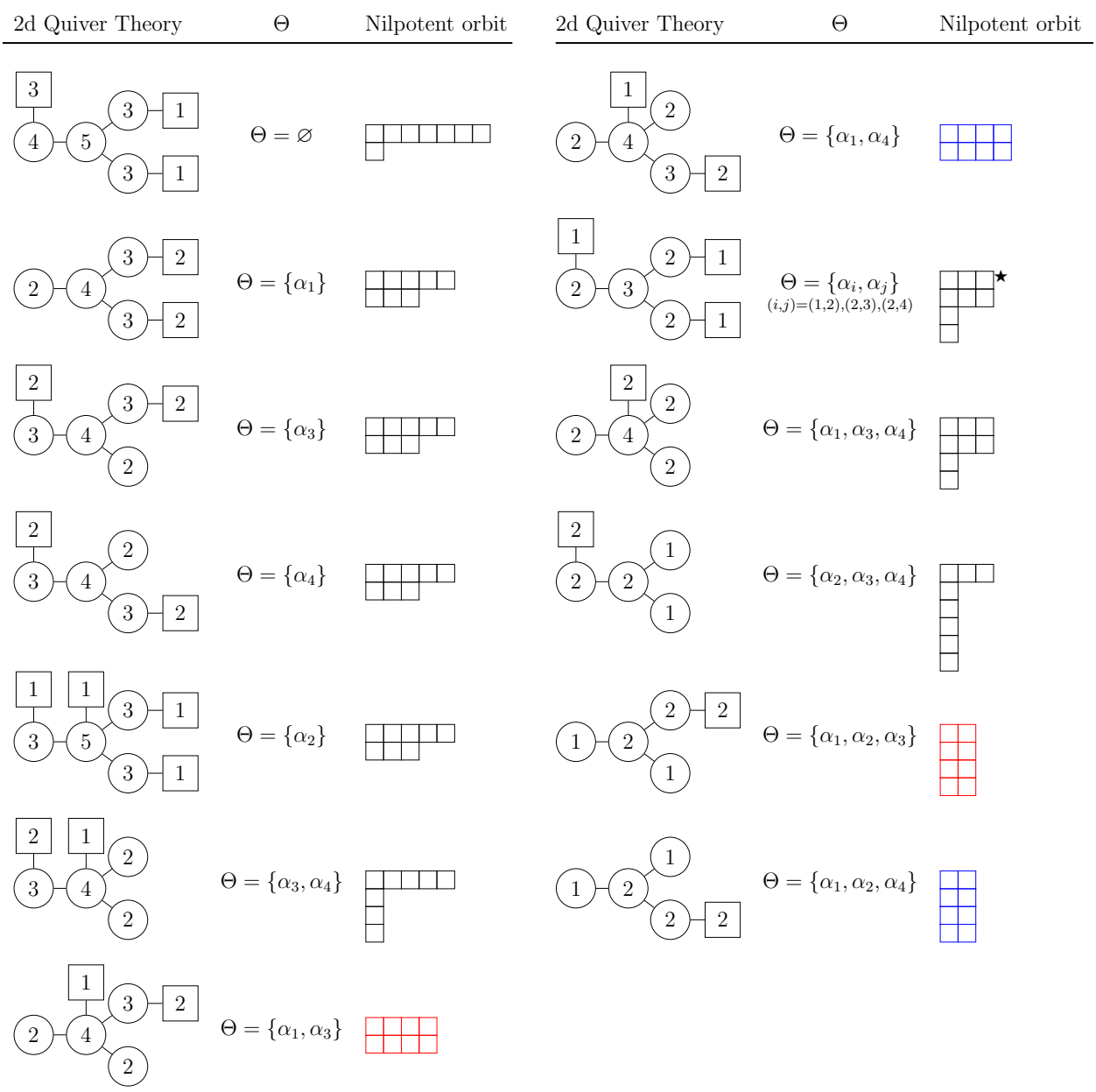

Figure 7.3: Surface defects of D_4. 2d quiver theories from the Little String are shown in the left column. Parabolic subalgebras that arise in the CFT limit $T^{2d}_{m_s\to\infty}$ are shown in the middle column. Nilpotent orbits from the defect classification of [16] are shown in the right column. We omitted writing down an explicit set of weights $\mathcal{W}_{\mathcal{S}}$ for each defect for brevity. The minimal nilpotent orbit is analyzed separately in section 7.4.

7.3 E_n Examples: Polarized Theories

Here, we give the quivers of E_n with the smallest number of Coulomb moduli that describe a polarized puncture.

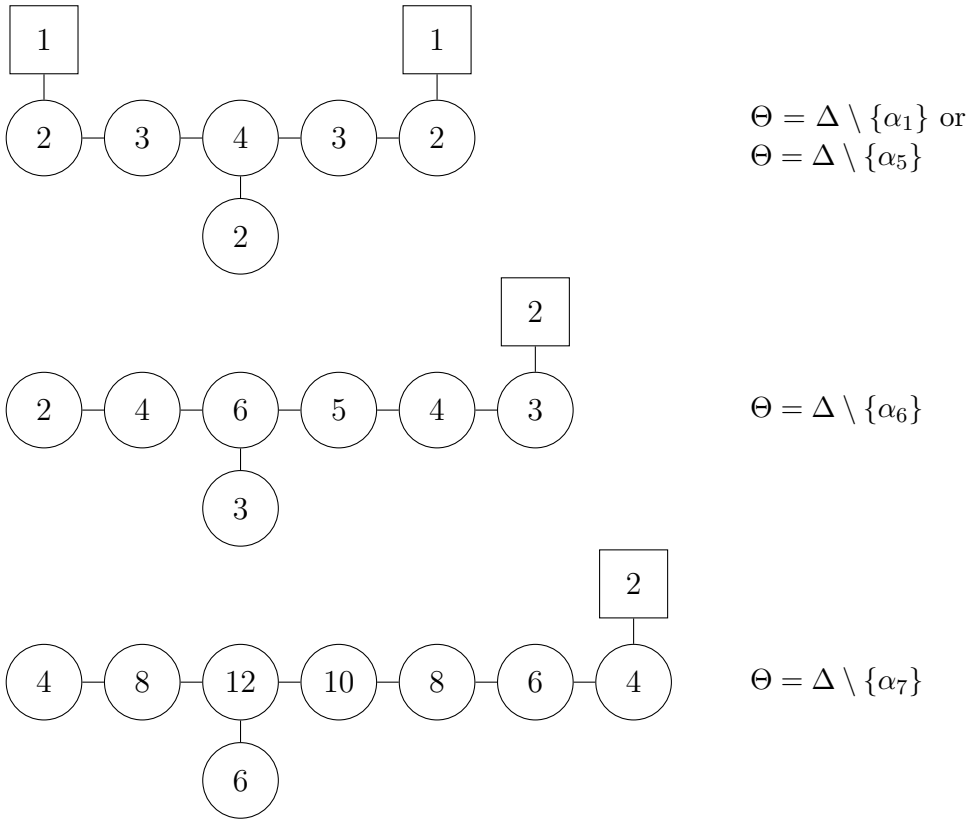

Figure 7.4: The top, middle, and bottom quivers are E_6, E_7, and E_8 2d theories respectively. The associated parabolic subalgebras are $\mathfrak{p}_{\Delta\setminus\{\alpha_1\}}$, $\mathfrak{p}_{\Delta\setminus\{\alpha_6\}}$, and $\mathfrak{p}_{\Delta\setminus\{\alpha_7\}}$ respectively. These punctures all have Bala-Carter label $2A_1$ in the classification of [17].

For E_6, we start with the set $\mathcal{W}_{\mathcal{S}}$:

$$\omega_1 \equiv [\ \ 1,0,0,0,0,0] = -w_5 + 2\alpha_1 + 3\alpha_2 + 4\alpha_3 + 2\alpha_4 + \alpha_5 + 2\alpha_6$$
$$\omega_2 \equiv [-1,0,0,0,0,0] = -w_1$$

This defines a 2d theory (shown in Figure 7.4). One checks at once from the positive roots that $\mathcal{W}_{\mathcal{S}}$ characterizes the nilradical $\mathfrak{n}_{\Delta\setminus\{\alpha_1\}}$, so the associated parabolic subalgebra is $\mathfrak{p}_{\Delta\setminus\{\alpha_1\}}$. In fact, no other set $\mathcal{W}_{\mathcal{S}}$ is associated to this parabolic subalgebra. The level 1 null state condition in the E_6-Toda CFT is:

$$\langle \beta, \alpha_i \rangle = 0, \qquad\qquad i = 2, \ldots, 6$$

The set $\mathcal{W}_{\mathcal{S}}$:

$$\omega_1 \equiv [0,0,0,0,\quad 1,0] = -w_1 + 2\alpha_1 + 3\alpha_2 + 4\alpha_3 + 2\alpha_4 + \alpha_5 + 2\alpha_6,$$
$$\omega_2 \equiv [0,0,0,0,-1,0] = -w_5,$$

produces the same 2d quiver as above, but the associated parabolic subalgebra is instead $\mathfrak{p}_{\Delta\setminus\{\alpha_5\}}$, and the level 1 null state condition is:

$$\langle \beta, \alpha_i \rangle = 0, \qquad i = 1,2,3,4,6.$$

All the other possible sets $\mathcal{W}_{\mathcal{S}}$ associated to $\mathfrak{p}_{\Delta\setminus\{\alpha_1\}}$ are obtained by Weyl reflection on the two weights (and the same is true about $\mathfrak{p}_{\Delta\setminus\{\alpha_5\}}$).

For E_7, we start with the set $\mathcal{W}_{\mathcal{S}}$:

$$\omega_1 \equiv [0,0,0,0,0,\quad 1,0] = -w_6 + 2\alpha_1 + 4\alpha_2 + 6\alpha_3 + 5\alpha_4 + 4\alpha_5 + 3\alpha_6 + 3\alpha_7$$
$$\omega_2 \equiv [0,0,0,0,0,-1,0] = -w_6$$

This defines a 2d theory (shown in the middle of Figure 7.4). One checks at once from the positive roots that $\mathcal{W}_{\mathcal{S}}$ characterizes the nilradical $\mathfrak{n}_{\Delta\setminus\{\alpha_6\}}$, so the associated parabolic subalgebra is $\mathfrak{p}_{\Delta\setminus\{\alpha_6\}}$. In fact, no other set $\mathcal{W}_{\mathcal{S}}$ is associated to this parabolic subalgebra. The level 1 null state condition in the E_7-Toda CFT is:

$$\langle \beta, \alpha_i \rangle = 0, \qquad i = 1,2,3,4,5,7.$$

All the other possible sets $\mathcal{W}_{\mathcal{S}}$ associated to $\mathfrak{p}_{\Delta\setminus\{\alpha_6\}}$ are obtained by Weyl reflection on the two weights.

For E_8, we start with the set $\mathcal{W}_{\mathcal{S}}$:

$$\omega_1 \equiv [0,0,0,0,0,0,\quad 1,0] = -w_7 + 4e_1 + 8e_2 + 12e_3 + 10e_4 + 8e_5 + 6e_6 + 4e_7 + 6e_8$$
$$\omega_2 \equiv [0,0,0,0,0,0,-1,0] = -w_7$$

This defines a 2d theory (shown at the bottom of Figure 7.4). One checks at once from the positive roots that $\mathcal{W}_{\mathcal{S}}$ characterizes the nilradical $\mathfrak{n}_{\Delta\setminus\{\alpha_7\}}$, so the associated parabolic subalgebra is $\mathfrak{p}_{\Delta\setminus\{\alpha_7\}}$. In fact, no other set $\mathcal{W}_{\mathcal{S}}$ is associated to this parabolic subalgebra. The level 1 null state condition in the E_8-Toda CFT is:

$$\langle \beta, \alpha_i \rangle = 0, \qquad i = 1,2,3,4,5,6,8.$$

All the other possible sets $\mathcal{W}_{\mathcal{S}}$ that are associated to $\mathfrak{p}_{\Delta\setminus\{\alpha_7\}}$ are obtained by Weyl reflection on the two weights.

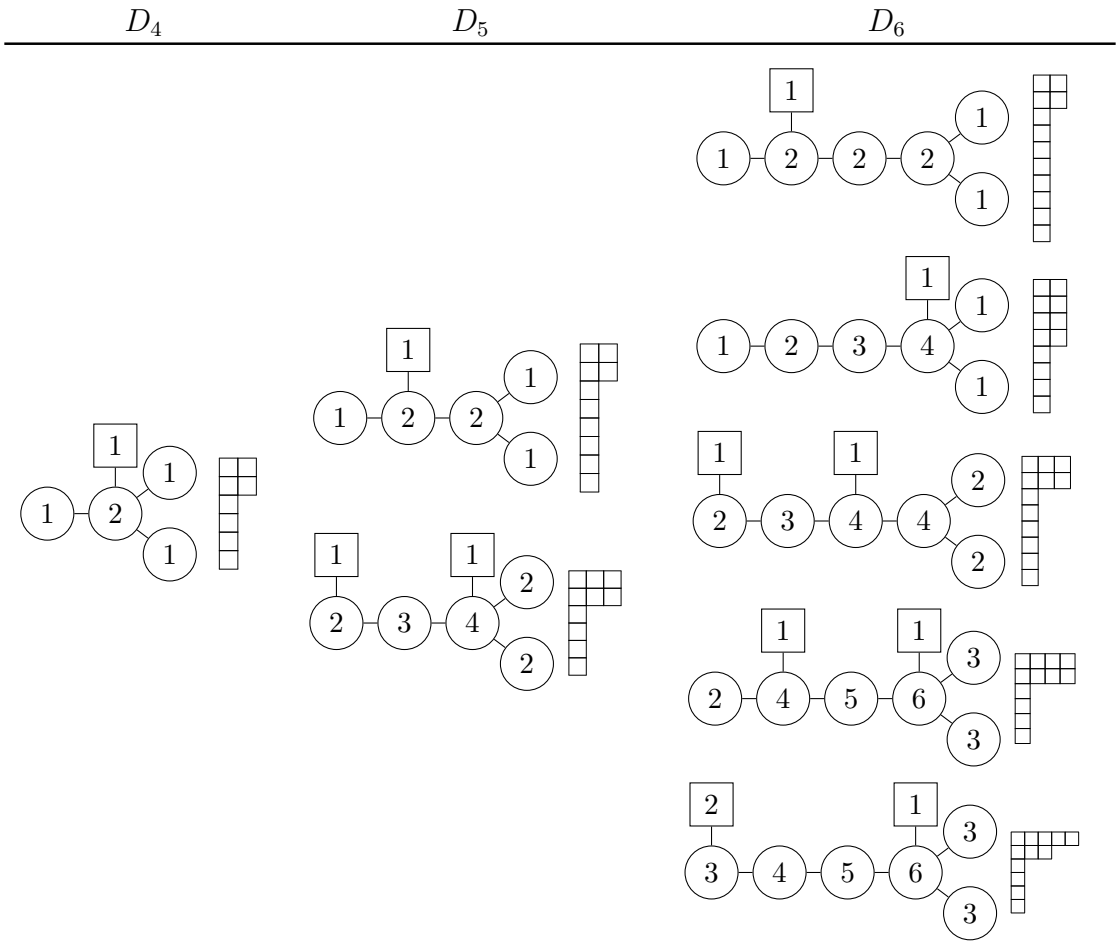

Figure 7.5: Exhaustive list of unpolarized quiver gauge theories T^{2d} for D_4, D_5, and D_6. The nilpotent orbit in the classification of [16] is also written for reference.

7.4 Unpolarized Theories

Here we give some examples of unpolarized theories for D_n and E_n only, since there is no such theory for A_n.

The simplest case of an unpolarized quiver gauge theory arises when only a single fundamental hypermultiplet is present, so there is only one mass. The corresponding weight is then the null weight, which is obviously not in the orbit of any fundamental weight. For instance, such a scenario occurs for the unique unpolarized theory of D_4, where the weight $[0, 0, 0, 0]$ is indeed in the second fundamental representation; see Figure 7.5 for examples in the D_n case, and Figure 7.6 for examples in the E_n case.

As explained in section 6.3, unpolarized theories can also have more than one weight: for

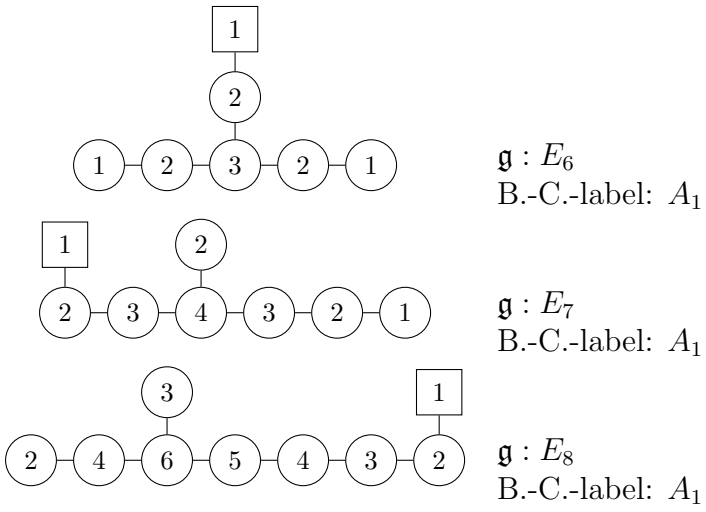

Figure 7.6: Examples of unpolarized quiver gauge theories for E_n. The ones shown here have the smallest Coulomb branch dimension. The Bala Carter label A_1 in the defect classification of [17] is also written for reference.

example, looking at D_5, it is possible to choose weights in the third fundamental representation that actually belong to the orbit of the first fundamental weight instead. One can then construct the bottom D_5 quiver of Figure 7.5. An example of two weights that make up such a quiver is $[1, 0, 0, 0, 0]$, chosen in the first fundamental representation, and $[-1, 0, 0, 0, 0]$, chosen in the third fundamental representation. If one wishes, it is always possible to flow on the Higgs branch and make these defects polarized, see 6.3.

Chapter 8

Bala–Carter Classification

As mentioned in chapter 4, defects of the 6d $(2,0)$ $\mathfrak{g}$-type CFT have been studied in the literature [17] in terms of *nilpotent orbits* of the algebra. We now want to give a more direct relationship between the physics construction of little string defects and these objects.

Recall that nilpotent orbits are directly related to the parabolic subalgebras we have been considering. Given a parabolic subalgebra with Levi decomposition $\mathfrak{p} = \mathfrak{l} \oplus \mathfrak{n}$, the nilpotent orbit $\mathcal{O}_\mathfrak{l}$ associated to $\mathfrak{p}$ is the maximal orbit containing a representative $X \in \mathcal{O}_\mathfrak{l}$ for which $X \in \mathfrak{n}$.

Many of the interesting properties of nilpotent orbits are related to the existence of a duality map: The *Spaltenstein map* [54] sends the set of nilpotent orbits of a simply-laced Lie algebra $\mathfrak{g}$ to itself, and reorganizes them.

For $\mathfrak{g} = A_n$, nilpotent orbits are in one-to-one correspondence with integer partitions of $n+1$ (or Young diagrams); for $\mathfrak{g} = D_n$, they can also be labeled by Young diagrams with $2n$ boxes that satisfy certain conditions (cf. the textbook [19] for more details.) However no such classification in terms of Young diagrams exists for the E_n algebras.

It proves fruitful instead to ignore Young diagrams altogether and resort to the classification of Bala and Carter [8, 9], which is valid for any semi-simple Lie algebra. We will see next that this is the natural language to describe the D3 brane defects in the low energy limit.

8.1 Bala–Carter Labeling of Nilpotent Orbits

Since there are only finitely many orbits in $\mathfrak{g}$, we want to find a convenient way of classifying them. One such classification scheme uses *Levi subalgebras* of $\mathfrak{g}$:

Recall that a Levi subalgebra $\mathfrak{l}$ of $\mathfrak{g}$ is a subalgebra of $\mathfrak{g}$ that can be written as:

$$\mathfrak{l} = \mathfrak{h} \oplus \bigoplus_{\alpha \in \langle \Theta \rangle} \mathfrak{g}_\alpha,$$

where $\mathfrak{h}$ is a Cartan subalgebra of $\mathfrak{g}$, Θ is an arbitrary subset of the simple roots of $\mathfrak{g}$, and $\mathfrak{g}_\alpha$ is the root space associated to a root in the additive closure of Θ.

Then, the idea of the Bala–Carter [8, 9] classification of nilpotent orbits is to label an orbit $\mathcal{O}$ by the smallest Levi subalgebra that contains a representative of $\mathcal{O}$. This is always unique if $\mathfrak{g} = A_n$, but for other algebras, two different nilpotent orbits can be associated to the same minimal Levi subalgebra.

In general, the following result holds: A nilpotent orbit $\mathcal{O}$ is uniquely specified by a Levi subalgebra $\mathfrak{l} \subset \mathfrak{g}$ and a certain (distinguished) parabolic subalgebra of $[\mathfrak{l}, \mathfrak{l}]$. These two algebras give the *Bala–Carter label* of $\mathcal{O}$. A parabolic subalgebra $\mathfrak{p} = \mathfrak{l}' \oplus \mathfrak{u}$, with nilradical $\mathfrak{u}$ and Levi part $\mathfrak{l}'$ is distinguished if $\dim \mathfrak{l}' = \dim (\mathfrak{u}/[\mathfrak{u}, \mathfrak{u}])$. One such distinguished parabolic subalgebra is the Borel subalgebra of $\mathfrak{l}$. The nilpotent orbit associated to it is called the *principal nilpotent orbit* of $\mathfrak{l}$.

Whenever the minimal Levi subalgebra associated to $\mathcal{O}$ only contains one distinguished parabolic subalgebra (so when $\mathfrak{l}$ uniquely specifies $\mathcal{O}$) we call the orbit $\mathcal{O}$ polarized. For simplicity of notation, the Bala–Carter label for such an orbit is just $\mathfrak{l}$. For an unpolarized orbit, it is given by $\mathfrak{l}$ and an additional label [1].

Example 8.1.1. For $\mathfrak{g} = A_3$, consider the orbit of the element

$$X = \begin{pmatrix} 0 & 1 & 0 & 0 \\ 0 & 0 & 0 & 0 \\ 0 & 0 & 0 & 1 \\ 0 & 0 & 0 & 0 \end{pmatrix}.$$

The algebra $\mathfrak{sl}_4$ has five different (conjugacy classes of) Levi subalgebras, corresponding to the five integer partitions of 4. X itself obviously is an element of the Levi subalgebra $\mathfrak{l}_{\{\alpha_1,\alpha_3\}}$:

$$\mathfrak{l}_{\{\alpha_1,\alpha_3\}} = \begin{pmatrix} * & * & 0 & 0 \\ * & * & 0 & 0 \\ 0 & 0 & * & * \\ 0 & 0 & * & * \end{pmatrix}.$$

This algebra contains

$$\mathfrak{l}_{\{\alpha_1\}} = \begin{pmatrix} * & * & 0 & 0 \\ * & * & 0 & 0 \\ 0 & 0 & * & 0 \\ 0 & 0 & 0 & * \end{pmatrix}.$$

Since every element in any conjugacy class of $\mathfrak{l}_{\{\alpha_1\}}$ has at most one non-trivial Jordan block, X can never be contained in any of them; thus, the orbit of X is associated to $\mathfrak{l}_{\{\alpha_1,\alpha_3\}}$ and has the Bala–Carter label $2A_1$.

[1] The additional label specifies the number of simple roots that live in a Levi subalgebra of $\mathfrak{p}$.

8.2 Physical Origin of Bala–Carter Labels

The relation to the little string defect classification of section 2 is immediate: since polarized defects of the little string distinguish the parabolic subalgebra $\mathfrak{p}_\Theta$ of $\mathfrak{g}$ in the CFT limit, we simply identify the set of simple roots Θ with the Bala–Carter label of the defect. Namely, the union of all the elements of Θ forms a subquiver of $\mathfrak{g}$, which denotes the Bala–Carter label for the defect. The corresponding nilpotent orbit is the principal nilpotent orbit of $\mathfrak{l}_\Theta$, defined in the previous section. Equivalently, the Bala–Carter label is given by the union of the simple roots α_i in the Toda level 1 null state condition:

$$\vec{\beta} \cdot \vec{\alpha}_i = 0 \quad \forall \vec{\alpha}_i \in \Theta,$$

for some highest weight state $|\vec{\beta}\rangle$ of the $\mathcal{W}(\mathfrak{g})$-algebra. See figure 8.1 below.

If the polarized theory T^{2d} is described by the Bala–Carter label denoting a nilpotent orbit $\mathcal{O}$, its Coulomb branch is a resolution of the Spaltenstein dual of $\mathcal{O}$.

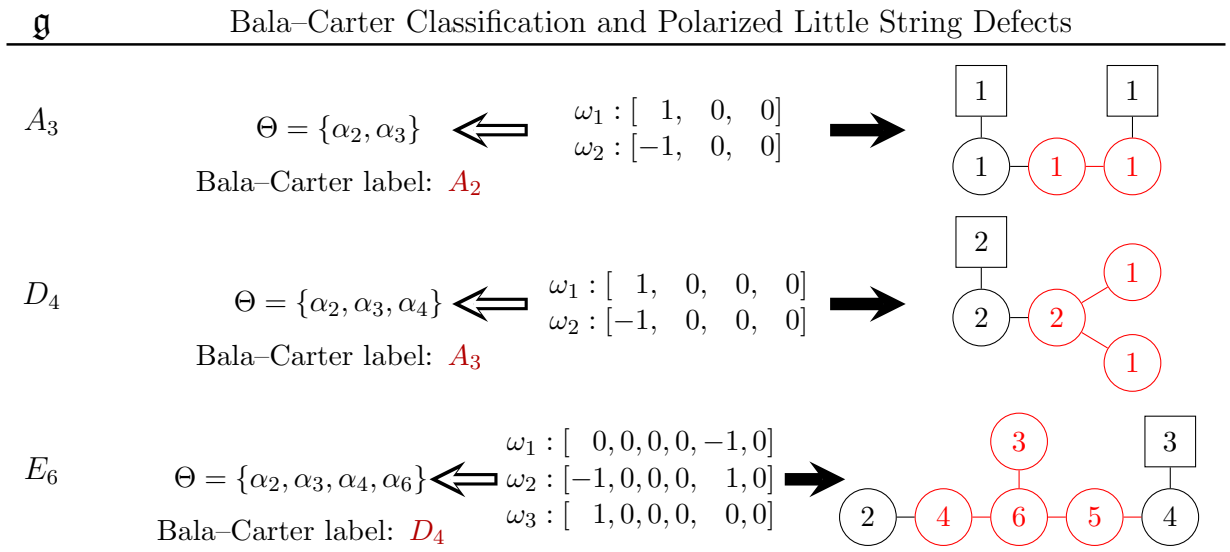

Figure 8.1: From a distinguished set of weights $\mathcal{W}_\mathcal{S}$ defining a polarized little string defect theory T^{2d}, one can extract a quiver gauge theory, shown on the right, and a parabolic subalgebra $\mathfrak{p}_\Theta$ in the $m_s \to \infty$ limit, shown on the left. The set Θ defines a Bala–Carter label, also shown in red as a subquiver of $\mathfrak{g}$ on the right. Note $\vec{\beta} \cdot \vec{\alpha}_i = 0$ for all $\vec{\alpha}_i \in \Theta$, which defines a null state at level 1 in $\mathfrak{g}$-Toda.

Concerning unpolarized defects of the little string, recall that they are characterized as follows: either $\mathcal{W}_\mathcal{S}$ is the set containing the zero weight $\omega = [0, 0, \ldots, 0]$ only (possibly multiple times), or $\mathcal{W}_\mathcal{S}$ contains a nonzero weight ω in the representation generated by (minus) a fundamental weight $-w_a$ without being in the Weyl orbit of $-w_a$.

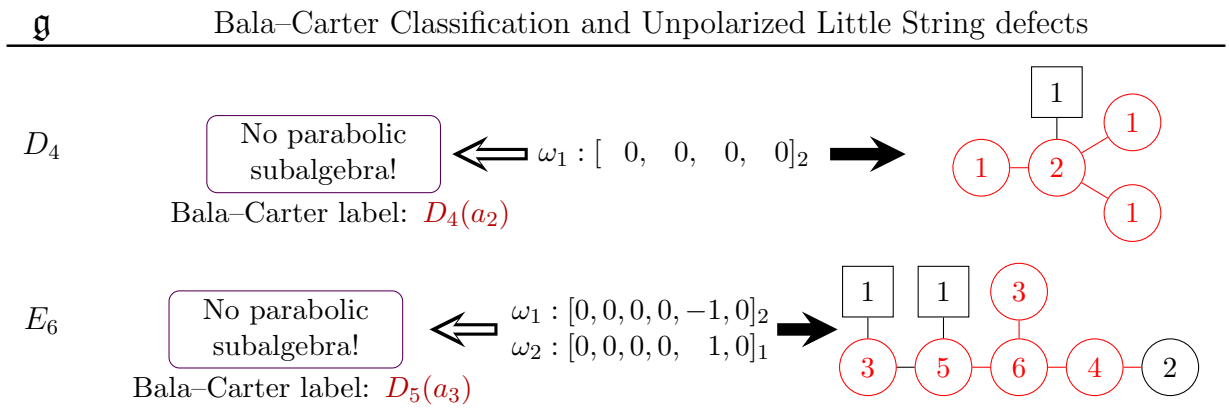

Figure 8.2: From a distinguished set of weights $\mathcal{W}_{\mathcal{S}}$ defining an unpolarized little string defect theory T^{2d}, one can extract a quiver gauge theory, shown on the right, but no parabolic subalgebra $\mathfrak{p}_\Theta$ in the $m_s \to \infty$ limit, as shown on the left. We added a subscript denoting which representation the weights ω_i belong in to fully specify the Bala–Carter label. The additional simple root data of the Bala–Carter label is written as a_i, where i is a number of simple roots.

Either way, additional data is needed to characterize such defects: in the end, it is sufficient to specify the representation ω belongs in. This prescription is in one-to-one correspondence with specifying a set of additional simple roots next to the Bala–Carter label of a non-principal nilpotent orbit, as we explained in section 8.1. To our knowledge, this extra simple root label unfortunately does not have a nice geometric interpretation for the defect. See figure 8.2 for examples.

At any rate, note that an unpolarized defect will still satisfy the relation

$$\vec{\beta} \cdot \vec{\alpha}_i = 0 \quad \forall \vec{\alpha}_i \in \Theta,$$

for some subset of positive simple roots Θ, with $\vec{\beta} = \sum_{i=1}^{|\mathcal{W}_{\mathcal{S}}|} \beta_i\ \omega_i$. This is the same level 1 null state condition of $\mathfrak{g}$-type Toda satisfied by polarized defects. There is however one crucial difference: the above constraint is no longer sufficient to characterize the defect, and one should specify the representation each ω_i belongs in.

Example 8.2.1. In the case of the single zero weight $\omega = [0, 0, \ldots, 0]$, we get $\vec{\beta} = 0$ and the null state condition is of course trivially satisfied; however, one should also specify which representation the weight ω is taken in, since for a given algebra $\mathfrak{g}$, ω belongs in general to many representations. This corresponds to specifying additional simple roots next to the Bala–Carter label $\mathfrak{g}$. Note the Bala–Carter label $\mathfrak{g}$ without any extra simple roots specified denotes the trivial nilpotent orbit, that is to say the absence of a defect.

In this way, one derives the full Bala–Carter classification of nilpotent orbits simply from a distinguished set $\mathcal{W}_{\mathcal{S}}$ of weights defining a little string defect. It's interesting to extend the analysis to the non-simply laced semi-simple Lie algebras, for which a Bala–Carter classification is also available. This was done in [31].

Chapter 9

Weighted Dynkin Diagrams

There is yet another way to classify nilpotent orbits of $\mathfrak{g}$, known as the so-called *weighted Dynkin diagrams.* We now show how to derive them.

9.1 Mathematical construction

Weighted Dynkin diagrams are vectors of integers $r_i \in \{0, 1, 2\}$, where $i = 1, \ldots, \mathrm{rk}\mathfrak{g}$; thus, we get one number for each node in the Dynkin diagram of $\mathfrak{g}$. We can associate such a vector to each nilpotent orbit of $\mathfrak{g}$, and each nilpotent orbit has a unique weighted Dynkin diagram. Note, however, that not all such labellings of the Dynkin diagram also have a nilpotent orbit corresponding to it.

To construct such a weighted Dynkin diagram, we use the following theorem by Jacobson and Morozov [45, 36].

Remember that $\mathfrak{sl}_2$ is the algebra generated by X, Y and H with the relations

$$[H, X] = 2X, \qquad [H, Y] = -2Y, \qquad [X, Y] = H. \tag{9.1}$$

Every nilpotent orbit in $\mathfrak{g}$ arises as the orbit of the image of X in an embedding $\rho : \mathfrak{sl}_2 \to \mathfrak{g}$.

In other words, for any embedding $\rho : \mathfrak{sl}_2 \to \mathfrak{g}$, the element $\rho(X)$ always is a nilpotent element of $\mathfrak{g}$. The Jacobson–Morozov theorem tells us that any nilpotent orbit uniquely arises (up to conjugation) as the orbit of such an element.

This means in particular that any nilpotent orbit also determines an element $\rho(H)$, which is semi-simple (we assume it to be diagonal). For simplicity, we'll just write $\rho(H)$ as H. The (diagonal) entries of H are always integers, and allow us to read off the weighted Dynkin diagram; the entry of the i-th node is defined to be $r_i = \alpha_i(H)$, where α_i is the i-th simple root of $\mathfrak{g}$. It turns out that these numbers are always 0, 1 or 2.

Example 9.1.1. We illustrate the above construction for the nilpotent orbit of

$$X = \begin{pmatrix} 0 & 1 & 0 & 0 \\ 0 & 0 & 0 & 0 \\ 0 & 0 & 0 & 1 \\ 0 & 0 & 0 & 0 \end{pmatrix}$$

in $\mathfrak{sl}_4$. One first constructs H; we won't do this explicitly here (see [19] for details), but the result is

$$H = \begin{pmatrix} 1 & 0 & 0 & 0 \\ 0 & -1 & 0 & 0 \\ 0 & 0 & 1 & 0 \\ 0 & 0 & 0 & -1 \end{pmatrix}.$$

The next step is to reorder the elements in the diagonal of H in a monotonically decreasing order. The quadruple we get is $(h_1, h_2, h_3, h_4) = (1, 1, -1, -1)$.

The nodes of the Dynkin diagram are labelled by the consecutive differences of these numbers, so $r_i = h_i - h_{i+1}$. This gives us $(r_1, r_2, r_3) = (0, 2, 0)$. So the weighted Dynkin diagram in this example looks as follows:

$$0 \text{ — } 2 \text{ — } 0$$

One can generalize the above construction to all semi-simple Lie algebras, with minor modifications.

9.2 From Weighted Dynkin Diagrams to Little String Defects

We make the following observations:

All weighted Dynkin diagrams can be interpreted as physical quiver theories: the label on each node of the weighted Dynkin diagram should be understood as the rank of a flavor symmetry group in a quiver. The quivers one reads in this way are always superconformal (in a 4d sense), and the flavor symmetry on each node is either nothing, a $U(1)$ group, or a $U(2)$ group. For instance, the full puncture, or maximal nilpotent orbit, denoted by the weighted Dynkin diagram $(2, 2, \ldots, 2, 2)$, can be understood as a quiver gauge theory with a $U(2)$ flavor attached to each node, for all semi-simple Lie algebras (see also [27]). Pushing this idea further, we find, surprisingly, that these quivers are little string defect theories T^{2d}, at finite m_s.

In the case of $\mathfrak{g} = A_n$, this correspondence between weighted Dynkin diagrams and defect theories T^{2d} can be made explicit. Indeed, all A_n weighted Dynkin diagrams are invariant under the $\mathbb{Z}_2$ outer automorphism action of the algebra; in other words, the quivers are all symmetric. For low dimensional defects, these quivers are precisely the little string quivers

T^{2d} studied in this note. For instance, consider the simple puncture of A_n, generated by the set of weights $\mathcal{W}_{\mathcal{S}} = \{[1, 0, \ldots, 0]\ ,\ [-1, 0, \ldots, 0]\}$, with Bala-Carter label A_{n-1}; the weighted Dynkin diagram with this Bala-Carter label can be shown to be $(1, 0, \ldots, 0, 1)$, in standard notation. This is precisely the little string quiver T^{2d} for the simple puncture! It has a $U(1)$ flavor symmetry on the first node, and a $U(1)$ flavor symmetry on the last node, as it should. See figure 9.1.

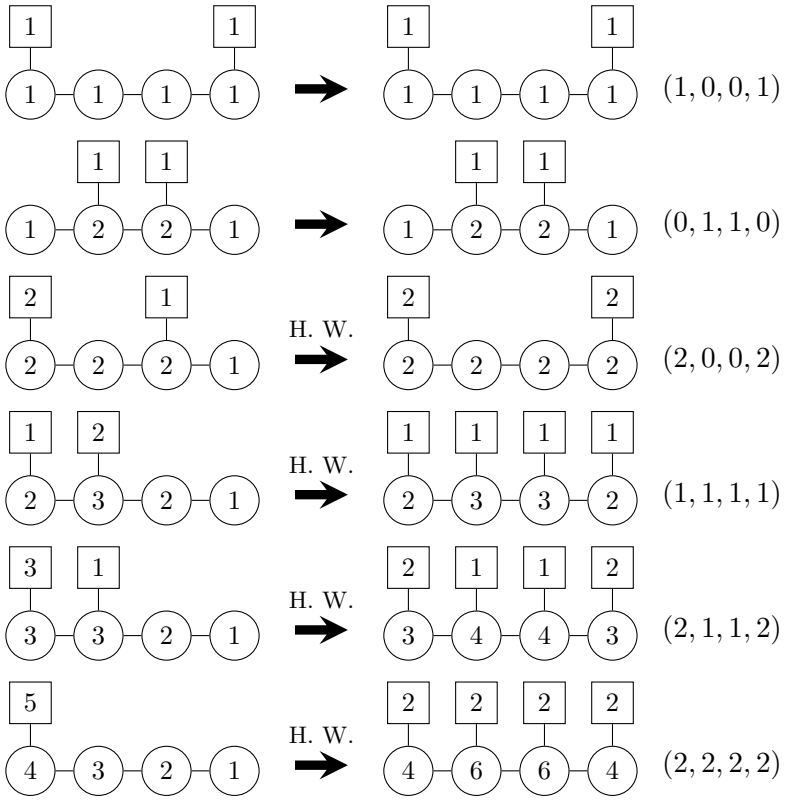

Figure 9.1: Either directly, or after flowing on the Higgs branch by Hanany-Witten transition to symmetrize the theories T^{2d}, the little string quivers (left) are precisely the weighted Dynkin diagrams of $\mathfrak{g}$ (right); the integers $0, 1, 2$ then get an interpretation as flavor symmetry ranks. Shown above is the case $\mathfrak{g} = A_4$.

Many of the little string quivers T^{2d} of A_n, however, are not weighted Dynkin diagrams. They are the quivers not invariant under $\mathbb{Z}_2$ reflection. We claim that such theories T^{2d} can however uniquely be turned into the correct weighted Dynkin diagrams, by moving on the Higgs branch of the theories.

Such a flow on the Higgs branch translates to a weight addition procedure in the algebra: this uses the fact that a weight in a fundamental representation can always be written as the sum of new weights in possibly different fundamental representations. Each of them should be in the orbit of some fundamental weight (possibly different orbits), while obeying the rule

that no subset adds up to zero. In the context of brane engineering, this weight addition procedure agrees with what is referred to as Hanany–Witten transitions [29]. See [33] for details, and figure 9.2 below for an example.

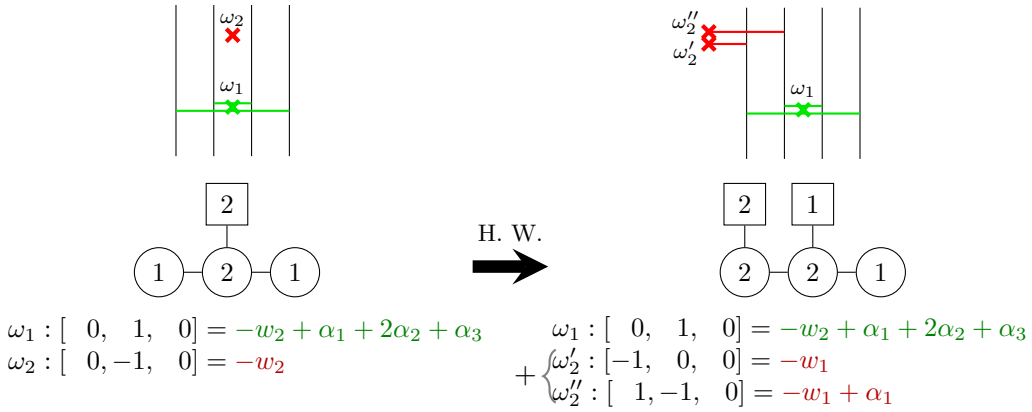

Figure 9.2: Writing a weight in a fundamental representation of $\mathfrak{g}$ as a sum of several weights in (possibly different) fundamental representations corresponds to flowing on the Higgs branch of T^{2d}. In the context of brane engineering, when $\mathfrak{g} = A_n$, this is the familiar Hanany–Witten transition [29]. In this example, we rewrite $[0, -1, 0]$ as the sum $[-1, 0, 0] + [1, -1, 0]$. As a result, the extra Coulomb parameter α_1 on the right is frozen to the value of the mass parameters denoted by ω_2' (and ω_2'').

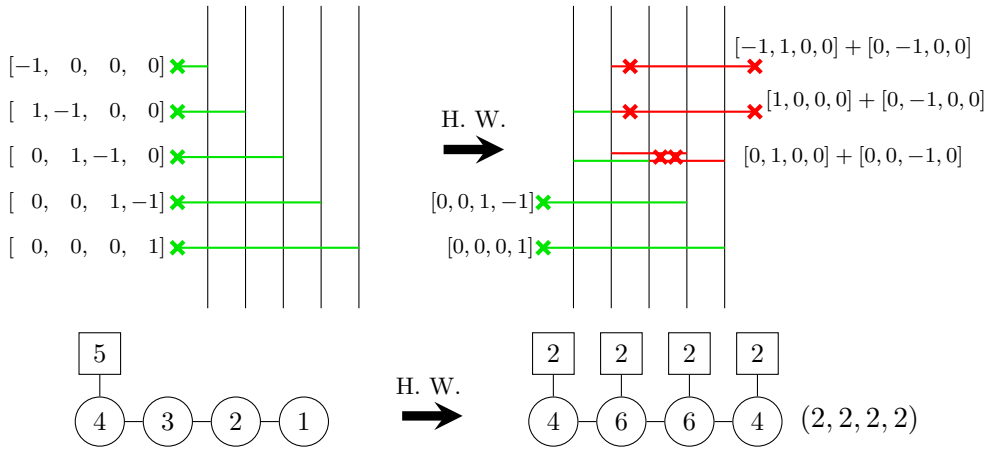

Figure 9.3: An example of how one symmetrizes a little string quiver of A_n using Hanany-Witten transitions, to end up with a weighted Dynkin diagram. The Coulomb parameters in red are frozen, and therefore do not increase the Coulomb branch dimension. In this example, no matter what the details of the transition are, the resulting symmetric quiver is always (2,2,2,2), the full puncture. Note some of the masses are equal to each other in the resulting quiver, as they should after Higgs flow.

Then, it turns out that all A_n little string quivers that are not symmetric under $\mathbb{Z}_2$ reflection can be uniquely written after Higgs flow as weighted Dynkin diagrams with correct Bala–Carter label. For instance, one can show that the full puncture of A_n, with Bala–Carter label $\varnothing$, can be symmetrized uniquely to give the weighted Dynkin diagram $(2, 2, \ldots, 2, 2)$. See figure 9.3.

This map between little string quivers and weighted Dynkin diagrams is one-to-one for $\mathfrak{g} = A_n$, but many-to-one for the other algebras, as a large number of different little string quivers typically describe one and the same defect in those cases. Nevertheless, the map always exists.

We now come to another result about weighted Dynkin diagrams, motivated by their apparent connection to little string defects we have pointed out: the dimension of a nilpotent orbit can be easily computed from its weighted Dynkin diagram.

9.3 Dimension Formula

Recall that the "flavor symmetry rank" of a weighted Dynkin diagram never exceeds 2 (as the flavor symmetry is always a product of $U(1)$ and $U(2)$ groups only). This is a claim about the hypermultiplets of the quiver theory. There exists a "vector multiplet" counterpart

to this statement, which is given by the following mathematical statement:

We interpret the weighted Dynkin diagram of a nilpotent orbit $\mathcal{O}$ as a weight ω, written down in the Dynkin basis. We then compute the sum of the inner products of all the positive roots of $\mathfrak{g}$ with this weight. This gives a vector of non-negative integers. Truncating the entries of this vector at 2 and taking the sum of the entries gives the (real) dimension of $\mathcal{O}$.

This result can be derived from the following dimension formula for nilpotent orbits[1] (cf. for instance [19]):

$$\dim \mathcal{O} = \dim \mathfrak{g} - \dim \mathfrak{g}_0 - \dim \mathfrak{g}_1, \tag{9.2}$$

where

$$\mathfrak{g}_i = \{Z \in \mathfrak{g} | [H, Z] = i \cdot Z\}, \tag{9.3}$$

and where H is the semisimple element in the $\mathfrak{sl}_2$ triple corresponding to $\mathcal{O}$.

Note that whenever $Z \in \mathfrak{g}_\beta$ for a root β, $[H, Z] = \beta(H)Z$. So

$$\mathfrak{g}_i = \bigoplus_{\substack{\beta \in \Phi, \\ \beta(H) = i}} \mathfrak{g}_\beta.$$

On the other hand, if $\mathfrak{g}$ is simply laced, then the inner product of the weighted Dynkin diagram weight ω with a root β is just

$$\left\langle \sum_{i=1}^{n} \alpha_i(H)\omega_i, \beta \right\rangle = \sum_{i=1}^{n} \alpha_i(H)\langle \omega_i, \beta \rangle = \beta(H),$$

where α_i and ω_i are the simple roots and fundamental weights of $\mathfrak{g}$, respectively.

Thus, if $\mathfrak{g}$ is simply laced, the above inner products just give us the grading 9.3.

The prescription we give is therefore equivalent to the dimension formula 9.2; namely,

$$\begin{aligned} \dim(\mathfrak{g}_1) + 2\sum_{i \geq 2} \dim(\mathfrak{g}_i) &= \dim(\mathfrak{g}_1) + \sum_{i \geq 2} \dim(\mathfrak{g}_i) + \sum_{i \leq -2} \dim(\mathfrak{g}_i) \\ &= \dim(\mathfrak{g}_1) + \dim(\mathfrak{g}) - \sum_{-1 \leq i \leq 1} \dim(\mathfrak{g}_i) \\ &= \dim(\mathfrak{g}_1) + \dim(\mathfrak{g}) - 2\dim(\mathfrak{g}_1) - \dim(\mathfrak{g}_0) \\ &= \dim(\mathfrak{g}) - \dim(\mathfrak{g}_0) - \dim(\mathfrak{g}_1). \end{aligned} \tag{9.4}$$

Example 9.3.1. Let us take the example of the weighted Dynkin diagram (2,1,1,2) in the algebra $\mathfrak{g} = A_4$. We write $\omega = [2, 1, 1, 2]$ as a weight in Dynkin basis.

[1] We thank Axel Kleinschmidt for pointing out this proof to us.

The positive roots Φ^+ of A_4 are

$$(h_1 - h_5,\ h_2 - h_5,\ h_1 - h_4,\ h_2 - h_4,\ h_3 - h_5,\ h_1 - h_3,\ h_2 - h_3,\ h_3 - h_4,\ h_4 - h_5,\ h_1 - h_2)$$

Calculating the inner product of all of these positive roots with ω gives the numbers

$$\langle \Phi^+, \omega \rangle = (6, 4, 4, 2, 3, 3, 1, 1, 2, 2).$$

Truncating at multiplicity 2, the sum of the inner products is $2 \times 8 + 1 \times 2 = 18$, which is indeed the dimension of the nilpotent orbit denoted by the diagram $(2, 1, 1, 2)$.

Note that the theories T^{2d} we have been studying can be interpreted as 3d $\mathcal{N} = 4$ theories. It is then interesting to compare this formula to the dimension of the Coulomb branch of a 3d $\mathcal{N} = 4$ quiver theory [13], which is given by a slice in the affine Grassmannian [12]. In that setup, the dimension can be calculated by the exact same procedure, coming from a monopole formula [44], but without truncating the inner products at the value 2. For conformal theories, this is simply the sum of the ranks of the gauge groups.

Lastly, we want to emphasize that the above formula we gave does not compute the Coulomb branch dimension of the defect theory $T^{2d}_{m_s \to \infty}$ denoted by the weighted Dynkin diagram. Instead, the Coulomb branch dimension is given by the dimension of the diagram's image under the Spaltenstein map. Note that not all nilpotent orbits are in the image of the Spaltenstein map, so in many cases, it is unclear what the physical interpretation of the dimension formula should be.

Chapter 10

Future Directions

The $\mathcal{W}$ algebras appearing in this thesis can be generalized to $\mathcal{W}$ algebras associated to any nilpotent orbit in $\mathfrak{g}$. It would be interesting to study their properties, and how they fit into this physical picture. An explanation might lie in the ubiquitous Ding-Iohara-Miki algebra [21, 43].

Also, this work ties into a general approach of using little string theory as a tool to understand mathematical structures appearing in gauge theory:

A powerful tool that was developed in this context are *elliptic stable envelopes* [5]. These objects appear in the study of certain difference equations (such as the quantum Knizhnik–Zamolodchikov equations), and act on the space of solutions by adding and substracting poles. The difference equations are satisfied by conformal blocks of deformed $\mathcal{W}$ algebras we encountered in this thesis. The corresponding three-dimensional $\mathcal{N} = 4$ quiver gauge theories give them a physical interpretation, that allows them to be calculated directly:

The partition function can be calculated by summing over poles as one integrates over the Coulomb branch. By doing this calculation on a cigar times S^1, we can change these poles by introducing fields on the boundary torus that couple to the bulk fields. This boundary theory directly gives the action of elliptic stable envelopes, which can be calculated explicitly for many theories.

They can be applied to a version of the geometric Langlands correspondence [2] and to three-dimensional mirror symmetry [52]. It would be interesting to perform explicit calculations in these setups.

Furthermore, the setup studied in this thesis has been related to qq-characters [47] in [30].

Appendix A

E_n little string defects

As an application of the Bala–Carter classification, we now present a table of the defects of the E_n little string. Unpolarized defects are shaded in yellow. For each defect type, we give a set $\mathcal{W}_{\mathcal{S}}$ of weights, along with the low energy 2d quiver gauge theory T^{2d} on the D3 branes that results from it. The Bala–Carter label that designates the nilpotent orbit in the CFT limit $m_s \to \infty$ is written in the left column. Each set $\mathcal{W}_{\mathcal{S}}$ is a distinguished set, in the sense of section 2; in particular, the weights ω_i of $\mathcal{W}_{\mathcal{S}}$ satisfy

$$\vec{\beta} \cdot \vec{\alpha}_i = 0 \quad \forall \vec{\alpha}_i \in \Theta,$$

with $\vec{\beta} = \sum_{i=1}^{|\mathcal{W}_{\mathcal{S}}|} \beta_i \, \omega_i$. This constraint has an interpretation as a level 1 null state condition of $\mathfrak{g}$-Toda. For unpolarized defects, a subscript is added to the weights, specifying the representation they are taken in. This corresponds to giving the additional simple root label a_i in the Bala–Carter picture. For polarized defects, no subscript is needed for the weights.

The dual orbit is the orbit describing the Coulomb branch of $T^{2d}_{m_s \to \infty}$; for polarized defects, this is given by the Spaltenstein dual of the Bala–Carter label. For unpolarized defects, these dual orbits had to be conjectured based on other approaches, such as dimension counting. The dimension of this dual orbit describing the Coulomb branch is given by d.

Note the quivers are either literally the weighted Dynkin diagrams as given in the literature, or are quivers that can be made to be weighted Dynkin diagrams after Higgs flow.

Table A.1: Results for E_6

Orbit	Θ	Weights	Quiver	Dual orbit	d
0	$\varnothing$	$\begin{bmatrix} 0, & 0, & 0, & 0, & 0, & -1 \\ -1, & 0, & 0, & 0, & -1, & 1 \\ 1, & 0, & 0, & -1, & 0, & 1 \\ 0, & -1, & 0, & 0, & 1, & 1 \\ 0, & 1, & -1, & 1, & 0, & 0 \\ 0, & 0, & 1, & 0, & 0, & -1 \\ 0, & 0, & 0, & 0, & 0, & -1 \end{bmatrix}$	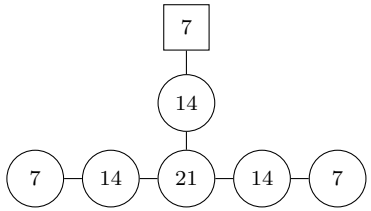	E_6	72
A_1	$\{\alpha_1\}$	$\begin{bmatrix} 0, & 0, & 0, & 0, & -1, & 0 \\ 0, & 0, & 0, & -1, & 1, & 0 \\ 0, & 1, & 0, & -1, & 0, & 0 \\ 0, & 0, & 0, & 1, & 0, & -1 \\ 0, & 0, & -1, & 1, & 0, & 1 \\ 0, & -1, & 1, & 0, & 0, & 0 \end{bmatrix}$	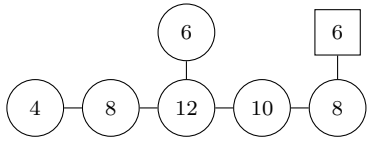	$E_6(a_1)$	70
$2A_1$	$\{\alpha_1, \alpha_3\}$	$\begin{bmatrix} 0, & 0, & 0, & 1, & -1, & -1 \\ 0, & 0, & 0, & 0, & 1, & -1 \\ 0, & -1, & 0, & 0, & 0, & 1 \\ 0, & 1, & 0, & -1, & 0, & 0 \\ 0, & 0, & 0, & 0, & 0, & 1 \end{bmatrix}$	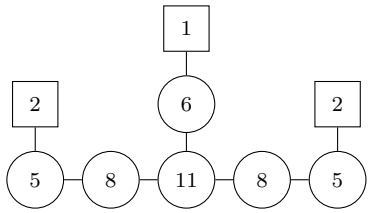	D_5	68
$3A_1$	$\{\alpha_1, \alpha_3, \alpha_5\}$	$\begin{bmatrix} 0, & -1, & 0, & 0, & 0, & 0 \\ 0, & 2, & 0, & -1, & 0, & -2 \\ 0, & -1, & 0, & 1, & 0, & 1 \\ 0, & 0, & 0, & 0, & 0, & 1 \end{bmatrix}$	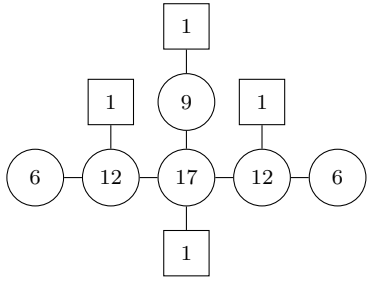	$E_6(a_3)$	66
A_2	$\{\alpha_1, \alpha_2\}$	$\begin{bmatrix} 0, & 0, & 1, & -1, & 0, & -1 \\ 0, & 0, & 0, & 0, & -1, & 0 \\ 0, & 0, & 0, & -1, & 2, & 0 \\ 0, & 0, & -1, & 2, & -1, & 0 \\ 0, & 0, & 0, & 0, & 0, & 1 \end{bmatrix}$	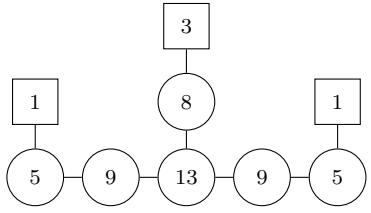	$E_6(a_3)$	66

Table A.1: Results for E_6

Orbit	Θ	Weights	Quiver	Dual orbit	d
$A_2 + A_1$	$\{\alpha_1, \alpha_2, \alpha_4\}$	$\begin{bmatrix} 0, & 0, & 0, & 0, & 1, & -1 \\ 0, & 0, & 0, & 0, & -1, & 0 \\ 0, & 0, & -1, & 0, & 0, & 2 \\ 0, & 0, & 1, & 0, & 0, & -1 \end{bmatrix}$	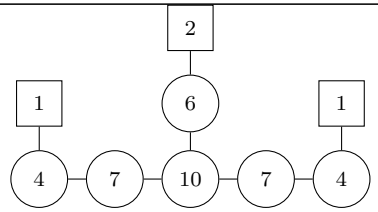	$D_5(a_1)$	64
$2A_2$	$\{\alpha_1, \alpha_2, \alpha_4, \alpha_5\}$	$\begin{bmatrix} 0, & 0, & 0, & 0, & 0, & -1 \\ 0, & 0, & -1, & 0, & 0, & 2 \\ 0, & 0, & 1, & 0, & 0, & -1 \end{bmatrix}$	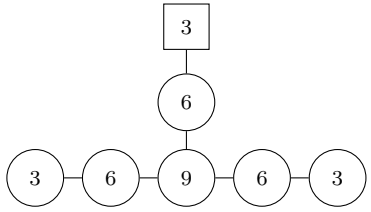	D_4	60
$A_2 + 2A_1$	$\{\alpha_1, \alpha_2, \alpha_4, \alpha_6\}$	$\begin{bmatrix} 0, & 0, & 0, & 0, & 1, & 0 \\ 0, & 0, & -1, & 0, & 1, & 0 \\ 0, & 0, & 1, & 0, & -2, & 0 \end{bmatrix}$	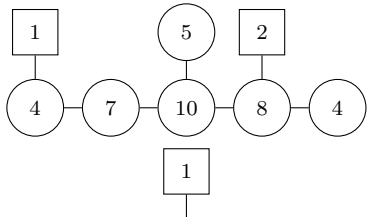	$A_4 + A_1$	62
A_3	$\{\alpha_1, \alpha_2, \alpha_3\}$	$\begin{bmatrix} 0, & 0, & 0, & 0, & -1, & 0 \\ 0, & 0, & 0, & -1, & 1, & 0 \\ 0, & 0, & 0, & 1, & 0, & -1 \\ 0, & 0, & 0, & 0, & 0, & 1 \end{bmatrix}$	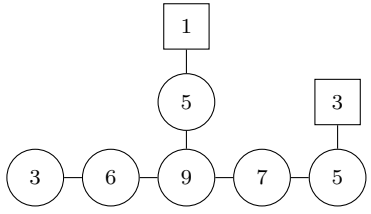	A_4	60
$2A_2 + A_1$	$\{\alpha_1, \alpha_2, \alpha_4, \alpha_5, \alpha_6\}$	$\begin{bmatrix} 0, & 0, & -1, & 0, & 0, & 0 \\ 0, & 0, & 1, & 0, & 0, & 0 \end{bmatrix}$	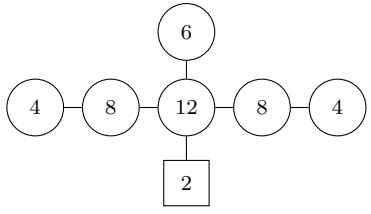	$D_4(a_1)$	58

Table A.1: Results for E_6

Orbit	Θ	Weights	Quiver	Dual orbit	d
$A_3 + A_1$	$\{\alpha_1, \alpha_2, \alpha_3, \alpha_5\}$	$\begin{bmatrix} 0, & 0, & 0, -1, & 0, & 0 \\ 0, & 0, & 0, & 1, & 0, -1 \\ 0, & 0, & 0, & 0, & 0, & 1 \end{bmatrix}$	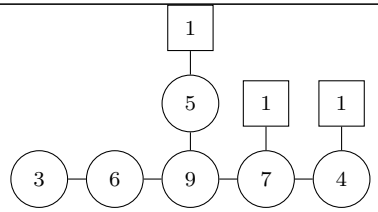	$D_4(a_1)$	58
$D_4(a_1)$	$\{\alpha_2, \alpha_3, \alpha_4, \alpha_6\}$	$\begin{bmatrix} 0, & 0, & 0, & 0, & 1, & 0 \end{bmatrix}_1$ $\begin{bmatrix} -1, & 0, & 0, & 0, -1, & 0 \end{bmatrix}_3$ $\begin{bmatrix} 1, & 0, & 0, & 0, & 0, & 0 \end{bmatrix}_5$	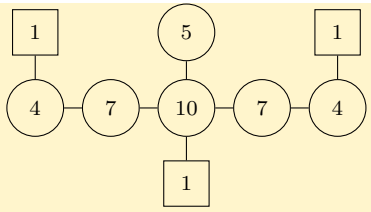	$2A_2 + A_1$	54
A_4	$\{\alpha_1, \alpha_2, \alpha_3, \alpha_4\}$	$\begin{bmatrix} 0, & 0, & 0, & 0, & 2, -1 \\ 0, & 0, & 0, & 0, -1, & 0 \\ 0, & 0, & 0, & 0, -1, & 1 \end{bmatrix}$	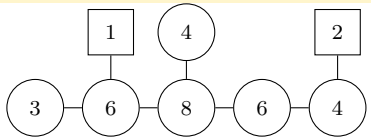	A_3	52
D_4	$\{\alpha_2, \alpha_3, \alpha_4, \alpha_6\}$	$\begin{bmatrix} 0, & 0, & 0, & 0, -1, & 0 \\ -1, & 0, & 0, & 0, & 1, & 0 \\ 1, & 0, & 0, & 0, & 0, & 0 \end{bmatrix}$	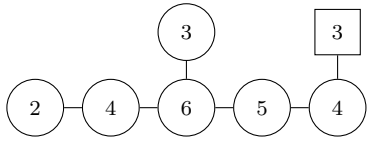	$2A_2$	48
$A_4 + A_1$	$\{\alpha_1, \alpha_2, \alpha_3, \alpha_5, \alpha_6\}$	$\begin{bmatrix} 0, & 0, & 0, & 1, & 0, & 0 \\ 0, & 0, & 0, -1, & 0, & 0 \end{bmatrix}$	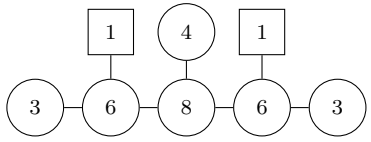	$A_2 + 2A_1$	50
A_5	$\{\alpha_1, \alpha_2, \alpha_3, \alpha_4, \alpha_5\}$	$\begin{bmatrix} 0, & 0, & 0, & 0, & 0, -1 \\ 0, & 0, & 0, & 0, & 0, & 1 \end{bmatrix}$	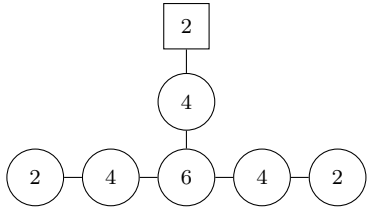	A_2	42

Table A.1: Results for E_6

Orbit	Θ	Weights	Quiver	Dual orbit	d
$D_5(a_1)$	$\{\alpha_1, \alpha_2, \alpha_3, \alpha_4, \alpha_6\}$	$[\ 0,\ 0,\ 0,\ 0,\ 1,\ 0]_1$ $[\ 0,\ 0,\ 0,\ 0,-1,\ 0]_2$	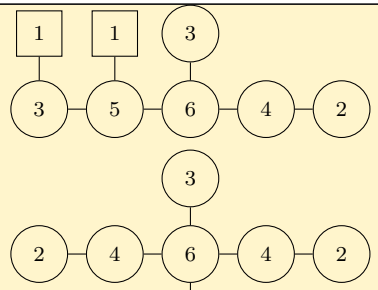	$A_2 + A_1$	46
$E_6(a_3)$	$\{\alpha_1, \alpha_2, \alpha_3, \alpha_4, \alpha_5, \alpha_6\}$	$[\ 0,\ 0,\ 0,\ 0,\ 0,\ 0]_3$		$3A_1$	40
D_5	$\{\alpha_1, \alpha_2, \alpha_3, \alpha_4, \alpha_6\}$	$[\ 0,\ 0,\ 0,\ 0,\ 1,\ 0]$ $[\ 0,\ 0,\ 0,\ 0,-1,\ 0]$	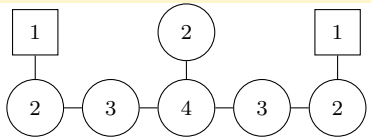	$2A_1$	32
$E_6(a_1)$	$\{\alpha_1, \alpha_2, \alpha_3, \alpha_4, \alpha_5, \alpha_6\}$	$[\ 0,\ 0,\ 0,\ 0,\ 0,\ 0]_7$	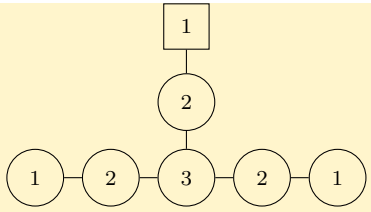	A_1	22

Table A.2: Results for E_7

Orbit	Θ	Weights	Quiver	Dual orbit	d
0	$\varnothing$	$\begin{bmatrix} -1, & 0, & 0, & 0, & 0, & 0, & 0 \\ 1, & 0, & 0, & -1, & 0, & 1, & 0 \\ 0, & -1, & 1, & 0, & 0, & -1, & 0 \\ -1, & 1, & 0, & 0, & 0, & -1, & 0 \\ 0, & 0, & 0, & 0, & 0, & 1, & 0 \\ 0, & 0, & -1, & 1, & 0, & 0, & 1 \\ 1, & 0, & -1, & 1, & -1, & 0, & 0 \\ 0, & 0, & 1, & -1, & 1, & 0, & -1 \end{bmatrix}$	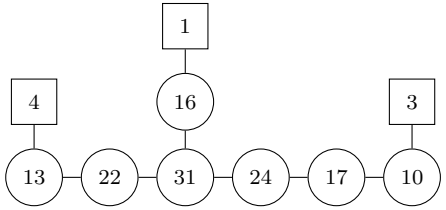	E_7	126
A_1	$\{\alpha_5\}$	$\begin{bmatrix} -1, & 0, & 0, & 0, & 0, & 0, & 0 \\ 1, & 0, & 0, & -1, & 0, & 1, & 0 \\ 0, & -1, & 1, & 0, & 0, & -1, & 0 \\ -1, & 1, & 0, & 0, & 0, & -1, & 0 \\ 0, & 0, & 0, & 0, & 0, & 1, & 0 \\ 0, & 0, & -1, & 1, & 0, & 0, & 1 \\ 1, & 0, & 0, & 0, & 0, & 0, & -1 \end{bmatrix}$	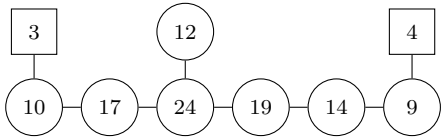	$E_7(a_1)$	124
$2A_1$	$\{\alpha_5, \alpha_7\}$	$\begin{bmatrix} -1, & 0, & 0, & 0, & 0, & 0, & 0 \\ 1, & 0, & 0, & -1, & 0, & 1, & 0 \\ 0, & -1, & 1, & 0, & 0, & -1, & 0 \\ -1, & 1, & 0, & 0, & 0, & -1, & 0 \\ 1, & 0, & -1, & 1, & 0, & 0, & 0 \\ 0, & 0, & 0, & 0, & 0, & 1, & 0 \end{bmatrix}$	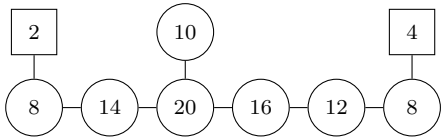	$E_7(a_2)$	122
$3A_1b$	$\{\alpha_4, \alpha_6, \alpha_7\}$	$\begin{bmatrix} 0, & 0, & 0, & 0, & -1, & 0, & 0 \\ 0, & 0, & -1, & 0, & 1, & 0, & 0 \\ -2, & 0, & 1, & 0, & 0, & 0, & 0 \\ 2, & -2, & 1, & 0, & 0, & 0, & 0 \\ 0, & 2, & -1, & 0, & 0, & 0, & 0 \end{bmatrix}$	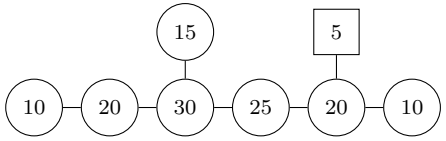	E_6	120
$3A_1a$	$\{\alpha_1, \alpha_4, \alpha_7\}$	$\begin{bmatrix} 0, & 0, & 0, & 0, & -1, & 0, & 0 \\ 0, & 0, & -1, & 0, & 1, & 0, & 0 \\ 0, & -1, & 1, & 0, & 1, & -2, & 0 \\ 0, & -1, & 1, & 0, & -1, & 2, & 0 \\ 0, & 2, & -1, & 0, & 0, & 0, & 0 \\ 0, & 0, & 0, & 0, & 0, & -1, & 0 \end{bmatrix}$	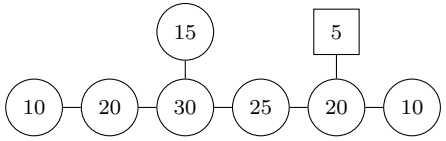	$E_7(a_3)$	120
A_2	$\{\alpha_1, \alpha_2\}$	$\begin{bmatrix} 0, & 0, & 0, & 0, & 1, & 0, & -1 \\ 0, & 0, & -1, & 0, & 1, & 0, & 1 \\ 0, & 0, & 1, & -1, & 0, & 0, & 0 \\ 0, & 0, & 0, & 1, & -1, & 0, & 0 \end{bmatrix}$	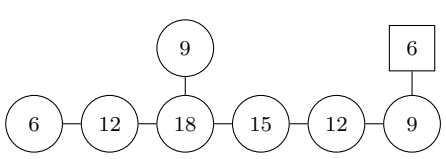	$E_7(a_3)$	120

Table A.2: Results for E_7

Orbit	Θ	Weights	Quiver	Dual orbit	d
$4A_1$	$\{\alpha_2, \alpha_4, \alpha_6, \alpha_7\}$	$\begin{bmatrix} 0, & 0, -1, & 0, & 0, & 0, & 0] \\ 0, & 0, & 1, & 0, -3, & 0, & 0] \\ 2, & 0, -1, & 0, & 2, & 0, & 0] \\ -2, & 0, & 1, & 0, & 1, & 0, & 0] \end{bmatrix}$	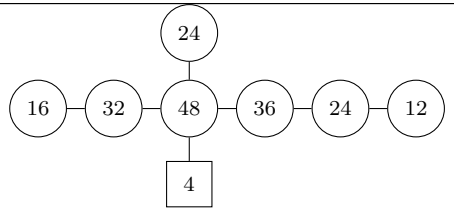	$E_6(a_1)$	118
$A_2 + A_1$	$\{\alpha_1, \alpha_2, \alpha_7\}$	$\begin{bmatrix} 0, & 0, & 1, -1, & 0, -1, & 0] \\ 0, & 0, -1, & 0, & 0, & 0, & 0] \\ 0, & 0, -1, & 2, -2, & 2, & 0] \\ 0, & 0, & 1, -1, & 1, -1, & 0] \\ 0, & 0, & 0, & 0, & 1, & 0, & 0] \end{bmatrix}$	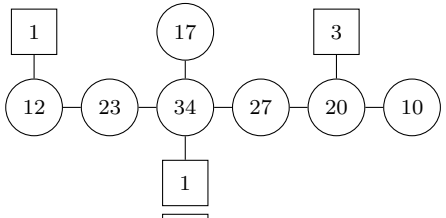	$E_6(a_1)$	118
$A_2 + 2A_1$	$\{\alpha_1, \alpha_2, \alpha_4, \alpha_7\}$	$\begin{bmatrix} 0, & 0, & 0, & 0, & 1, -2, & 0] \\ 0, & 0, -1, & 0, & 0, & 1, & 0] \\ 0, & 0, & 0, & 0, & 1, & 0, & 0] \\ 0, & 0, & 1, & 0, -2, & 1, & 0] \end{bmatrix}$	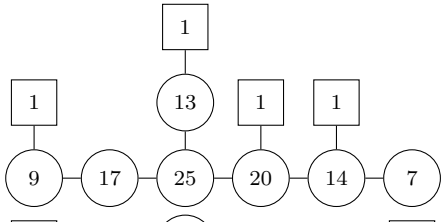	$E_7(a_4)$	116
A_3	$\{\alpha_1, \alpha_2, \alpha_3\}$	$\begin{bmatrix} 0, & 0, & 0, & 1, -1, & 0, -1] \\ 0, & 0, & 0, -1, & 1, & 0, & 0] \\ 0, & 0, & 0, & 0, -1, & 0, & 1] \\ 0, & 0, & 0, & 0, & 1, -1, & 0] \\ 0, & 0, & 0, & 0, & 0, & 1, & 0] \end{bmatrix}$	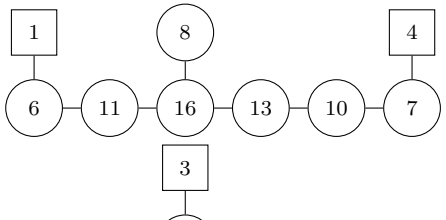	$D_6(a_1)$	114
$2A_2$	$\{\alpha_1, \alpha_2, \alpha_5, \alpha_6\}$	$\begin{bmatrix} 0, & 0, -1, & 1, & 0, & 0, & 0] \\ 0, & 0, & 0, & 0, & 0, & 0, -1] \\ 0, & 0, & 0, -1, & 0, & 0, & 2] \\ 0, & 0, & 1, & 0, & 0, & 0, -1] \end{bmatrix}$	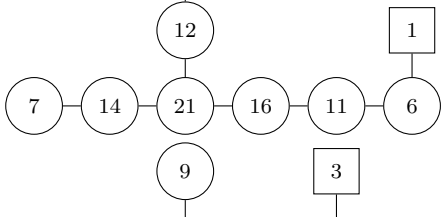	$D_5 + A_1$	114
$A_2 + 3A_1$	$\{\alpha_1, \alpha_2, \alpha_4, \alpha_6, \alpha_7\}$	$\begin{bmatrix} 0, & 0, & 0, & 0, -1, & 0, & 0] \\ 0, & 0, -1, & 0, & 2, & 0, & 0] \\ 0, & 0, & 1, & 0, -1, & 0, & 0] \end{bmatrix}$		A_6	114

Table A.2: Results for E_7

Orbit	Θ	Weights	Quiver	Dual orbit	d
$A_3b + A_1b$	$\{\alpha_3, \alpha_4, \alpha_6, \alpha_7\}$	$[-1, 0, 0, 0, 0, 0, 0]$ $[1, 0, 0, 0, -1, 0, 0]$ $[1, -1, 0, 0, 1, 0, 0]$ $[-1, 1, 0, 0, 0, 0, 0]$	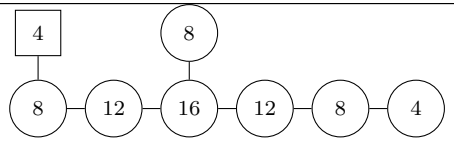	D_5	112
$2A_2 + A_1$	$\{\alpha_1, \alpha_2, \alpha_4, \alpha_5, \alpha_7\}$	$[0, 0, -1, 0, 0, 0, 0]$ $[0, 0, 1, 0, 0, -1, 0]$ $[0, 0, 0, 0, 0, 1, 0]$	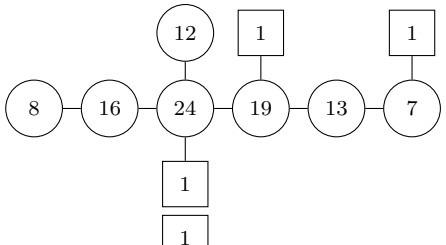	$E_7(a_5)$	112
$A_3a + A_1a$	$\{\alpha_1, \alpha_3, \alpha_4, \alpha_7\}$	$[0, -1, 0, 0, 1, 0, 0]$ $[0, 0, 0, 0, -1, 0, 0]$ $[0, 0, 0, 0, 1, -1, 0]$ $[0, 1, 0, 0, -1, 1, 0]$	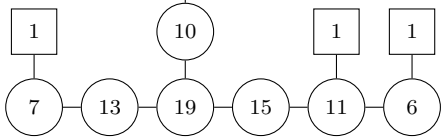	$E_7(a_5)$	112
$D_4(a_1)$	$\{\alpha_2, \alpha_3, \alpha_4, \alpha_7\}$	$[1, 0, 0, 0, 0, 0, 0]_1$ $[-1, 0, 0, 0, -1, 0, 0]_3$ $[0, 0, 0, 0, 0, 1, 0]_6$ $[0, 0, 0, 0, 1, -1, 0]_6$	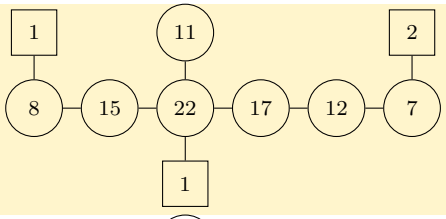	$D_6(a_2)$	110
$A_3 + 2A_1$	$\{\alpha_1, \alpha_4, \alpha_5, \alpha_6, \alpha_7\}$	$[0, 1, -1, 0, 0, 0, 0]$ $[0, -1, 0, 0, 0, 0, 0]$ $[0, 0, 1, 0, 0, 0, 0]$	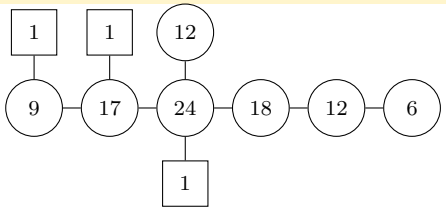	$E_6(a_3)$	110
D_4	$\{\alpha_2, \alpha_3, \alpha_4, \alpha_7\}$	$[0, 0, 0, 0, 0, -1, 0]$ $[-1, 0, 0, 0, 0, 1, 0]$ $[1, 0, 0, 0, -1, 1, 0]$ $[0, 0, 0, 0, 1, -1, 0]$	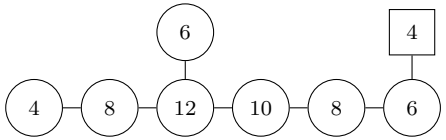	A_5b	102

Table A.2: Results for E_7

Orbit	Θ	Weights	Quiver	Dual orbit	d
$D_4(a_1)+A_1$	$\{\alpha_2,\alpha_3,\alpha_4,\alpha_6,\alpha_7\}$	$[1,0,0,0,0,0,0]_1$ $[-1,0,0,0,-1,0,0]_3$ $[0,0,0,0,1,0,0]_5$	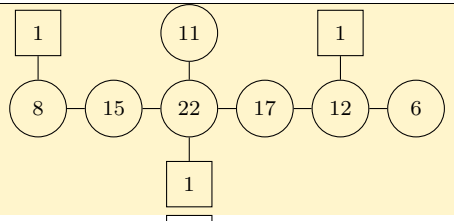	A_5a	108
A_3+A_2	$\{\alpha_1,\alpha_2,\alpha_3,\alpha_5,\alpha_6\}$	$[0,0,0,-1,0,0,1]$ $[0,0,0,1,0,0,-2]$ $[0,0,0,0,0,0,1]$	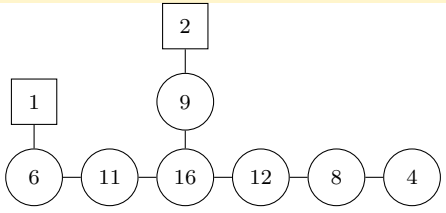	$D_5(a_1)+A_1$	108
A_4	$\{\alpha_1,\alpha_2,\alpha_3,\alpha_4\}$	$[0,0,0,0,0,-1,0]$ $[0,0,0,0,-1,1,0]$ $[0,0,0,0,1,0,-1]$ $[0,0,0,0,0,0,1]$	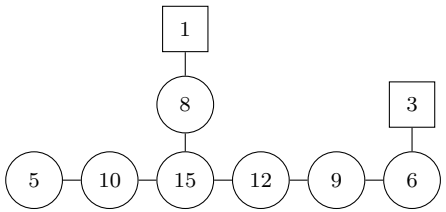	$D_5(a_1)$	106
$A_3+A_2+A_1$	$\{\alpha_1,\alpha_2,\alpha_4,\alpha_5,\alpha_6,\alpha_7\}$	$[0,0,-1,0,0,0,0]$ $[0,0,1,0,0,0,0]$	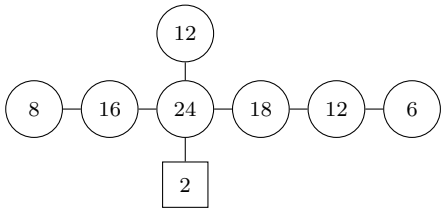	A_4+A_2	106
A_5b	$\{\alpha_3,\alpha_4,\alpha_5,\alpha_6,\alpha_7\}$	$[-1,0,0,0,0,0,0]$ $[2,-1,0,0,0,0,0]$ $[-1,1,0,0,0,0,0]$	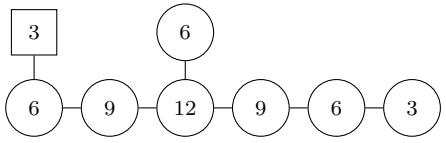	D_4	96
D_4+A_1	$\{\alpha_2,\alpha_3,\alpha_4,\alpha_6,\alpha_7\}$	$[-1,0,0,0,0,0,0]$ $[1,0,0,0,-1,0,0]$ $[0,0,0,0,1,0,0]$	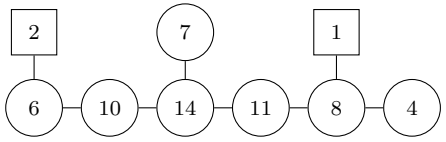	A_4	100

Table A.2: Results for E_7

Orbit	Θ	Weights	Quiver	Dual orbit	d
$A_4 + A_1$	$\{\alpha_1, \alpha_2, \alpha_3, \alpha_4, \alpha_6\}$	$\begin{bmatrix} 0, & 0, & 0, & 0, & -1, & 0, & 0 \\ 0, & 0, & 0, & 0, & 1, & 0, & -1 \\ 0, & 0, & 0, & 0, & 0, & 0, & 1 \end{bmatrix}$	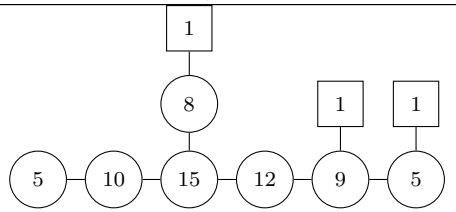	$A_4 + A_1$	104
$D_5(a_1)$	$\{\alpha_2, \alpha_3, \alpha_4, \alpha_5, \alpha_7\}$	$\begin{bmatrix} 1, & 0, & 0, & 0, & 0, & 0, & 0 \\ -1, & 0, & 0, & 0, & 0, & -1, & 0 \\ 0, & 0, & 0, & 0, & 0, & 1, & 0 \end{bmatrix}_{1,4,6}$	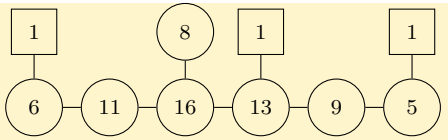	A_4	100
$A_4 + A_2$	$\{\alpha_1, \alpha_2, \alpha_3, \alpha_5, \alpha_6, \alpha_7\}$	$\begin{bmatrix} 0, & 0, & 0, & -1, & 0, & 0, & 0 \\ 0, & 0, & 0, & 1, & 0, & 0, & 0 \end{bmatrix}$	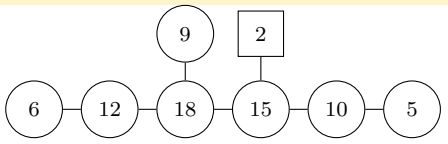	$A_3 + A_2 + A_1$	100
A_5a	$\{\alpha_1, \alpha_2, \alpha_3, \alpha_4, \alpha_5\}$	$\begin{bmatrix} 0, & 0, & 0, & 0, & 0, & 1, & -1 \\ 0, & 0, & 0, & 0, & 0, & -1, & 0 \\ 0, & 0, & 0, & 0, & 0, & 0, & 1 \end{bmatrix}$	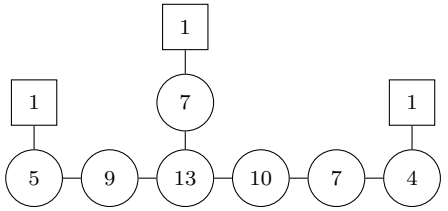	$D_4(a_1) + A_1$	96
$A_5 + A_1$	$\{\alpha_1, \alpha_3, \alpha_4, \alpha_5, \alpha_6, \alpha_7\}$	$\begin{bmatrix} 0, & -1, & 0, & 0, & 0, & 0, & 0 \\ 0, & 1, & 0, & 0, & 0, & 0, & 0 \end{bmatrix}$	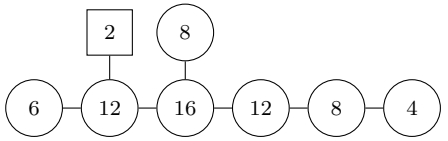	$D_4(a_1)$	94
$D_5(a_1) + A_1$	$\{\alpha_1, \alpha_2, \alpha_3, \alpha_4, \alpha_6, \alpha_7\}$	$\begin{bmatrix} 0, & 0, & 0, & 0, & -1, & 0, & 0 \\ 0, & 0, & 0, & 0, & 1, & 0, & 0 \end{bmatrix}_{3,5}$	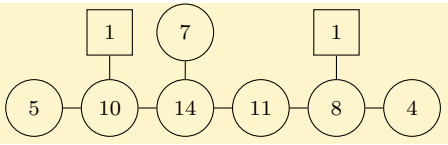	$A_3 + A_2$	98

Table A.2: Results for E_7

Orbit	Θ	Weights	Quiver	Dual orbit	d
$D_6(a_2)$	$\{\alpha_2,\alpha_3,\alpha_4,\alpha_5,\alpha_6,\alpha_7\}$	$[1,0,0,0,0,0,0]_1$ $[-1,0,0,0,0,0,0]_3$	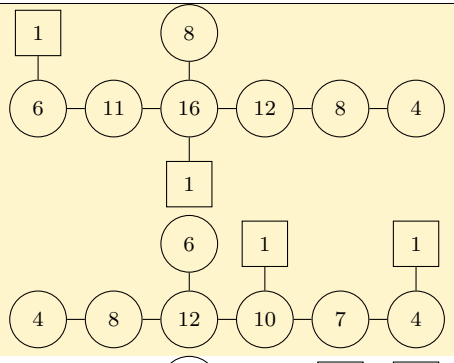	$A_3a + A_1a$	92
$E_6(a_3)$	$\{\alpha_1,\alpha_2,\alpha_3,\alpha_4,\alpha_5,\alpha_7\}$	$[0,0,0,0,0,-1,0]_4$ $[0,0,0,0,0,1,0]_6$		$A_3 + 2A_1$	94
D_5	$\{\alpha_1,\alpha_2,\alpha_3,\alpha_4,\alpha_7\}$	$[0,0,0,0,-1,0,0]$ $[0,0,0,0,1,-1,0]$ $[0,0,0,0,0,1,0]$	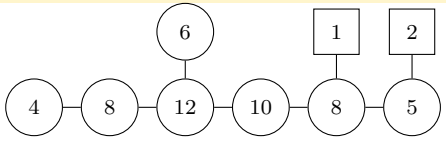	$A_3b + A_1b$	86
$E_7(a_5)$	$\{\alpha_1,\alpha_2,\alpha_3,\alpha_4,\alpha_5,\alpha_6,\alpha_7\}$	$[0,0,0,0,0,0,0]_2$ $[0,0,0,0,0,0,0]_5$	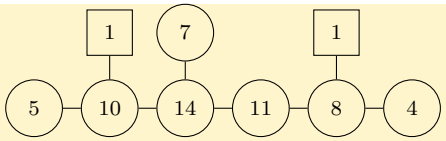	$2A_2 + A_1$	90
A_6	$\{\alpha_1,\alpha_2,\alpha_3,\alpha_4,\alpha_5,\alpha_6\}$	$[0,0,0,0,0,0,-1]$ $[0,0,0,0,0,0,1]$	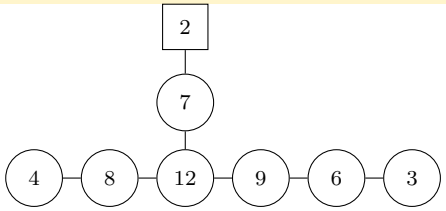	$A_2 + 3A_1$	84
$D_5 + A_1$	$\{\alpha_1,\alpha_2,\alpha_3,\alpha_4,\alpha_6,\alpha_7\}$	$[0,0,0,0,-1,0,0]$ $[0,0,0,0,1,0,0]$	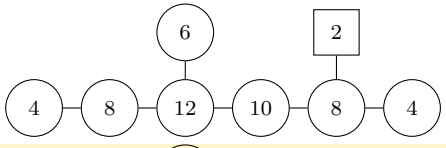	$2A_2$	84
$D_6(a_1)$	$\{\alpha_2,\alpha_3,\alpha_4,\alpha_5,\alpha_6,\alpha_7\}$	$[1,0,0,0,0,0,0]_1$ $[-1,0,0,0,0,0,0]_5$	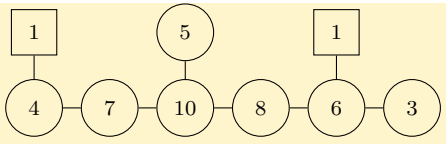	A_3	84

Table A.2: Results for E_7

Orbit	Θ	Weights	Quiver	Dual orbit	d
$E_7(a_4)$	$\{\alpha_1,\alpha_2,\alpha_3,\alpha_4,\alpha_5,\alpha_6,\alpha_7\}$	$[\ 0,\ 0,\ 0,\ 0,\ 0,\ 0,\ 0]_3$	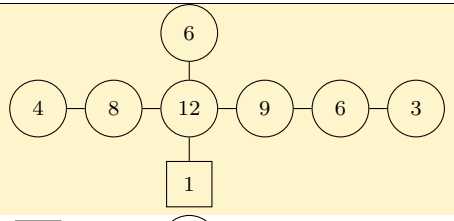	A_2+2A_1	82
D_6	$\{\alpha_2,\alpha_3,\alpha_4,\alpha_5,\alpha_6,\alpha_7\}$	$[-1,\ 0,\ 0,\ 0,\ 0,\ 0,\ 0]$ $[\ 1,\ 0,\ 0,\ 0,\ 0,\ 0,\ 0]$	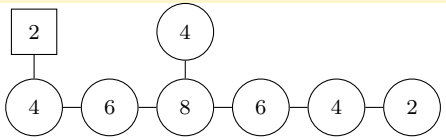	A_2	66
$E_6(a_1)$	$\{\alpha_1,\alpha_2,\alpha_3,\alpha_4,\alpha_5,\alpha_7\}$	$[\ 0,\ 0,\ 0,\ 0,\ 0,\ 1,\ 0]_6$ $[\ 0,\ 0,\ 0,\ 0,\ 0,-1,\ 0]_7$	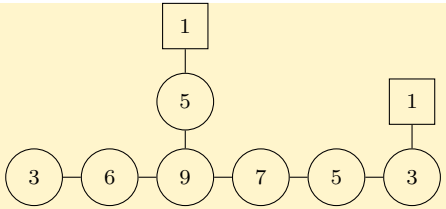	$4A_1$	70
E_6	$\{\alpha_1,\alpha_2,\alpha_3,\alpha_4,\alpha_5,\alpha_7\}$	$[\ 0,\ 0,\ 0,\ 0,\ 0,-1,\ 0]$ $[\ 0,\ 0,\ 0,\ 0,\ 0,\ 1,\ 0]$	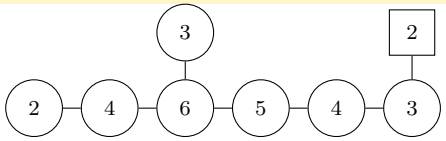	$3A_1b$	54
$E_7(a_3)$	$\{\alpha_1,\alpha_2,\alpha_3,\alpha_4,\alpha_5,\alpha_6,\alpha_7\}$	$[\ 0,\ 0,\ 0,\ 0,\ 0,\ 0,\ 0]_2$	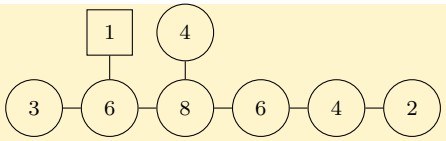	$3A_1a$	64
$E_7(a_2)$	$\{\alpha_1,\alpha_2,\alpha_3,\alpha_4,\alpha_5,\alpha_6,\alpha_7\}$	$[\ 0,\ 0,\ 0,\ 0,\ 0,\ 0,\ 0]_5$	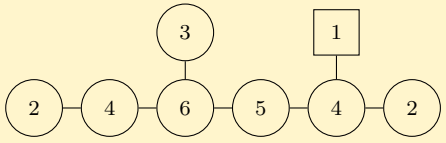	$2A_1$	52
$E_7(a_1)$	$\{\alpha_1,\alpha_2,\alpha_3,\alpha_4,\alpha_5,\alpha_6,\alpha_7\}$	$[\ 0,\ 0,\ 0,\ 0,\ 0,\ 0,\ 0]_1$	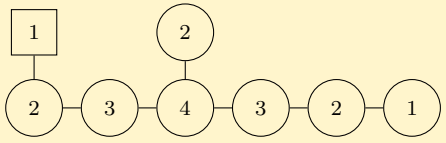	A_1	34

Table A.3: Results for E_8

Orbit	Θ	Weights	Quiver	Dual orbit	d
0	$\varnothing$	$\begin{bmatrix}-1, & 0, & 0, & 0, & 0, & 0, & 0, & 0\\ 1, & -1, & 1, & -1, & 0, & 0, & 0, & 0\\ 0, & 1, & -1, & 1, & 0, & -1, & 0, & 0\\ -1, & -1, & 1, & -1, & 0, & 1, & -1, & 0\\ 1, & 2, & -2, & 1, & 0, & 0, & 1, & 0\\ -1, & 0, & 0, & 1, & -1, & 0, & 0, & -1\\ 1, & -1, & 0, & 0, & 1, & 0, & 0, & 1\\ 0, & 0, & 2, & -2, & 0, & 0, & 0, & -1\\ 0, & 0, & -1, & 1, & 0, & 0, & 0, & 1\\ -1, & 0, & 0, & 0, & 0, & 0, & 0, & 0\end{bmatrix}$	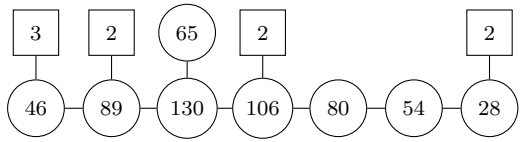	E_8	240
A_1	$\{\alpha_7\}$	$\begin{bmatrix}1, & -1, & 0, & 0, & 1, & 0, & 0, & 1\\ 0, & 0, & 2, & -2, & 0, & 0, & 0, & -1\\ 0, & 0, & -1, & 1, & 0, & 0, & 0, & 1\\ -1, & 0, & 0, & 0, & 0, & 0, & 0, & 0\\ 1, & -1, & 1, & -1, & 0, & 0, & 0, & 0\\ 0, & 1, & -1, & 1, & 0, & -1, & 0, & 0\\ 0, & 1, & -1, & 0, & 0, & 1, & 0, & 0\\ 0, & -1, & 0, & 1, & 0, & 0, & 0, & 0\end{bmatrix}$	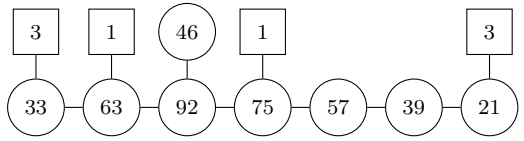	$E_8(a_1)$	238
$2A_1$	$\{\alpha_5, \alpha_7\}$	$\begin{bmatrix}0, & 0, & 2, & -2, & 0, & 0, & 0, & -1\\ 0, & 0, & -1, & 1, & 0, & 0, & 0, & 1\\ -1, & 0, & 0, & 0, & 0, & 0, & 0, & 0\\ 1, & -1, & 1, & -1, & 0, & 0, & 0, & 0\\ 0, & 1, & -1, & 1, & 0, & -1, & 0, & 0\\ 0, & 1, & -1, & 0, & 0, & 1, & 0, & 0\\ 0, & -1, & 0, & 1, & 0, & 0, & 0, & 0\end{bmatrix}$	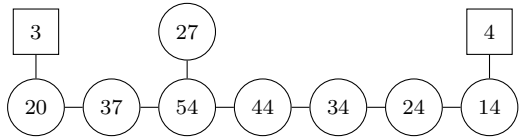	$E_8(a_2)$	236
$3A_1$	$\{\alpha_5, \alpha_7, \alpha_8\}$	$\begin{bmatrix}1, & -1, & 1, & -1, & 0, & 0, & 0, & 0\\ 0, & 1, & -1, & 1, & 0, & -1, & 0, & 0\\ 0, & 1, & -1, & 0, & 0, & 1, & 0, & 0\\ 0, & -1, & 0, & 1, & 0, & 0, & 0, & 0\\ 0, & 0, & 1, & -1, & 0, & 0, & 0, & 0\end{bmatrix}$	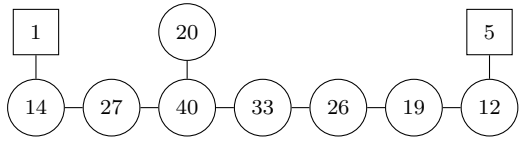	$E_8(a_3)$	234
A_2	$\{\alpha_2, \alpha_3\}$	$\begin{bmatrix}2, & 0, & 0, & -1, & 0, & -1, & 0, & 0\\ 0, & 0, & 0, & 0, & 0, & -1, & 0, & 0\\ -1, & 0, & 0, & 0, & -1, & 3, & -1, & 0\\ 0, & 0, & 0, & 0, & 2, & -2, & 0, & -1\\ 0, & 0, & 0, & 0, & -1, & 1, & 0, & 1\\ 0, & 0, & 0, & 0, & 0, & 0, & 1, & 0\\ -1, & 0, & 0, & 1, & 0, & 0, & 0, & 0\end{bmatrix}$	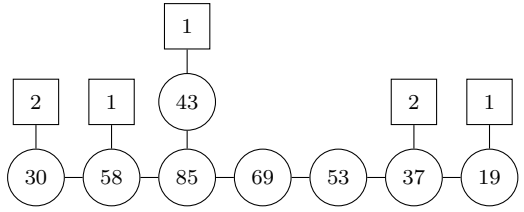	$E_8(a_3)$	234

Table A.3: Results for E_8

Orbit	Θ	Weights	Quiver	Dual orbit	d
$4A_1$	$\{\alpha_1, \alpha_3, \alpha_5, \alpha_7\}$	$\begin{bmatrix} 0,-1, & 0, & 0, & 0,-1, & 0, & 1] \\ [\ 0,-1, & 0, & 0, & 0,-1, & 0, & 1] \\ [\ 0, & 3, & 0,-1, & 0, & 1, & 0,-3] \\ [\ 0,-1, & 0, & 1, & 0, & 1, & 0, & 0] \\ [\ 0, & 0, & 0, & 0, & 0, & 0, & 1] \end{bmatrix}$	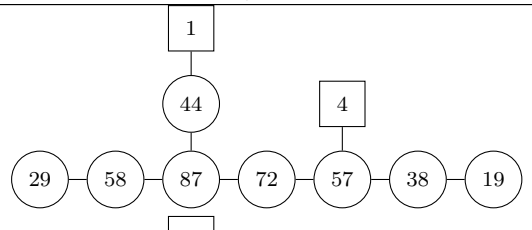	$E_8(a_4)$	232
$A_2 + A_1$	$\{\alpha_2, \alpha_3, \alpha_7\}$	$\begin{bmatrix} 0, & 0, & 0,-1, & 0, & 0, & 0, & 0] \\ [\ 0, & 0, & 0, & 0,-1, & 1, & 0, & 0] \\ [-1, & 0, & 0, & 0, & 1,-1, & 0, & 0] \\ [\ 0, & 0, & 0, & 1,-1, & 0, & 0, & 0] \\ [\ 1, & 0, & 0, & 0, & 1, & 0, & 0,-1] \\ [\ 0, & 0, & 0, & 0, & 0, & 0, & 0, & 1] \end{bmatrix}$	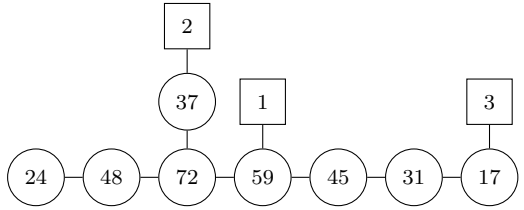	$E_8(a_4)$	232
$A_2 + 2A_1$	$\{\alpha_1, \alpha_2, \alpha_4, \alpha_6\}$	$\begin{bmatrix} 0, & 0, & 1, & 0,-3, & 0, & 0, & 0] \\ [\ 0, & 0, & 0, & 0, & 1, & 0,-1, & 0] \\ [\ 0, & 0, & 0, & 0, & 1, & 0, & 0,-1] \\ [\ 0, & 0,-1, & 0, & 1, & 0, & 0, & 1] \\ [\ 0, & 0, & 0, & 0, & 0, & 1, & 0] \end{bmatrix}$	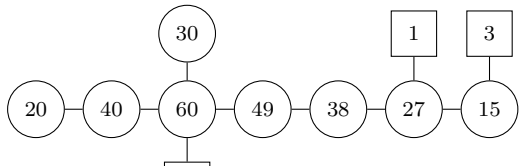	$E_8(b_4)$	230
A_3	$\{\alpha_2, \alpha_3, \alpha_8\}$	$\begin{bmatrix} 2, & 0, & 0,-1, & 0,-1, & 0, & 0] \\ [\ 0, & 0, & 0, & 0, & 0,-1, & 0, & 0] \\ [-1, & 0, & 0, & 0,-1, & 3,-1, & 0] \\ [\ 0, & 0, & 0, & 0, & 1,-1, & 0, & 0] \\ [\ 0, & 0, & 0, & 0, & 0, & 0, & 1, & 0] \\ [-1, & 0, & 0, & 1, & 0, & 0, & 0, & 0] \end{bmatrix}$	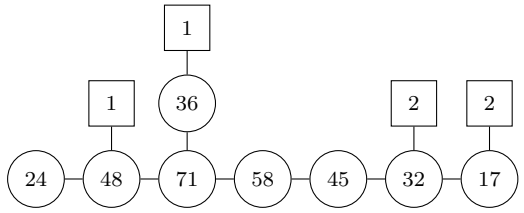	$E_7(a_1)$	228
$A_2 + 3A_1$	$\{\alpha_1, \alpha_3, \alpha_5, \alpha_7, \alpha_8\}$	$\begin{bmatrix} 0, & 0, & 0, & 0, & 0,-1, & 0, & 0] \\ [\ 0, & 1, & 0,-2, & 0, & 2, & 0, & 0] \\ [\ 0, & 0, & 0, & 1, & 0,-1, & 0, & 0] \\ [\ 0,-1, & 0, & 1, & 0, & 0, & 0, & 0] \end{bmatrix}$	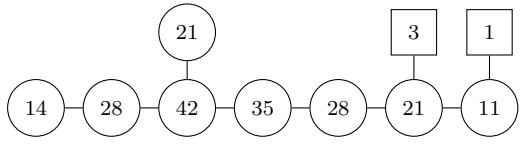	$E_8(a_5)$	228

Table A.3: Results for E_8

Orbit	Θ	Weights	Quiver	Dual orbit	d
$2A_2$	$\{\alpha_1, \alpha_2, \alpha_4, \alpha_5\}$	$\begin{bmatrix} 0, & 0, & 0, & 0, & 0, & 0, & 0, & -1 \\ 0, & 0, & 0, & 0, & 0, & 0, & 0, & -1 \\ 0, & 0, & -2, & 0, & 0, & 2, & -1, & 3 \\ 0, & 0, & 1, & 0, & 0, & -2, & 1, & 0 \\ 0, & 0, & 1, & 0, & 0, & 0, & 0, & -1 \end{bmatrix}$	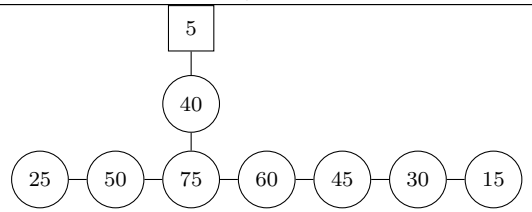	$E_8(a_5)$	228
$2A_2 + A_1$	$\{\alpha_1, \alpha_2, \alpha_4, \alpha_5, \alpha_7\}$	$\begin{bmatrix} 0, & 0, & -1, & 0, & 0, & 1, & 0, & 0 \\ 0, & 0, & 0, & 0, & 0, & 1, & 0, & 0 \\ 0, & 0, & 1, & 0, & 0, & -1, & 0, & -1 \\ 0, & 0, & 0, & 0, & 0, & -1, & 0, & 1 \end{bmatrix}$	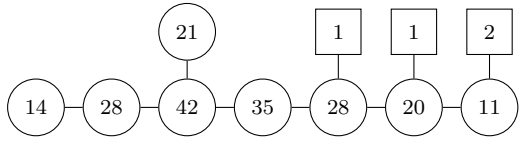	$E_8(b_5)$	226
$A_3 + A_1$	$\{\alpha_1, \alpha_2, \alpha_3, \alpha_5\}$	$\begin{bmatrix} 0, & 0, & 0, & 0, & 0, & 0, & -1, & 0 \\ 0, & 0, & 0, & 0, & 0, & 1, & 0, & -1 \\ 0, & 0, & 0, & 0, & 0, & 0, & 0, & -1 \\ 0, & 0, & 0, & 1, & 0, & -2, & 2, & 0 \\ 0, & 0, & 0, & -1, & 0, & 1, & -1, & 2 \end{bmatrix}$	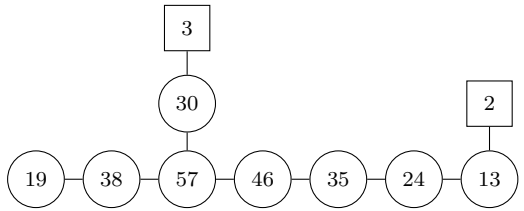	$E_8(b_5)$	226
$D_4(a_1)$	$\{\alpha_2, \alpha_3, \alpha_4, \alpha_8\}$	$\begin{bmatrix} 0, & 0, & 0, & 0, & -1, & 1, & 0, & 0 \\ 0, & 0, & 0, & 0, & 0, & 0, & 1, & 0 \\ 0, & 0, & 0, & 0, & 0, & 1, & -1, & 0 \\ 1, & 0, & 0, & 0, & 0, & -1, & 0, & 0 \\ -1, & 0, & 0, & 0, & 1, & -1, & 0, & 0 \end{bmatrix}_7$	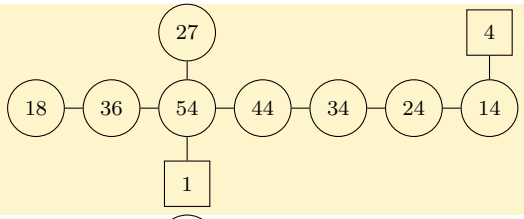	$E_8(b_5)$	226
D_4	$\{\alpha_2, \alpha_3, \alpha_4, \alpha_8\}$	$\begin{bmatrix} 0, & 0, & 0, & 0, & 0, & 0, & -1, & 0 \\ 0, & 0, & 0, & 0, & 0, & -1, & 1, & 0 \\ -1, & 0, & 0, & 0, & 0, & 1, & 0, & 0 \\ 1, & 0, & 0, & 0, & -1, & 1, & 0, & 0 \\ 0, & 0, & 0, & 0, & 1, & -1, & 0, & 0 \end{bmatrix}$	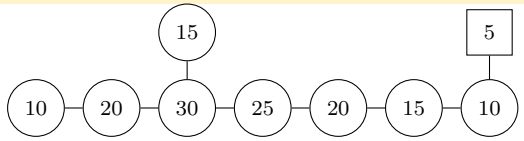	E_6	216
$2A_2 + 2A_1$	$\{\alpha_1, \alpha_2, \alpha_4, \alpha_5, \alpha_7, \alpha_8\}$	$\begin{bmatrix} 0, & 0, & -1, & 0, & 0, & 1, & 0, & 0 \\ 0, & 0, & 1, & 0, & 0, & -2, & 0, & 0 \\ 0, & 0, & 0, & 0, & 0, & 1, & 0, & 0 \end{bmatrix}$	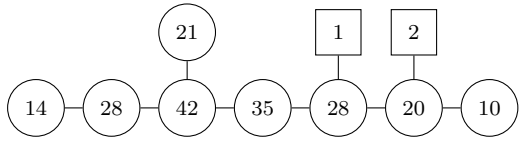	$E_8(a_6)$	224

Table A.3: Results for E_8

Orbit	Θ	Weights	Quiver	Dual orbit	d
$A_3 + 2A_1$	$\{\alpha_1, \alpha_2, \alpha_3, \alpha_5, \alpha_7\}$	$\begin{bmatrix} 0, & 0, & 0, & 1, & 0, & 0, & 0, -2 \\ 0, & 0, & 0, & 0, & 0, -1, & 0, & 0 \\ 0, & 0, & 0, -1, & 0, & 1, & 0, & 1 \\ 0, & 0, & 0, & 0, & 0, & 0, & 0, & 1 \end{bmatrix}$	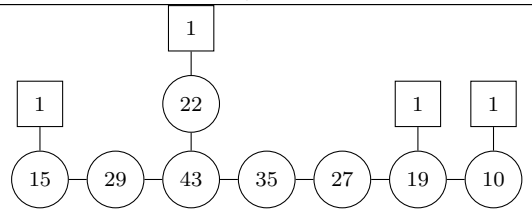	$E_8(a_6)$	224
$D_4(a_1) + A_1$	$\{\alpha_2, \alpha_3, \alpha_4, \alpha_7, \alpha_8\}$	$\begin{bmatrix} 0, & 0, & 0, & 0, -1, & 1, & 0, & 0 \\ 0, & 0, & 0, & 0, & 0, & 1, & 0, & 0 \\ 1, & 0, & 0, & 0, & 0, -1, & 0, & 0 \\ -1, & 0, & 0, & 0, & 1, -1, & 0, & 0 \end{bmatrix}_3 \begin{matrix} \\ _6 \\ _7 \\ _7 \end{matrix}$	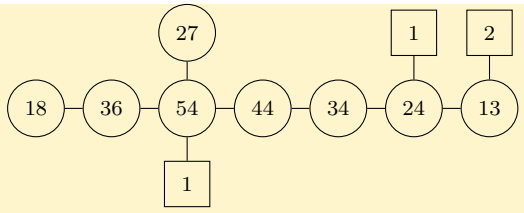	$E_8(a_6)$	224
$A_3 + A_2$	$\{\alpha_1, \alpha_2, \alpha_3, \alpha_5, \alpha_6\}$	$\begin{bmatrix} 0, & 0, & 0, -1, & 0, & 0, & 0, & 1 \\ 0, & 0, & 0, & 1, & 0, & 0, & 0, -2 \\ 0, & 0, & 0, & 0, & 0, & 0, -1, & 1 \\ 0, & 0, & 0, & 0, & 0, & 0, & 1, & 0 \end{bmatrix}$	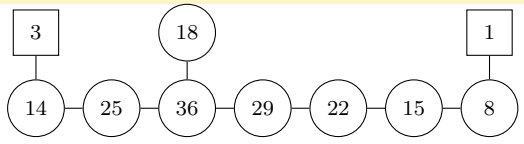	$D_7(a_1)$	222
A_4	$\{\alpha_1, \alpha_2, \alpha_3, \alpha_4\}$	$\begin{bmatrix} 0, & 0, & 0, & 0, & 0, & 0, & 0, -1 \\ 0, & 0, & 0, & 0, & 1, & 0, & 0, -2 \\ 0, & 0, & 0, & 0, & 1, -1, & -2, & 1 \\ 0, & 0, & 0, & 0, & 0, -2, & 3, & 1 \\ 0, & 0, & 0, & 0, -2, & 3, & -1, & 1 \end{bmatrix}$	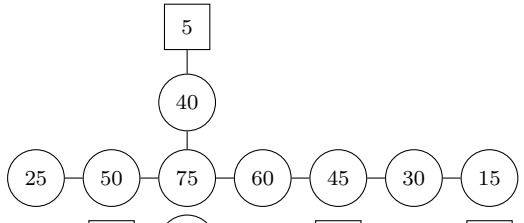	$E_7(a_3)$	220
$A_3 + A_2 + A_1$	$\{\alpha_1, \alpha_3, \alpha_5, \alpha_6, \alpha_7, \alpha_8\}$	$\begin{bmatrix} 0, -1, & 0, & 0, & 0, & 0, & 0, & 0 \\ 0, & 2, & 0, -1, & 0, & 0, & 0, & 0 \\ 0, -1, & 0, & 1, & 0, & 0, & 0, & 0 \end{bmatrix}$	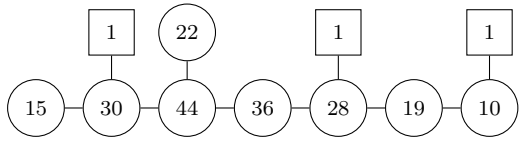	$E_8(b_6)$	220
$D_4 + A_1$	$\{\alpha_2, \alpha_3, \alpha_4, \alpha_6, \alpha_8\}$	$\begin{bmatrix} -1, & 0, & 0, & 0, & 0, & 0, & 0 \\ 1, & 0, & 0, & 0, -1, & 0, & 0, & 0 \\ 0, & 0, & 0, & 0, & 1, & 0, -1, & 0 \\ 0, & 0, & 0, & 0, & 0, & 1, & 0 \end{bmatrix}$	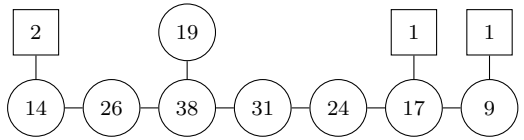	$E_6(a_1)$	214

Table A.3: Results for E_8

Orbit	Θ	Weights	Quiver	Dual orbit	d
$D_4(a_1)+A_2$	$\{\alpha_2,\alpha_3,\alpha_4,\alpha_6,\alpha_7,\alpha_8\}$	$[1,0,0,0,0,0,0,0]_1$ $[-1,0,0,0,1,0,0,0]_1$ $[0,0,0,0,-1,0,0,0]_4$	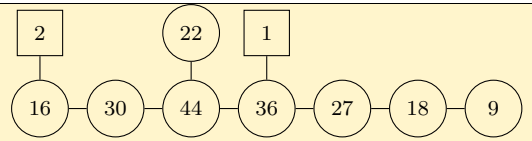	A_7	218
A_4+A_1	$\{\alpha_1,\alpha_2,\alpha_3,\alpha_4,\alpha_6\}$	$[0,0,0,0,-1,0,1,0]$ $[0,0,0,0,0,0,-1,0]$ $[0,0,0,0,1,0,0,-1]$ $[0,0,0,0,0,0,0,1]$	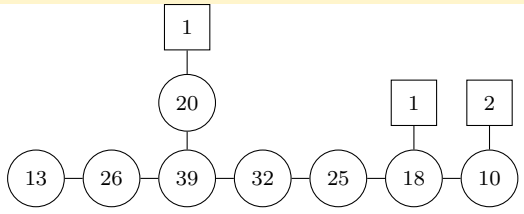	$E_6(a_1)+A_1$	218
$2A_3$	$\{\alpha_1,\alpha_2,\alpha_3,\alpha_5,\alpha_6,\alpha_7\}$	$[0,0,0,-1,0,0,0,1]$ $[0,0,0,1,0,0,0,-2]$ $[0,0,0,0,0,0,0,1]$	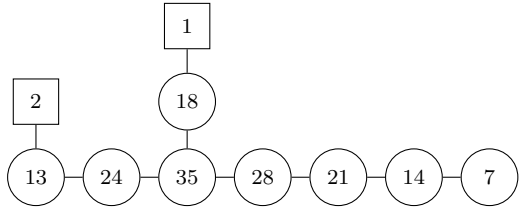	$D_7(a_2)$	216
$D_5(a_1)$	$\{\alpha_1,\alpha_2,\alpha_3,\alpha_4,\alpha_8\}$	$[0,0,0,0,0,0,1,0]_2$ $[0,0,0,0,-1,2,-1,0]_7$ $[0,0,0,0,1,-1,-1,0]_7$ $[0,0,0,0,0,-1,1,0]_7$	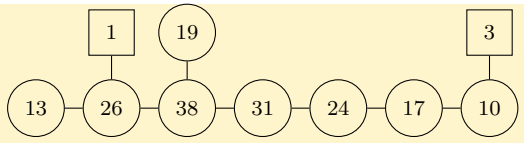	$E_6(a_1)$	214
A_4+2A_1	$\{\alpha_1,\alpha_4,\alpha_5,\alpha_6,\alpha_7,\alpha_8\}$	$[0,1,-1,0,0,0,0,0]$ $[0,-1,0,0,0,0,0,0]$ $[0,0,1,0,0,0,0,0]$	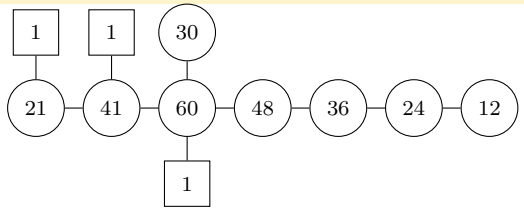	$D_7(a_2)$	216
A_4+A_2	$\{\alpha_1,\alpha_2,\alpha_4,\alpha_5,\alpha_6,\alpha_7\}$	$[0,0,1,0,0,0,0,-2]$ $[0,0,-1,0,0,0,0,1]$ $[0,0,0,0,0,0,0,1]$	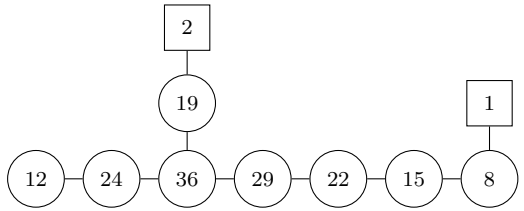	D_5+A_2	214

Table A.3: Results for E_8

Orbit	Θ	Weights	Quiver	Dual orbit	d
A_5	$\{\alpha_1,\alpha_2,\alpha_3,\alpha_4,\alpha_5\}$	$\begin{bmatrix}0,&0,&0,&0,&0,&0,&-1,&0\\0,&0,&0,&0,&0,&-1,&1,&0\\0,&0,&0,&0,&0,&1,&0,&-1\\0,&0,&0,&0,&0,&0,&0,&1\end{bmatrix}$	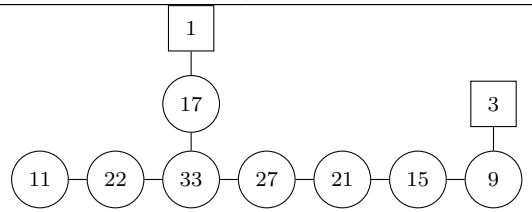	$D_6(a_1)$	210
$D_5(a_1)+A_1$	$\{\alpha_1,\alpha_2,\alpha_3,\alpha_4,\alpha_6,\alpha_8\}$	$\begin{bmatrix}0,&0,&0,&0,&-1,&0,&1,&0\\0,&0,&0,&0,&1,&0,&0,&0\\0,&0,&0,&0,&0,&0,&-1,&0\end{bmatrix}_{3,5,7}$	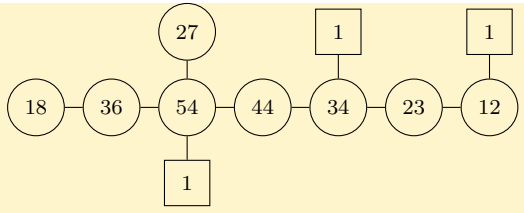	$E_7(a_4)$	212
$A_4+A_2+A_1$	$\{\alpha_1,\alpha_2,\alpha_4,\alpha_5,\alpha_6,\alpha_7,\alpha_8\}$	$\begin{bmatrix}0,&0,&-1,&0,&0,&0,&0,&0\\0,&0,&1,&0,&0,&0,&0,&0\end{bmatrix}$	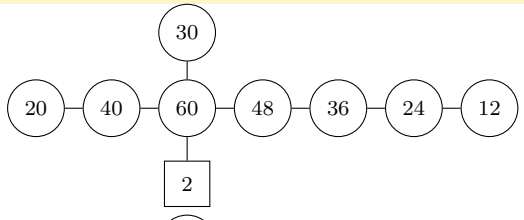	A_6+A_1	212
D_4+A_2	$\{\alpha_2,\alpha_3,\alpha_4,\alpha_6,\alpha_7,\alpha_8\}$	$\begin{bmatrix}-1,&0,&0,&0,&0,&0,&0,&0\\1,&0,&0,&0,&-1,&0,&0,&0\\0,&0,&0,&0,&1,&0,&0,&0\end{bmatrix}$	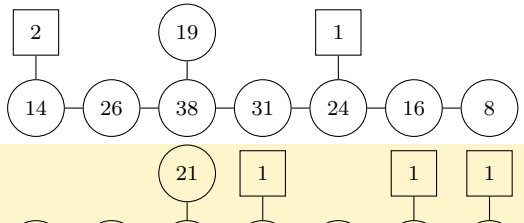	A_6	210
$E_6(a_3)$	$\{\alpha_1,\alpha_2,\alpha_3,\alpha_4,\alpha_5,\alpha_8\}$	$\begin{bmatrix}0,&0,&0,&0,&0,&-1,&-1,&0\\0,&0,&0,&0,&0,&1,&0,&0\\0,&0,&0,&0,&0,&0,&1,&0\end{bmatrix}_{4,6,7}$	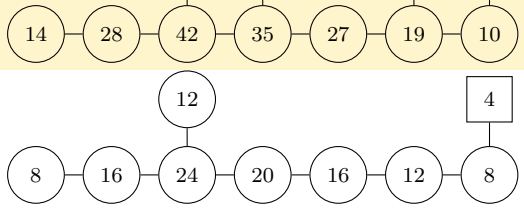	D_5+A_1	208
D_5	$\{\alpha_1,\alpha_2,\alpha_3,\alpha_4,\alpha_8\}$	$\begin{bmatrix}0,&0,&0,&0,&0,&0,&-1,&0\\0,&0,&0,&0,&1,&-2,&1,&0\\0,&0,&0,&0,&-1,&1,&1,&0\\0,&0,&0,&0,&0,&1,&-1,&0\end{bmatrix}$		D_5	200

Table A.3: Results for E_8

Orbit	Θ	Weights	Quiver	Dual orbit	d
$A_4 + A_3$	$\{\alpha_1, \alpha_2, \alpha_3, \alpha_5, \alpha_6, \alpha_7, \alpha_8\}$	$\begin{bmatrix} 0, & 0, & 0, & 0, -1, & 0, & 0, & 0, & 0 \\ 0, & 0, & 0, & 1, & 0, & 0, & 0, & 0 \end{bmatrix}$	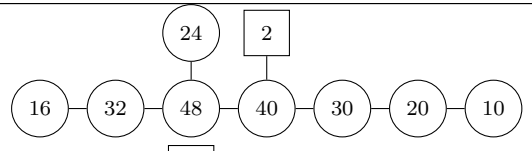	$E_8(a_7)$	208
$A_5 + A_1$	$\{\alpha_1, \alpha_2, \alpha_3, \alpha_4, \alpha_5, \alpha_7\}$	$\begin{bmatrix} 0, & 0, & 0, & 0, & 0, -1, & 0, & 0 \\ 0, & 0, & 0, & 0, & 0, & 1, & 0, -1 \\ 0, & 0, & 0, & 0, & 0, & 0, & 0, & 1 \end{bmatrix}$	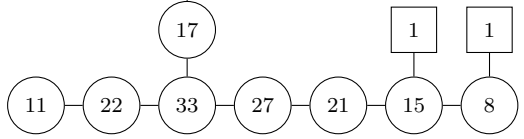	$E_8(a_7)$	208
$D_5(a_1) + A_2$	$\{\alpha_1, \alpha_2, \alpha_3, \alpha_4, \alpha_6, \alpha_7, \alpha_8\}$	$\begin{bmatrix} 0, & 0, & 0, & 0, -1, & 0, & 0, & 0 \end{bmatrix}_3$ $\begin{bmatrix} 0, & 0, & 0, & 0, & 1, & 0, & 0, & 0 \end{bmatrix}_5$	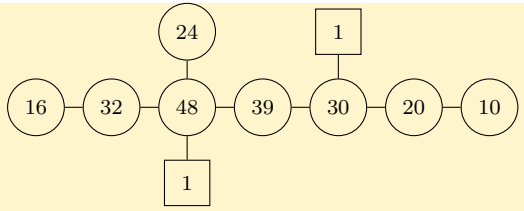	$E_7(a_5)$	206
$D_6(a_2)$	$\{\alpha_2, \alpha_3, \alpha_4, \alpha_5, \alpha_6, \alpha_8\}$	$\begin{bmatrix} 1, & 0, & 0, & 0, & 0, & 0, & 0, & 0 \end{bmatrix}_1$ $\begin{bmatrix} -1, & 0, & 0, & 0, & 0, & 0, -1, & 0 \end{bmatrix}_4$ $\begin{bmatrix} 0, & 0, & 0, & 0, & 0, & 0, & 1, & 0 \end{bmatrix}_7$	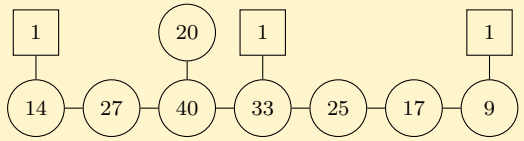	$D_5(a_1) + A_2$	202
$E_6(a_3) + A_1$	$\{\alpha_1, \alpha_2, \alpha_3, \alpha_4, \alpha_5, \alpha_7, \alpha_8\}$	$\begin{bmatrix} 0, & 0, & 0, & 0, & 0, -1, & 0, & 0 \end{bmatrix}_3$ $\begin{bmatrix} 0, & 0, & 0, & 0, & 0, & 1, & 0, & 0 \end{bmatrix}_6$	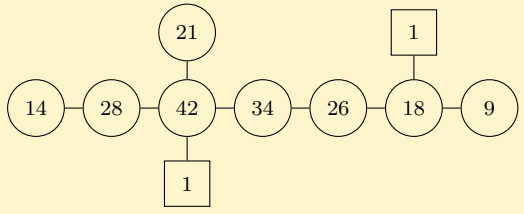	$A_5 + A_1$	202
$E_7(a_5)$	$\{\alpha_1, \alpha_2, \alpha_3, \alpha_4, \alpha_5, \alpha_6, \alpha_8\}$	$\begin{bmatrix} 0, & 0, & 0, & 0, & 0, & 0, -1, & 0 \end{bmatrix}_3$ $\begin{bmatrix} 0, & 0, & 0, & 0, & 0, & 0, & 1, & 0 \end{bmatrix}_7$	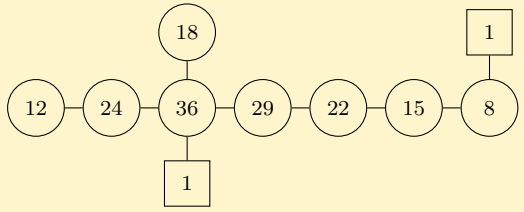	$A_4 + A_3$	200

Table A.3: Results for E_8

Orbit	Θ	Weights	Quiver	Dual orbit	d
$D_5 + A_1$	$\{\alpha_1, \alpha_2, \alpha_3, \alpha_4, \alpha_6, \alpha_8\}$	$\begin{bmatrix} 0, & 0, & 0, & 0, & -1, & 0, & 0, & 0 \\ 0, & 0, & 0, & 0, & 1, & 0, & -1, & 0 \\ 0, & 0, & 0, & 0, & 0, & 0, & 1, & 0 \end{bmatrix}$	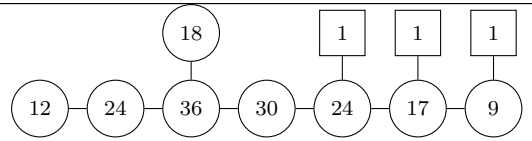	$E_6(a_3)$	198
$E_8(a_7)$	$\{\alpha_1, \alpha_2, \alpha_3, \alpha_4, \alpha_5, \alpha_6, \alpha_7, \alpha_8\}$	$\begin{bmatrix} 0, & 0, & 0, & 0, & 0, & 0, & 0, & 0 \end{bmatrix}_4$ $\begin{bmatrix} 0, & 0, & 0, & 0, & 0, & 0, & 0, & 0 \end{bmatrix}_4$	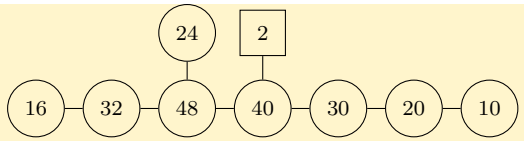	$E_8(a_7)$	208
A_6	$\{\alpha_1, \alpha_2, \alpha_3, \alpha_4, \alpha_5, \alpha_6\}$	$\begin{bmatrix} 0, & 0, & 0, & 0, & 0, & 0, & 1, & -1 \\ 0, & 0, & 0, & 0, & 0, & 0, & -1, & 0 \\ 0, & 0, & 0, & 0, & 0, & 0, & 0, & 1 \end{bmatrix}$	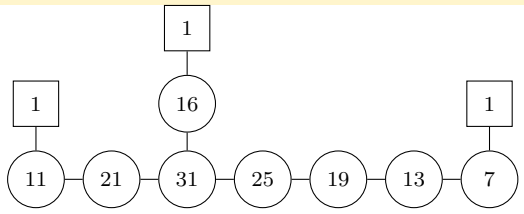	$D_4 + A_2$	198
$D_6(a_1)$	$\{\alpha_2, \alpha_3, \alpha_4, \alpha_5, \alpha_6, \alpha_8\}$	$\begin{bmatrix} 1, & 0, & 0, & 0, & 0, & 0, & 0, & 0 \end{bmatrix}_1$ $\begin{bmatrix} -1, & 0, & 0, & 0, & 0, & 0, & -1, & 0 \end{bmatrix}_5$ $\begin{bmatrix} 0, & 0, & 0, & 0, & 0, & 0, & 1, & 0 \end{bmatrix}_7$	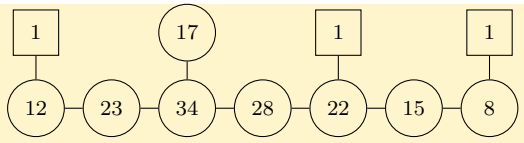	A_5	196
$A_6 + A_1$	$\{\alpha_1, \alpha_3, \alpha_4, \alpha_5, \alpha_6, \alpha_7, \alpha_8\}$	$\begin{bmatrix} 0, & -1, & 0, & 0, & 0, & 0, & 0, & 0 \\ 0, & 1, & 0, & 0, & 0, & 0, & 0, & 0 \end{bmatrix}$	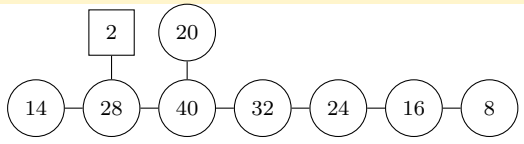	$A_4 + A_2 + A_1$	196
$E_7(a_4)$	$\{\alpha_1, \alpha_2, \alpha_3, \alpha_4, \alpha_5, \alpha_6, \alpha_8\}$	$\begin{bmatrix} 0, & 0, & 0, & 0, & 0, & 0, & -1, & 0 \end{bmatrix}_4$ $\begin{bmatrix} 0, & 0, & 0, & 0, & 0, & 0, & 1, & 0 \end{bmatrix}_7$	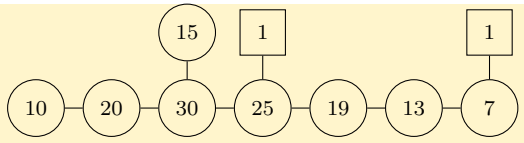	$D_5(a_1) + A_1$	196
$E_6(a_1)$	$\{\alpha_1, \alpha_2, \alpha_3, \alpha_4, \alpha_5, \alpha_8\}$	$\begin{bmatrix} 0, & 0, & 0, & 0, & 0, & 0, & -1, & 0 \end{bmatrix}_2$ $\begin{bmatrix} 0, & 0, & 0, & 0, & 0, & 1, & 0, & 0 \end{bmatrix}_6$ $\begin{bmatrix} 0, & 0, & 0, & 0, & 0, & -1, & 1, & 0 \end{bmatrix}_7$	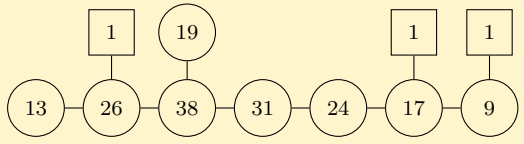	$D_4 + A_1$	184

Table A.3: Results for E_8

Orbit	Θ	Weights	Quiver	Dual orbit	d
$D_5 + A_2$	$\{\alpha_1, \alpha_2, \alpha_3, \alpha_4, \alpha_6, \alpha_7, \alpha_8\}$	$\begin{bmatrix} 0, & 0, & 0, & 0, & -1, & 0, & 0, & 0 \\ 0, & 0, & 0, & 0, & 1, & 0, & 0, & 0 \end{bmatrix}$	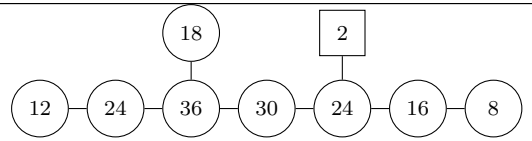	$A_4 + A_2$	194
D_6	$\{\alpha_2, \alpha_3, \alpha_4, \alpha_5, \alpha_6, \alpha_8\}$	$\begin{bmatrix} -1, & 0, & 0, & 0, & 0, & 0, & 0, & 0 \\ 1, & 0, & 0, & 0, & 0, & 0, & -1, & 0 \\ 0, & 0, & 0, & 0, & 0, & 0, & 1, & 0 \end{bmatrix}$	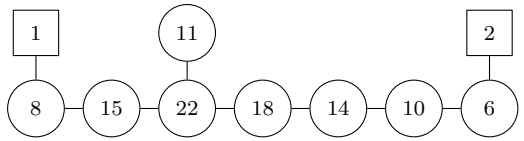	A_4	180
E_6	$\{\alpha_1, \alpha_2, \alpha_3, \alpha_4, \alpha_5, \alpha_8\}$	$\begin{bmatrix} 0, & 0, & 0, & 0, & 0, & -1, & 0, & 0 \\ 0, & 0, & 0, & 0, & 0, & 1, & -1, & 0 \\ 0, & 0, & 0, & 0, & 0, & 0, & 1, & 0 \end{bmatrix}$	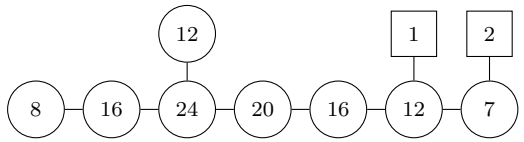	D_4	168
$D_7(a_2)$	$\{\alpha_2, \alpha_3, \alpha_4, \alpha_5, \alpha_6, \alpha_7, \alpha_8\}$	$\begin{bmatrix} 1, & 0, & 0, & 0, & 0, & 0, & 0, & 0 \\ -1, & 0, & 0, & 0, & 0, & 0, & 0, & 0 \end{bmatrix}_{1,4}$	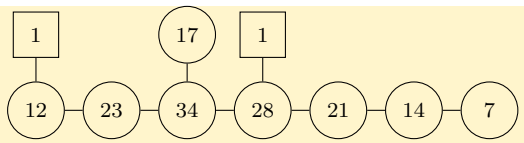	$2A_3$	188
A_7	$\{\alpha_1, \alpha_2, \alpha_3, \alpha_4, \alpha_5, \alpha_6, \alpha_7\}$	$\begin{bmatrix} 0, & 0, & 0, & 0, & 0, & 0, & 0, & -1 \\ 0, & 0, & 0, & 0, & 0, & 0, & 0, & 1 \end{bmatrix}$	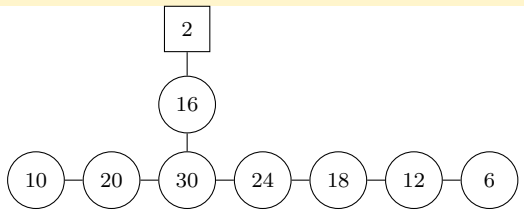	$D_4(a_1) + A_2$	184
$E_6(a_1) + A_1$	$\{\alpha_1, \alpha_2, \alpha_3, \alpha_4, \alpha_5, \alpha_7, \alpha_8\}$	$\begin{bmatrix} 0, & 0, & 0, & 0, & 0, & -1, & 0, & 0 \\ 0, & 0, & 0, & 0, & 0, & 1, & 0, & 0 \end{bmatrix}_{5,6}$	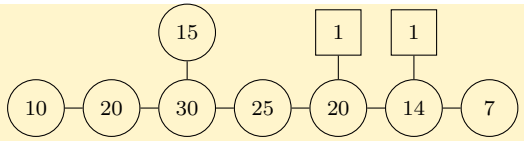	$A_4 + A_1$	188
$E_7(a_3)$	$\{\alpha_1, \alpha_2, \alpha_3, \alpha_4, \alpha_5, \alpha_6, \alpha_8\}$	$\begin{bmatrix} 0, & 0, & 0, & 0, & 0, & 0, & -1, & 0 \\ 0, & 0, & 0, & 0, & 0, & 0, & 1, & 0 \end{bmatrix}_{2,7}$	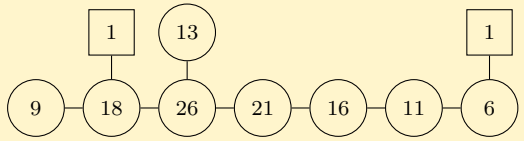	A_4	180

Table A.3: Results for E_8

Orbit	Θ	Weights	Quiver	Dual orbit	d
$E_8(b_6)$	$\{\alpha_1,\alpha_2,\alpha_3,\alpha_4,\alpha_5,\alpha_6,\alpha_7,\alpha_8\}$	$[\ 0,\ 0,\ 0,\ 0,\ 0,\ 0,\ 0,\ 0]_3$	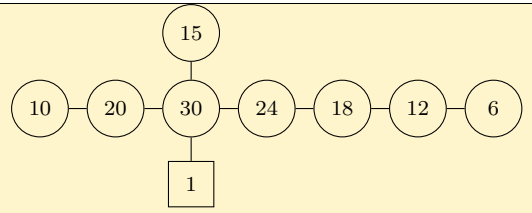	$A_3+A_2+A_1$	182
$D_7(a_1)$	$\{\alpha_2,\alpha_3,\alpha_4,\alpha_5,\alpha_6,\alpha_7,\alpha_8\}$	$[\ 1,\ 0,\ 0,\ 0,\ 0,\ 0,\ 0,\ 0]_1$ $[-1,\ 0,\ 0,\ 0,\ 0,\ 0,\ 0,\ 0]_5$	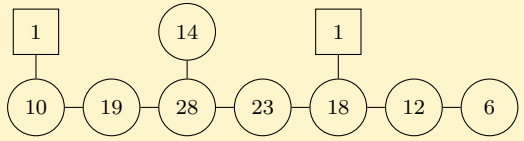	A_3+A_2	178
E_6+A_1	$\{\alpha_1,\alpha_2,\alpha_3,\alpha_4,\alpha_5,\alpha_7,\alpha_8\}$	$[\ 0,\ 0,\ 0,\ 0,\ 0,-1,\ 0,\ 0]$ $[\ 0,\ 0,\ 0,\ 0,\ 0,\ 1,\ 0,\ 0]$	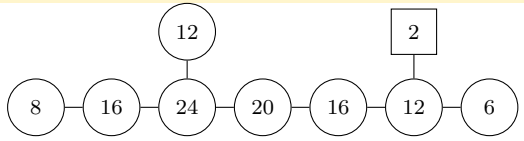	$D_4(A_1)$	166
$E_7(a_2)$	$\{\alpha_1,\alpha_2,\alpha_3,\alpha_4,\alpha_5,\alpha_6,\alpha_8\}$	$[\ 0,\ 0,\ 0,\ 0,\ 0,\ 0,-1,\ 0]_5$ $[\ 0,\ 0,\ 0,\ 0,\ 0,\ 0,\ 1,\ 0]_7$	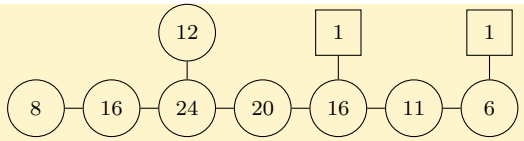	A_3+A_1	164
$E_8(a_6)$	$\{\alpha_1,\alpha_2,\alpha_3,\alpha_4,\alpha_5,\alpha_6,\alpha_7,\alpha_8\}$	$[\ 0,\ 0,\ 0,\ 0,\ 0,\ 0,\ 0,\ 0]_4$	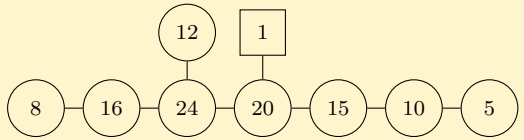	$2A_2+2A_1$	168
D_7	$\{\alpha_2,\alpha_3,\alpha_4,\alpha_5,\alpha_6,\alpha_7,\alpha_8\}$	$[-1,\ 0,\ 0,\ 0,\ 0,\ 0,\ 0,\ 0]$ $[\ 1,\ 0,\ 0,\ 0,\ 0,\ 0,\ 0,\ 0]$	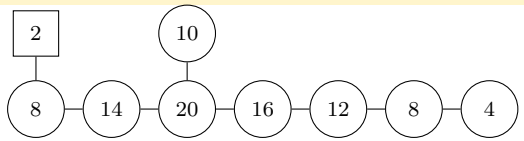	$2A_2$	156
$E_8(b_5)$	$\{\alpha_1,\alpha_2,\alpha_3,\alpha_4,\alpha_5,\alpha_6,\alpha_7,\alpha_8\}$	$[\ 0,\ 0,\ 0,\ 0,\ 0,\ 0,\ 0,\ 0]_1$ $[\ 0,\ 0,\ 0,\ 0,\ 0,\ 0,\ 0,\ 0]_6$	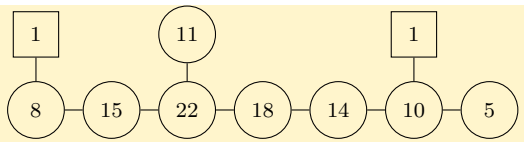	$2A_2+A_1$	162

Table A.3: Results for E_8

Orbit	Θ	Weights	Quiver	Dual orbit	d
$E_7(a_1)$	$\{\alpha_1,\alpha_2,\alpha_3,\alpha_4,\alpha_5,\alpha_6,\alpha_8\}$	$[0,0,0,0,0,0,-1,0]_1$ $[0,0,0,0,0,0,1,0]_7$	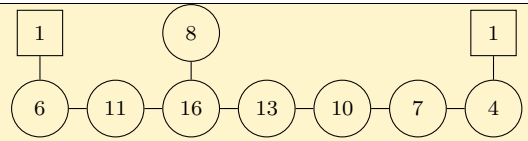	A_3	148
$E_8(a_5)$	$\{\alpha_1,\alpha_2,\alpha_3,\alpha_4,\alpha_5,\alpha_6,\alpha_7,\alpha_8\}$	$[0,0,0,0,0,0,0,0]_2$	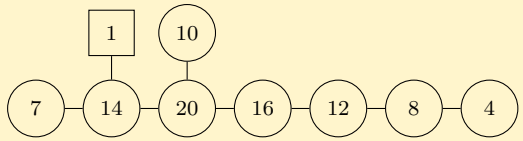	A_2+3A_1	154
$E_8(b_4)$	$\{\alpha_1,\alpha_2,\alpha_3,\alpha_4,\alpha_5,\alpha_6,\alpha_7,\alpha_8\}$	$[0,0,0,0,0,0,0,0]_5$	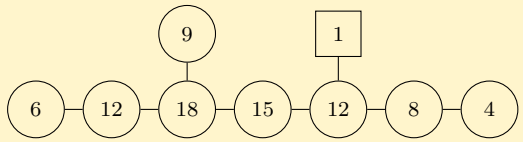	A_2+2A_1	146
E_7	$\{\alpha_1,\alpha_2,\alpha_3,\alpha_4,\alpha_5,\alpha_6,\alpha_8\}$	$[0,0,0,0,0,0,-1,0]$ $[0,0,0,0,0,0,1,0]$	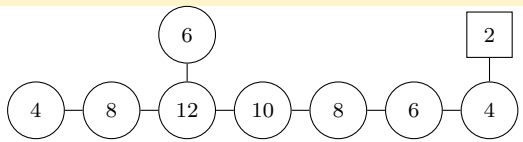	A_2	114
$E_8(a_4)$	$\{\alpha_1,\alpha_2,\alpha_3,\alpha_4,\alpha_5,\alpha_6,\alpha_7,\alpha_8\}$	$[0,0,0,0,0,0,0,0]_8$	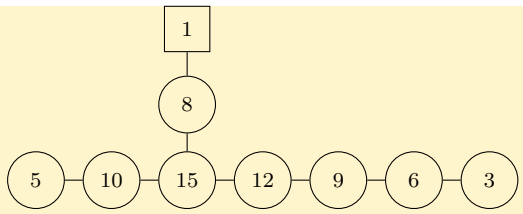	$4A_1$	128
$E_8(a_3)$	$\{\alpha_1,\alpha_2,\alpha_3,\alpha_4,\alpha_5,\alpha_6,\alpha_7,\alpha_8\}$	$[0,0,0,0,0,0,0,0]_6$	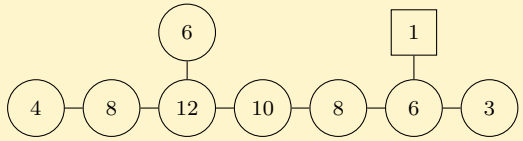	$3A_1$	112
$E_8(a_2)$	$\{\alpha_1,\alpha_2,\alpha_3,\alpha_4,\alpha_5,\alpha_6,\alpha_7,\alpha_8\}$	$[0,0,0,0,0,0,0,0]_1$	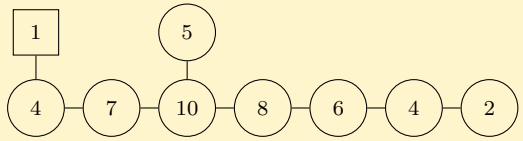	$2A_1$	92

Table A.3: Results for E_8

Orbit	Θ	Weights	Quiver	Dual orbit	d
$E_8(a_1)$	$\{\alpha_1, \alpha_2, \alpha_3, \alpha_4, \alpha_5, \alpha_6, \alpha_7, \alpha_8\}$	$[\ 0,\ 0,\ 0,\ 0,\ 0,\ 0,\ 0,\ 0]_7$		A_1	58

Appendix B

Zero Weight Multiplicity

We make a comment about the multiplicity of the zero weight in unpolarized defects. This is relevant for two of the defects analyzed in appendix A: one has Bala–Carter label $E_7(a_5)$ in $\mathfrak{g} = E_7$, and the other has Bala–Carter label $E_8(b_5)$ in $\mathfrak{g} = E_8$. For both of these, $\mathcal{W}_{\mathcal{S}}$ is the set of the zero weight only, but appearing *twice*. In the little string, at finite m_s, defects usually add up in a linear fashion [4, 3]. If a subset of weights in $\mathcal{W}_{\mathcal{S}}$ adds up to zero, then one is simply describing more than one elementary defect. In the case of polarized defects, where a direct Toda interpretation is available, we would refer to this situation as a higher-than-three point function on the sphere. We note here that for the two unpolarized defects we mentioned, this is not the case. For both cases, the zero weight is required to appear twice and does characterize a single exotic defect, with Bala–Carter label given above. In particular, $E_7(a_5)$ and $E_8(b_5)$ are not engineered in the little string as the sum of two elementary defects with a single zero weight. See Figure B.1 for the example of $E_7(a_5)$.

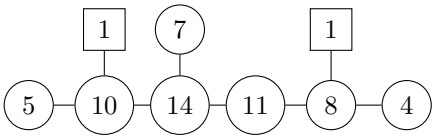

$\omega_1 : [0,0,0,0,0,0,0]$
$\omega_2 : [0,0,0,0,0,0,0]$

Bala–Carter label: $E_7(a_5)$ Coulomb dim. of $T^{2d}_{m_s\to\infty}$: 45

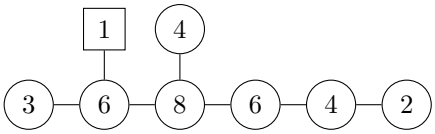

$\omega_1 : [0,0,0,0,0,0,0]$

Bala–Carter label: $E_7(a_3)$ Coulomb dim. of $T^{2d}_{m_s\to\infty}$: 32

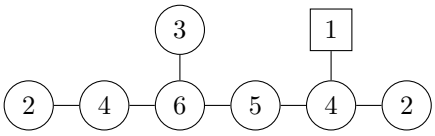

$\omega_2 : [0,0,0,0,0,0,0]$

Bala–Carter label: $E_7(a_2)$ Coulomb dim. of $T^{2d}_{m_s\to\infty}$: 26

Figure B.1: In the little string, at finite m_s, defects add up in a linear fashion. For instance, the E_7 defect shown on top is the sum of the two defects shown under it. For polarized defects, we usually refer to this situation as a four-punctured sphere: two full punctures and two punctures each labeled by the zero weight. However, in the $m_s \to \infty$, the defect really should be thought of as a three punctured sphere, with two full punctures and an exotic puncture given by a combination of the two zero weights, which cannot be split apart. As a quick check, this is confirmed by noting that the Coulomb branch dimension of $T^{2d}_{m_s\to\infty}$ is not additive.

Bibliography

[1] Mina Aganagic. "String theory and math: Why this marriage may last. Mathematics and dualities of quantum physics". In: *Bull. Am. Math. Soc.* 53.1 (2016), pp. 93–115. DOI: 10.1090/bull/1517. arXiv: 1508.06642 [hep-th].

[2] Mina Aganagic, Edward Frenkel, and Andrei Okounkov. "Quantum q-Langlands Correspondence". In: *Trans. Moscow Math. Soc.* 79 (2018), pp. 1–83. DOI: 10.1090/mosc/278. arXiv: 1701.03146 [hep-th].

[3] Mina Aganagic and Nathan Haouzi. "ADE Little String Theory on a Riemann Surface (and Triality)". In: (2015). arXiv: 1506.04183 [hep-th].

[4] Mina Aganagic, Nathan Haouzi, and Shamil Shakirov. "A_n-Triality". In: (2014). arXiv: 1403.3657 [hep-th].

[5] Mina Aganagic and Andrei Okounkov. "Elliptic stable envelopes". In: (Apr. 2016). arXiv: 1604.00423 [math.AG].

[6] Mina Aganagic et al. "Gauge/Liouville Triality". In: (2013). arXiv: 1309.1687 [hep-th].

[7] Ofer Aharony. "A Brief review of 'little string theories'". In: *Class. Quant. Grav.* 17 (2000), pp. 929–938. DOI: 10.1088/0264-9381/17/5/302. arXiv: hep-th/9911147 [hep-th].

[8] P. Bala and R. W. Carter. "Classes of unipotent elements in simple algebraic groups. I". In: *Math. Proc. Cambridge Philos. Soc.* 79.3 (1976), pp. 401–425. ISSN: 0305-0041. DOI: 10.1017/S0305004100052403.

[9] P. Bala and R. W. Carter. "Classes of unipotent elements in simple algebraic groups. II". In: *Math. Proc. Cambridge Philos. Soc.* 80.1 (1976), pp. 1–17. ISSN: 0305-0041. DOI: 10.1017/S0305004100052610.

[10] Peter Bouwknegt and Krzysztof Pilch. "On deformed W algebras and quantum affine algebras". In: *Adv. Theor. Math. Phys.* 2 (1998), pp. 357–397. arXiv: math/9801112 [math].

[11] Peter Bouwknegt and Kareljan Schoutens. "W symmetry in conformal field theory". In: *Phys. Rept.* 223 (1993), pp. 183–276. DOI: 10.1016/0370-1573(93)90111-P. arXiv: hep-th/9210010 [hep-th].

[12] Alexander Braverman, Michael Finkelberg, and Hiraku Nakajima. "Coulomb branches of $3d$ $\mathcal{N} = 4$ quiver gauge theories and slices in the affine Grassmannian (with appendices by Alexander Braverman, Michael Finkelberg, Joel Kamnitzer, Ryosuke Kodera, Hiraku Nakajima, Ben Webster, and Alex Weekes)". In: (2016). arXiv: 1604.03625 [math.RT].

[13] Mathew Bullimore, Tudor Dimofte, and Davide Gaiotto. "The Coulomb Branch of 3d $\mathcal{N} = 4$ Theories". In: (2015). arXiv: 1503.04817 [hep-th].

[14] F. Cachazo, S. Katz, and C. Vafa. "Geometric transitions and $\mathcal{N} = 1$ quiver theories". In: (2001). arXiv: hep-th/0108120 [hep-th].

[15] Oscar Chacaltana and Jacques Distler. "Tinkertoys for Gaiotto Duality". In: *JHEP* 11 (2010), p. 099. DOI: 10.1007/JHEP11(2010)099. arXiv: 1008.5203 [hep-th].

[16] Oscar Chacaltana and Jacques Distler. "Tinkertoys for the D_N series". In: *JHEP* 02 (2013), p. 110. DOI: 10.1007/JHEP02(2013)110. arXiv: 1106.5410 [hep-th].

[17] Oscar Chacaltana, Jacques Distler, and Yuji Tachikawa. "Nilpotent orbits and codimension-two defects of 6d $\mathcal{N} = (2, 0)$ theories". In: *Int. J. Mod. Phys.* A28 (2013), p. 1340006. DOI: 10.1142/S0217751X1340006X. arXiv: 1203.2930 [hep-th].

[18] Oscar Chacaltana, Jacques Distler, and Anderson Trimm. "Tinkertoys for the E_6 theory". In: *JHEP* 09 (2015), p. 007. DOI: 10.1007/JHEP09(2015)007. arXiv: 1403.4604 [hep-th].

[19] David H. Collingwood and William M. McGovern. *Nilpotent orbits in semisimple Lie algebras*. Van Nostrand Reinhold Mathematics Series. Van Nostrand Reinhold Co., New York, 1993, pp. xiv+186. ISBN: 0-534-18834-6.

[20] Stefano Cremonesi et al. "$\mathrm{T}_\rho^\sigma(G)$ theories and their Hilbert series". In: *JHEP* 01 (2015), p. 150. DOI: 10.1007/JHEP01(2015)150. arXiv: 1410.1548 [hep-th].

[21] Jin-tai Ding and Kenji Iohara. "Generalization and deformation of Drinfeld quantum affine algebras". In: *Lett. Math. Phys.* 41 (1997), pp. 181–193. DOI: 10.1023/A:1007341410987.

[22] Michael R. Douglas and Gregory W. Moore. "D-branes, quivers, and ALE instantons". In: (1996). arXiv: hep-th/9603167 [hep-th].

[23] Edward Frenkel and Nicolai Reshetikhin. "Deformations of $\mathcal{W}$-algebras associated to simple Lie algebras". In: *Comm. Math. Phys.* 197.1 (1998), pp. 1–32. ISSN: 0010-3616. arXiv: q-alg/9708006 [math.QA].

[24] Davide Gaiotto, Gregory W. Moore, and Andrew Neitzke. "Wall-crossing, Hitchin Systems, and the WKB Approximation". In: (2009). arXiv: 0907.3987 [hep-th].

[25] Davide Gaiotto and Edward Witten. "S-Duality of Boundary Conditions In $\mathcal{N} = 4$ Super Yang-Mills Theory". In: *Adv. Theor. Math. Phys.* 13.3 (2009), pp. 721–896. DOI: 10.4310/ATMP.2009.v13.n3.a5. arXiv: 0807.3720 [hep-th].

[26] Sergei Gukov and Edward Witten. "Gauge Theory, Ramification, And The Geometric Langlands Program". In: (2006). arXiv: hep-th/0612073 [hep-th].

[27] Amihay Hanany and Rudolph Kalveks. "Quiver Theories for Moduli Spaces of Classical Group Nilpotent Orbits". In: *JHEP* 06 (2016), p. 130. DOI: 10.1007/JHEP06(2016)130. arXiv: 1601.04020 [hep-th].

[28] Amihay Hanany and Noppadol Mekareeya. "Complete Intersection Moduli Spaces in $\mathcal{N} = 4$ Gauge Theories in Three Dimensions". In: *JHEP* 01 (2012), p. 079. DOI: 10.1007/JHEP01(2012)079. arXiv: 1110.6203 [hep-th].

[29] Amihay Hanany and Edward Witten. "Type IIB superstrings, BPS monopoles, and three-dimensional gauge dynamics". In: *Nucl. Phys.* B492 (1997), pp. 152–190. DOI: 10.1016/S0550-3213(97)00157-0, 10.1016/S0550-3213(97)80030-2. arXiv: hep-th/9611230 [hep-th].

[30] Nathan Haouzi and Can Kozçaz. "Supersymmetric Wilson Loops, Instantons, and Deformed W-Algebras". In: (July 2019). arXiv: 1907.03838 [hep-th].

[31] Nathan Haouzi and Can Kozçaz. "The ABCDEFG of Little Strings". In: (Nov. 2017). arXiv: 1711.11065 [hep-th].

[32] Nathan Haouzi and Christian Schmid. "Little String Defects and Bala-Carter Theory". In: (Dec. 2016). arXiv: 1612.02008 [hep-th].

[33] Nathan Haouzi and Christian Schmid. "Little String Origin of Surface Defects". In: (2016). arXiv: 1608.07279 [hep-th].

[34] Sean A. Hartnoll, Andrew Lucas, and Subir Sachdev. "Holographic quantum matter". In: (Dec. 2016). arXiv: 1612.07324 [hep-th].

[35] Nigel J. Hitchin. "The Selfduality equations on a Riemann surface". In: *Proc. Lond. Math. Soc.* 55 (1987), pp. 59–131. DOI: 10.1112/plms/s3-55.1.59.

[36] Nathan Jacobson. "Completely reducible Lie algebras of linear transformations". In: *Proc. Amer. Math. Soc.* 2 (1951), pp. 105–113. ISSN: 0002-9939.

[37] Shoichi Kanno et al. "$\mathcal{N} = 2$ gauge theories and degenerate fields of Toda theory". In: *Phys. Rev.* D81 (2010), p. 046004. DOI: 10.1103/PhysRevD.81.046004. arXiv: 0911.4787 [hep-th].

[38] Christoph A. Keller et al. "The ABCDEFG of Instantons and W-algebras". In: *JHEP* 03 (2012), p. 045. DOI: 10.1007/JHEP03(2012)045. arXiv: 1111.5624 [hep-th].

[39] Taro Kimura and Vasily Pestun. "Quiver W-algebras". In: (2015). arXiv: 1512.08533 [hep-th].

[40] Andrei Losev, Gregory W. Moore, and Samson L. Shatashvili. "M & m's". In: *Nucl. Phys.* B522 (1998), pp. 105–124. DOI: 10.1016/S0550-3213(98)00262-4. arXiv: hep-th/9707250 [hep-th].

[41] A. Malcev. "On the representation of an algebra as a direct sum of the radical and a semi-simple subalgebra". In: *C. R. (Doklady) Acad. Sci. URSS (N.S.)* 36 (1942), pp. 42–45.

[42] Travis Maxfield and Savdeep Sethi. "The Conformal Anomaly of M5-Branes". In: *JHEP* 06 (2012), p. 075. DOI: 10.1007/JHEP06(2012)075. arXiv: 1204.2002 [hep-th].

[43] Kei Miki. "A (q,γ) analog of the $\mathcal{W}_{1+\infty}$ algebra". In: *Journal of Mathematical Physics* 48.12 (2007), p. 123520. DOI: 10.1063/1.2823979. eprint: https://doi.org/10.1063/1.2823979. URL: https://doi.org/10.1063/1.2823979.

[44] Gregory W. Moore, Andrew B. Royston, and Dieter Van den Bleeken. "Parameter counting for singular monopoles on $\mathbb{R}^3$". In: *JHEP* 10 (2014), p. 142. DOI: 10.1007/JHEP10(2014)142. arXiv: 1404.5616 [hep-th].

[45] V. V. Morozov. "On a nilpotent element in a semi-simple Lie algebra". In: *C. R. (Doklady) Acad. Sci. URSS (N.S.)* 36 (1942), pp. 83–86.

[46] Dimitri Nanopoulos and Dan Xie. "Hitchin Equation, Singularity, and $\mathcal{N} = 2$ Superconformal Field Theories". In: *JHEP* 1003 (2010), p. 043. DOI: 10.1007/JHEP03(2010)043. arXiv: 0911.1990 [hep-th].

[47] Nikita Nekrasov. "BPS/CFT correspondence: non-perturbative Dyson-Schwinger equations and qq-characters". In: *JHEP* 03 (2016), p. 181. DOI: 10.1007/JHEP03(2016)181. arXiv: 1512.05388 [hep-th].

[48] Nikita Nekrasov and Vasily Pestun. "Seiberg-Witten geometry of four dimensional $\mathcal{N} = 2$ quiver gauge theories". In: (2012). arXiv: 1211.2240 [hep-th].

[49] Nikita Nekrasov, Vasily Pestun, and Samson Shatashvili. "Quantum geometry and quiver gauge theories". In: (2013). arXiv: 1312.6689 [hep-th].

[50] Hirosi Ooguri and Cumrun Vafa. "Two-dimensional black hole and singularities of CY manifolds". In: *Nucl. Phys. B* 463 (1996), pp. 55–72. DOI: 10.1016/0550-3213(96)00008-9. arXiv: hep-th/9511164.

[51] Miles Reid. "McKay correspondence". In: (1997). arXiv: alg-geom/9702016 [alg-geom].

[52] Richárd Rimányi et al. "3d Mirror Symmetry and Elliptic Stable Envelopes". In: (Feb. 2019). arXiv: 1902.03677 [math.AG].

[53] Nathan Seiberg. "New theories in six-dimensions and Matrix description of M theory on T^5 and $T^5/\mathbb{Z}_2$". In: *Phys. Lett.* B408 (1997), pp. 98–104. DOI: 10.1016/S0370-2693(97)00805-8. arXiv: hep-th/9705221 [hep-th].

[54] Nicolas Spaltenstein. *Classes unipotentes et sous-groupes de Borel*. Vol. 946. Lecture Notes in Mathematics. Springer-Verlag, Berlin-New York, 1982, pp. ix+259. ISBN: 3-540-11585-4.

[55] K. Thielemans. "A Mathematica package for computing operator product expansions". In: *Int. J. Mod. Phys.* C2 (1991), pp. 787–798. DOI: 10.1142/S0129183191001001.

[56] Cumrun Vafa. "Geometric origin of Montonen-Olive duality". In: *Adv. Theor. Math. Phys.* 1 (1998), pp. 158–166. arXiv: hep-th/9707131 [hep-th].

[57] Edward Witten. "Geometric Langlands From Six Dimensions". In: (2009). arXiv: 0905.2720 [hep-th].

[58] Edward Witten. "Quantum Field Theory and the Jones Polynomial". In: *Commun. Math. Phys.* 121 (1989). Ed. by Asoke N. Mitra, pp. 351–399. DOI: 10.1007/BF01217730.

[59] Edward Witten. "Some comments on string dynamics". In: *Future perspectives in string theory. Proceedings, Conference, Strings'95, Los Angeles, USA, March 13-18, 1995.* 1995. arXiv: hep-th/9507121 [hep-th].

[60] Edward Witten. "Two-dimensional gravity and intersection theory on moduli space". In: *Surveys Diff. Geom.* 1 (1991), pp. 243–310. DOI: 10.4310/SDG.1990.v1.n1.a5.